

1-30

COPY NO. _____

Support Under Concrete Pavements

APPENDICES

Prepared for
National Cooperative Highway Research Program
Transportation Research Board
National Research Council

Michael I. Darter
Kathleen T. Hall
Chen-Ming Kuo

Department of Civil Engineering
University of Illinois at Urbana-Champaign

December 1994

Acknowledgment

This work was sponsored by the American Association of State Highway and Transportation Officials, in cooperation with the Federal Highway Administration, and was conducted in the National Cooperative Highway Research Program which is administered by the Transportation Research Board of the National Research Council.

Disclaimer

The opinions and conclusions expressed or implied in the report are those of the research agency. They are not necessarily those of the Transportation Research Board, the National Research Council, or the Federal Highway Administration, American Association of State Highway and Transportation Officials, or of the individual states participating in the National Cooperative Highway Research Program.

TABLE OF CONTENTS

	Page
LIST OF FIGURES	vii
LIST OF TABLES	xv
APPENDIX A DEVELOPMENT OF K VALUE CONCEPTS AND METHODS	
DEVELOPMENT OF K VALUE CONCEPTS AND PROCEDURES	A-1
INTRODUCTION OF DENSE LIQUID SUPPORT MODEL	A-1
WESTERGAARD'S EQUATIONS FOR SLAB ON A DENSE LIQUID	A-6
ARLINGTON ROAD TESTS	A-8
CORPS OF ENGINEERS FIELD STUDIES	A-25
EFFECT OF BASE LAYERS ON K	A-31
ASTM PLATE BEARING TEST METHODS	A-32
AASHO ROAD TEST	A-34
PORTLAND CEMENT ASSOCIATION	A-44
1972 AASHO INTERIM GUIDE	A-54
CORRELATION OF K TO SOIL TYPE AND MOISTURE	A-55
1986 AASHO GUIDE K TO VALUE METHODS	A-58
K VALUE BACKCALCULATION METHODS	A-85
BACKCALCULATION FIELD RESULTS	A-95
REFERENCES FOR APPENDIX A	A-114

TABLE OF CONTENTS, CONTINUED

	Page
APPENDIX B METHODS FOR ESTIMATING K VALUE	
INTRODUCTION	B-1
CORRELATION METHODS	B-2
DEFLECTION TESTING AND BACKCALCULATION METHODS	B-19
PLATE TESTING METHODS	B-38
REFERENCES FOR APPENDIX B	B-47
APPENDIX C LOSS OF SUPPORT CONCEPTS AND METHODS	
LOSS OF SUPPORT OVER THE DESIGN LIFE	C-1
LOSS OF SUPPORT FROM EROSION	C-1
LOSS OF SUPPORT FROM TEMPERATURE CURLING AND MOISTURE WARPING	C-8
METHODS OF ASSESSING LOSS OF SUPPORT IN THE FIELD	C-20
CONSIDERATION OF LOSS OF SUPPORT IN DESIGN	C-21
REFERENCES FOR APPENDIX C	C-23
APPENDIX D THREE-DIMENSIONAL FINITE ELEMENT MODEL DEVELOPMENT AND VALIDATION	
OVERVIEW OF ABAQUS	D-2
FEASIBILITY STUDY OF ELEMENT TYPES	D-8
MOTIVATION FOR 3-D MODEL DEVELOPMENT	D-31
DEVELOPMENT OF THE 3DPAVE MODEL	D-33

TABLE OF CONTENTS, CONTINUED

	Page
VALIDATION OF 3DPAVE	D-49
REFERENCES FOR APPENDIX D	D-73
APPENDIX E IMPROVED CONSIDERATION OF SUPPORT IN CURRENT AASHTO METHODOLOGY	
EXISTING AASHTO DESIGN MODEL FOR CONCRETE PAVEMENTS ..	E-2
DEFICIENCIES IN 1993 AASHTO PROCEDURE RELATED TO PAVEMENT SUPPORT	E-18
IMPROVED AASHTO METHODOLOGY RECOMMENDED	E-22
FIELD VERIFICATION OF NEW MODELS	E-57
SENSITIVITY OF PROPOSED AASHTO CONCRETE PAVEMENT DESIGN MODEL	E-61
COMPARISON WITH AASHTO DESIGN PROCEDURE	E-61
NEW DESIGN TABLES	E-61
DESIGN OF JOINT LOAD TRANSFER TO CONTROL FAULTING	E-66
DESIGN OF THE BASE COURSE	E-75
DESIGN CHECK FOR CRITICAL JOINT LOAD POSITION STRESSES ..	E-77
DESIGN OF DIFFERENT TYPES OF CONCRETE PAVEMENT	E-93
SUMMARY COMPARISON OF EXISTING AASHTO DESIGN PROCEDURE AND PROPOSED REVISED PROCEDURE WITH IMPROVED SUPPORT CONSIDERATIONS	E-93
REFERENCES FOR APPENDIX E	E-95

TABLE OF CONTENTS, CONTINUED

	Page
APPENDIX F PROPOSED REVISION TO AASHTO GUIDE, PART II, SECTION 3.2 RIGID PAVEMENT DESIGN AND SECTION 3.3 RIGID PAVEMENT JOINT DESIGN	
3.2 RIGID PAVEMENT DESIGN	F-1
3.3 RIGID PAVEMENT JOINT DESIGN	F-57
APPENDIX G RIGID PAVEMENT DESIGN EXAMPLE (PROPOSED REVISION TO AASHTO GUIDE APPENDIX I)	G-1
APPENDIX H DEVELOPMENT OF EFFECTIVE ROADBED SOIL K VALUE (PROPOSED REVISION TO AASHTO GUIDE APPENDIX HH)	H-1

LIST OF FIGURES

Figure	Page
A-1 Dense liquid and elastic solid extremes of elastic soil response	A-2
A-2 Schematic illustration and calculation of k from deflected volume	A-13
A-3 Typical load-displacement data from Arlington plate tests	A-16
A-4 Effect of load size and deflection magnitude on k	A-17
A-5 Effect of seasonal variation and deformation level on k value	A-21
A-6 Correlation of k value, CBR, and soil classification	A-28
A-7 Bureau of Public Roads and Unified soil classes versus k values	A-30
A-8 Seasonal variation in moisture content, dry density, CBR, and k_E AASHO Road Test Loop 1 flexible tangent data	A-35
A-9 Seasonal variation in moisture content, dry density, CBR, and k_E AASHO Road Test Loop 1 rigid tangent data	A-36
A-10 Effect of moisture and density of k_E and CBR, AASHO Road Test main loop data	A-38
A-11 Plate load test apparatus used at AASHO Road Test	A-39
A-12 Schematic illustration of AASHO Road Test plate load test results	A-41
A-13 Correlation of K_E and k_C , AASHO Road Test data	A-42
A-14 Results of PCA plate tests on granular and cement-treated bases	A-45
A-15 Base k curves from 1973 PCA airport pavement design manual	A-47
A-16 Correlations between k , soil type, and other tests	A-48
A-17 PCA's alternate procedure for effect of base on l	A-52
A-18 k values for fine-grained AASHTO soil classes and degrees of saturation	A-56
A-19 k values for coarse-grained AASHTO soil classes and degrees of saturation	A-57

LIST OF FIGURES, CONTINUED

Figure	Page
A-20 Comparison of field subgrade bearing values and laboratory triaxial test results, from Palmer	A-60
A-21 Elastic layer simulation of plate load test, from AASHTO Guide Appendix HH	A-64
A-22 Comparison of AASHTO k value equation and backcalculated k values for unprotected subgrades	A-66
A-23 Inputs to 1986 AASHTO Guide composite k analysis	A-68
A-24 Composite k nomograph (1986 AASHTO Guide, Figure 3.3)	A-70
A-25 Comparison of k values from 1986 AASHTO Guide Appendix LL and k values backcalculated from concrete slab deflections	A-71
A-26 Example of subgrade and base effects on k value and slab response	A-74
A-27 Adjustment to k for rigid foundation within 10 ft [3 m], from 1986 AASHTO Guide	A-77
A-28 Relative damage nomograph from 1986 AASHTO Guide	A-79
A-29 Loss of support nomograph from 1986 AASHTO Guide	A-81
A-30 Relationship of backcalculated k value to static k value	A-88
A-31 Backcalculated k value determination from d_0 and AREA	A-90
A-32 Concrete E determination from k value, AREA, and slab thickness	A-91
A-33 Effect of fill and bedrock on backcalculated k values at Dulles International Airport	A-110
B-1 k value versus degree of saturation for fine-grained soils	B-5
B-2 Approximate relationship of k value range to CBR	B-14
B-3 Approximate relationship of k value to R-value	B-15
B-4 Approximate relationship of k value range to DCP penetration rate	B-16

LIST OF FIGURES, CONTINUED

Figure	Page
B-5 Adjustment to k for fill and/or rigid layer	B-18
B-6 Relationship of AREA to ℓ . [2]	B-20
B-7 Dynamic k value determination from d_0 and AREA. [2]	B-21
B-8 Concrete E determination from k value, AREA, and slab thickness. [2] . . .	B-22
B-9 Nondimensional deflection coefficients versus ℓ_k . [4]	B-26
B-10 Nondimensional deflection versus normalized radial distance	B-30
B-11 Iowa Road Rater method for determining springtime static k value. [6] . .	B-37
C-1 Illustration of corner deflection due to a negative temperature differential through the slab, computed using 3DPAVE	C-10
C-2 Increase in tensile stress at top of slab from increased negative temperature differential from top to bottom of slab	C-11
C-3 Development of upward curling within 48 hours after paving in Munich, Germany. [37]	C-13
C-4 Deflection profiles along a joint due to change in the temperature differential. [5]	C-15
C-5 Annual cyclic variations of slab deflections and its relation to rainfall in Chile (note: these data taken when no temperature differential existed through the slab). [8]	C-19
D-1 Example of mesh generated by PATRAN	D-4
D-2 Components of data deck in ABAQUS	D-6
D-3 Mesh fineness and element type comparison	D-13
D-4 Major brick elements in ABAQUS	D-15
D-5 Finite element meshes used for interior loading in case 1	D-16
D-6 Change of load size in interior loading of case 2	D-20

LIST OF FIGURES, CONTINUED

Figure	Page
D-7 Westergaard, 2-D, and 3-D finite element interior stress results	D-22
D-8 Westergaard, 2-D, and 3-D finite element interior deflection results	D-23
D-9 Change of load size in edge loading of case 2	D-25
D-10 Westergaard, 2-D, and 3-D finite element edge stress results	D-26
D-11 Westergaard, 2-D, and 3-D finite element edge deflection results	D-27
D-12 Steps in development of 3-D model	D-34
D-13 C3D27R element	D-36
D-14 Nonlinear temperature distribution with C3D27R element	D-36
D-15 INTER9 interface element	D-37
D-16 Model of slab resting on Winkler foundation	D-39
D-17 Model of slab resting on elastic solid foundation	D-39
D-18 Friction model in ABAQUS	D-41
D-19 Implementation of friction in ABAQUS	D-41
D-20 Dowel bar model	D-44
D-21 Dowel model comparison between ABAQUS and ILLI-SLAB	D-46
D-22 3-D displaced shape of jointed slabs modelled by ABAQUS	D-47
D-23 Aggregate interlock model	D-48
D-24 3-D single slab model in ABAQUS	D-50
D-25 Configuration of main loop test setup at AASHO Road Test	D-51
D-26 3DPAVE meshes for AASHO Road Test single and tandem axles	D-53
D-27 Moving truck edge stress comparisons for AASHO Road Test	D-54

LIST OF FIGURES, CONTINUED

Figure	Page
D-28 3DPAVE stress versus AASHO Road Test stress from measured strain . . .	D-56
D-29 Percent reduction in edge strain with increase in vehicle speed	D-58
D-30 Speed versus k value matching stress, AASHO Road Test	D-61
D-31 Crack progression in 3.5-in [89 mm] unreinforced slabs at AASHO Road Test	D-62
D-32 Crack progression in 8-in [203 mm] unreinforced slabs at AASHO Road Test	D-62
D-33 Load positions simulating traffic loading	D-63
D-34 3DPAVE stress contours for thin slab for different load positions	D-64
D-35 3DPAVE stress contours for thick slab for different load positions	D-65
D-36 Configuration of slabs on cement-treated bases in PCA tests	D-68
D-37 Comparison of results for interior loading condition	D-69
D-38 Comparison of results for edge loading condition	D-69
D-39 Comparison of measured and computed edge stress due to curling, Arlington Road Test	D-72
E-1 Original 1961 plot of "extension" to the rigid pavement design equation. [1]	E-8
E-2 Seasonal variation in elastic k value at the AASHO Road Test, Loop 1. [2]	E-16
E-3 Midslab and joint loading positions	E-25
E-4 Illustration of Equation E-22, total stress versus load-only stress.	E-28
E-5 Mean annual wind speed, mph. [18]	E-35
E-6 Mean annual air temperature, °F. [18]	E-36
E-7 Mean annual wind precipitation, in. [18]	E-37

LIST OF FIGURES, CONTINUED

Figure	Page
E-8 Relationship of W to $\log S'_c/\sigma_t$ for three terminal serviceability levels for the proposed revised AASHTO extended concrete pavement design model.	E-40
E-9 Relationship between terminal serviceability P2 and $\log W$ for proposed revised AASHTO extended concrete pavement design model.	E-41
E-10 Relationship between $\log W$ and $\log S'_c/\sigma_t$	E-44
E-11 Effect of slab thickness, base modulus, and friction coefficient on ratio of stress computed with friction coefficient to stress computed with full friction, for midslab loading and daytime temperature gradient.	E-54
E-12 Predicted versus actual $\log W$ for test sections from the two-year AASHTO Road Test using the proposed revised concrete pavement model.	E-59
E-13 Predicted versus actual $\log W$ for test sections from the 2-year AASHTO Road Test, the 14-year extended tests on I-80 and other data from North America using the proposed revised concrete pavement design model.	E-63
E-14 Effect of slab thickness, base modulus, and friction coefficient on ratio of stress computed with friction coefficient to stress computed with full friction, for joint loading and nighttime temperature gradient. ...	E-78
E-15 Critical location of maximum tensile stresses for the midslab load position and joint load position	E-81
E-16a Maximum tensile stress on top of slab for joint loading position versus a negative temperature differential through the slab for specific design conditions (aggregate base, soft subgrade)	E-86
E-16b Maximum tensile stress on top of slab for joint loading position versus a negative temperature differential through the slab for specific design conditions (treated base, soft subgrade)	E-87
E-16c Maximum tensile stress on top of slab for joint loading position versus a negative temperature differential through the slab for specific design conditions (aggregate base, medium subgrade)	E-88
E-16d Maximum tensile stress on top of slab for joint loading position versus a negative temperature differential through the slab for specific design conditions (treated base, medium subgrade)	E-89

LIST OF FIGURES, CONTINUED

Figure	Page
E-16e Maximum tensile stress on top of slab for joint loading position versus a negative temperature differential through the slab for specific design conditions (aggregate base, stiff subgrade)	E-90
E-16f Maximum tensile stress on top of slab for joint loading position versus a negative temperature differential through the slab for specific design conditions (treated base, stiff subgrade)	E-91
F-1 k values versus degree of saturation for cohesive soils	F-7
F-2 Approximate relationship of k value range to CBR	F-11
F-3 Approximate relationship of k value range to R-value	F-12
F-4 Approximate relationship of k value range to DCP penetration rate	F-13
F-5 Dynamic elastic k value determination from d_0 and AREA	F-16
F-6 Adjustment to k for fill and/or rigid layer	F-20
F-7 Midslab and joint loading positions defined	F-22
F-8 Mean annual wind speed, mph	F-27
F-9 Mean annual air temperature, °F	F-28
F-10 Mean annual precipitation, in	F-29
F-11a Maximum tensile stress at bottom of slab for midslab loading position versus a positive temperature differential through the slab for specific design conditions (aggregate base, soft subgrade)	F-41
F-11b Maximum tensile stress at bottom of slab for midslab loading position versus a positive temperature differential through the slab for specific design conditions (treated base, soft subgrade)	F-42
F-11c Maximum tensile stress at bottom of slab for midslab loading position versus a positive temperature differential through the slab for specific design conditions (aggregate base, medium subgrade) ..	F-43

LIST OF FIGURES, CONTINUED

Figure	Page
F-11d	Maximum tensile stress at bottom of slab for midslab loading position versus a positive temperature differential through the slab for specific design conditions (treated base, medium subgrade) F-44
F-11e	Maximum tensile stress at bottom of slab for midslab loading position versus a positive temperature differential through the slab for specific design conditions (aggregate base, stiff subgrade) F-45
F-11f	Maximum tensile stress at bottom of slab for midslab loading position versus a positive temperature differential through the slab for specific design conditions (treated base, stiff subgrade) F-46
F-12	Friction adjustment factor for stress at bottom of slab for midslab loading F-47
F-13a	Maximum tensile stress at top of slab for joint loading position versus a negative temperature differential through the slab for specific design conditions (aggregate base, soft subgrade) F-49
F-13b	Maximum tensile stress at top of slab for joint loading position versus a negative temperature differential through the slab for specific design conditions (treated base, soft subgrade) F-50
F-13c	Maximum tensile stress at top of slab for joint loading position versus a negative temperature differential through the slab for specific design conditions (aggregate base, medium subgrade) F-51
F-13d	Maximum tensile stress at top of slab for joint loading position versus a negative temperature differential through the slab for specific design conditions (treated base, medium subgrade) F-52
F-13e	Maximum tensile stress at top of slab for joint loading position versus a negative temperature differential through the slab for specific design conditions (aggregate base, stiff subgrade) F-53
F-13f	Maximum tensile stress at top of slab for joint loading position versus a negative temperature differential through the slab for specific design conditions (treated base, stiff subgrade) F-54
F-14	Friction adjustment factor for stress at top of slab for joint loading F-55

LIST OF TABLES

Table	Page
A-1	Subgrade k values and concrete elastic moduli backcalculated from slab deflections at Arlington Road Test A-19
A-2	AASHO Road Test k values from spring trenching program A-44
A-3	Sections in PCA tests of slabs with cement-treated bases A-53
A-4	Backcalculation results for PCA test slabs A-54
A-5	Comparison of composite k values from Appendix LL and nomograph A-72
A-6	AASHO Road Test Loop 1 rigid pavement backcalculation results A-97
A-7	AASHO Road Test Loop 1 flexible pavement backcalculation results A-100
A-8	Backcalculation results for concrete pavements and concrete overlays at Willard Airport A-102
A-9	Backcalculated k values by soil class, from RPPR data A-103
A-10	Effect of treated and untreated bases on k, for projects with different bases at the same location, from RPPR data A-105
A-11	Backcalculated k values by soil class, from LTPP GPS 3 and 4 A-106
A-12	Mean backcalculated k values from 20 Chilean JPCP test sections A-113
B-1	Regression coefficients for d^* versus l relationships B-28
C-1	Design provisions proposed for combatting pumping in concrete pavements by PIARC C-6
D-1	Characteristics of shell elements in ABAQUS D-10
D-2	Comparison of maximum tensile stress, psi [1 psi = 6.89 kPa] D-11
D-3	Comparison of maximum deflection, mils [1 mil = 25.4 μ m] D-11
D-4	Deflections at center of load, mils [1 mil = 25.4 μ m] D-17
D-5	Stresses at center of load, psi [1 psi = 6.89 kPa] D-17

LIST OF TABLES, CONTINUED

Table	Page
D-6 Maximum interior stress comparison, psi [1 psi = 6.89 kPa]	D-21
D-7 Maximum interior deflection comparison, mils [1 mil = 25.4 μm]	D-21
D-8 Maximum edge stress comparison, psi [1 psi = 6.89 kPa]	D-25
D-9 Maximum edge deflection comparison, mils [1 mil = 25.4 μm]	D-25
D-10 Stress comparison between AASHO Road Test and 3DPAVE	D-55
D-11 Measured and computed stress due to curling (without applied load) Arlington Road Test	D-71
E-1 Summary of daytime positive effective temperature differentials over year for several sites, based on equivalent fatigue damage	E-33
E-2 Comparison of maximum tensile stresses for conventional lane width (12 ft [3.66 m]), widened slab (2 ft [0.6 m]) and tied concrete shoulder (deflection load transfer 74 percent)	E-47
E-3 Summary of measured coefficients of friction between concrete slab and base course from various references and typical ranges of base modulus of elasticity	E-50
E-4 Some results for the friction adjustment factor, F (ratio of σ_t computed with friction coefficient to σ_t computed with full friction)	E-53
E-5 Predicted versus actual ESALs for seven groups of JPCP sections from the extended AASHO Road Test (1958-1974)	E-60
E-6 Predicted versus actual ESALs for pavement sections from the RPPR database	E-62
E-7 Slab thickness required for given inputs for untreated aggregate base . . .	E-64
E-8 Slab thickness required for given inputs for treated aggregate base	E-65
E-9 Mean joint faulting predictions for dowelled jointed plain concrete pavement using Equation E-37	E-71
E-10 Mean joint faulting predictions for dowelled jointed reinforced concrete pavement using Equation E-37	E-72

LIST OF TABLES, CONTINUED

Table	Page
E-11	Mean joint faulting predictions for undowelled jointed plain concrete pavement using Equation E-42 E-73
E-12	Recommended critical joint faulting levels for design E-74
E-13	Effect of base widening on critical stress in slab for midslab loading position using 3DPAVE E-79
E-14	Summary of nighttime negative effective temperature differentials over year for several sites based on equivalent fatigue damage E-83
E-15	Summary of comparison between existing and proposed revised design considerations E-94
F-1	Recommended k value ranges for A-1 and A-3 soils F-8
F-2	Recommended k value ranges for A-2 soils F-10
F-3	Determination of effective subgrade k value for a specific project site and design features F-19
F-4	Summary of measured coefficient of friction between concrete slab and base course from various references and typical ranges of base modulus of elasticity F-26
F-5	A_0 and A_1 constants for model $D = A_0 + A_1 \log W$, for $P_2 = 2.5$, conventional 12-ft lane F-31
F-6	Example slab thickness required for given inputs for untreated aggregate base, conventional width traffic lane with no tied concrete shoulders for Midwestern location F-36
F-7	Slab thickness required for given inputs for treated aggregate base F-37
F-8	Mean joint faulting predictions for dowelled jointed plain concrete pavement using Equation F-17 F-64
F-9	Mean joint faulting predictions for dowelled jointed reinforced concrete pavement using Equation F-17 F-65

LIST OF TABLES, CONTINUED

Table	Page
F-10 Mean joint faulting predictions for undowelled jointed plain concrete pavement using Equation F-22	F-66
F-11 Recommended critical joint faulting levels for design	F-67
H-1 Example calculation of effective k value	H-5
H-2 Effective k value calculation for second example	H-7
H-3 Effective subgrade k value for AASHO Road Test site	H-8
H-4 Worksheet for computation of effective subgrade k value	H-8

APPENDIX A

DEVELOPMENT OF K VALUE CONCEPTS AND PROCEDURES

INTRODUCTION OF DENSE LIQUID SUPPORT MODEL

The conceptual model of a plate supported by a "dense liquid" foundation is attributed to Winkler [1] in 1867, although it may have been suggested earlier. Such a foundation is assumed to deflect under an applied vertical force in direct proportion to the force, without shear transmission to adjacent areas of the foundation not under the loaded area. The constant of proportionality between deflection and force is the k value. "A popular physical interpretation of this model," according to McCullough, "indicates that the foundation acts as a bed of springs [with spring constant k] or as a dense liquid with a density equal to k times the deflection of a given load." [2] The first application of this concept, to floating ice sheets, was presented by Hertz in 1884. [3] Applications of the dense liquid concept to slab support were subsequently proposed by Föppl [4] in 1907, and Koch [5] and Schleicher [6] in 1925.

Dense Liquid and Elastic Solid Idealizations

The dense liquid model represents one end of the spectrum of elastic soil response. At the other end of the spectrum is the elastic solid model, according to which a load applied to the surface of a foundation is assumed to produce a continuous and infinite deflection basin. The key features of these two models are illustrated in Figure A-1 and summarized below.

Dense Liquid Model

Real Soil

Elastic Solid Model

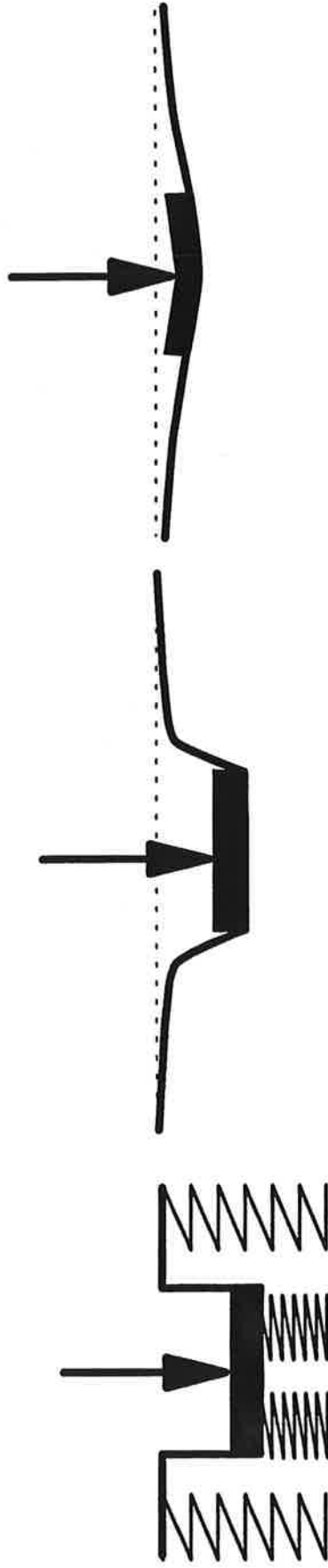


Figure A-1. Dense liquid and elastic solid extremes of elastic soil response.

Dense Liquid Model

- The deflection under the plate equals plate pressure divided by k value.
- Deflection equals zero beyond the edge of the plate.
- Deflection is the same for rigid and flexible plates.
- For a given pressure and deflection, k is independent of plate size.

Elastic Solid Model

- Deflection depends on subgrade elastic modulus, plate size, and distance.
- The deflection basin is continuous and infinite.
- Rigid and flexible load plates produce different deflections.

The elastic response of real soils (i.e., unbound sands, silts, and clays) lies somewhere between these two extremes. In a static plate load test on a real soil, the following responses are likely to be observed:

Real Soil

- Plate punches down somewhat, producing discontinuous deflection basin.
- Some surface deflection occurs beyond edge of load plate.
- Deflection equals zero at some finite distance.
- For a given pressure and deflection, k varies with plate size.

Choice of Soil Model for Concrete Pavement Analysis

The dense liquid model has traditionally been favored over the elastic solid model in concrete pavement analysis. One reason for this is that the calculations for slab deflection and stress are simpler using the dense liquid model than using the

elastic solid model. In the modern era of high-speed computers this is a less significant concern than it was in the past. Another reason the dense liquid model is preferred for concrete pavement analysis is that, for slabs on natural soil subgrades or granular bases, the dense liquid model more accurately predicts slab responses at edges and corners.

For example, if a load were placed adjacent to a joint with no physical load transfer (e.g., no dowels or aggregate interlock) on a pavement with an untreated foundation, the loaded slab would deflect and the unloaded slab would not deflect. This is the response the dense liquid model would predict. The elastic solid model, on the other hand, would predict equal deflections on both sides of the joint, even though the shear stress produced in the foundation may be substantially higher than the shear strength of the foundation material. Because concrete slab responses at edges and corners are considered critical for design purposes, the dense liquid model is considered more appropriate.

Two-Parameter Elastic Models

Both of the models described above are idealizations of real soil behavior. The dense liquid model is better suited for materials of relatively low shear strength (e.g., natural subgrade soils and granular bases), while the elastic solid model is better suited for materials of high shear strength (e.g., treated bases). Several researchers have proposed two-parameter models to characterize the range of soil response between the dense liquid (k) and elastic solid (E) extremes. [7] Although two-parameter soil models have some theoretical appeal, their usefulness in concrete pavement design is limited by lack of guidance on selection of the needed model parameters for various soils.

Inelastic and Time-Dependent Behavior of Real Soils

In addition to elastic behavior, real soils exhibit irreversible (plastic) behavior and time-dependent behavior. Plastic deformation is not generally considered a significant concern in concrete pavement design due to the low stresses on the subgrade, although repeated loading of free slab corners can conceivably result in permanent deformation of subgrade or base materials. Erosion due to water pumping beneath the slab may be far more significant to corner support.

A more significant concern in concrete pavement design is the effect of loading rate on soil stresses and deformations, particularly for cohesive saturated soils. The stiffness (e.g., k-value) of these soils may be substantially higher under rapid loading (e.g., moving vehicles or impulse loads) than under slow loading, because under rapid loading pore water pressures are not dissipated. [7] This is a practical concern for concrete pavement design because the available performance models are based on k-values determined from static load tests, while the actual loads applied by traffic are usually dynamic, as are the loads applied by deflection testing devices used for evaluation of in-service pavements and foundations.

Under slow loading, primary consolidation occurs gradually as pore water pressures dissipate, until (in most cases) the deformation of the soil reaches some stable value. [7] However, it is possible for soils to exhibit secondary (creep) deformation, if the magnitude of load exceeds the creep strength of the soil. [7, 8] In such a case the deformation may not reach a stable value, even in a load test which is allowed to continue for several hours. The consolidation and creep responses of soils to slow loading necessitate some standardization in soil load test methods. For example, a typical load test procedure may specify that the test may be stopped when the rate of change of deformation has slowed to some given value.

WESTERGAARD'S EQUATIONS FOR SLAB ON A DENSE LIQUID

In 1925, Westergaard presented equations for deflection of a concrete slab on a dense liquid foundation, for interior, edge, and corner loading conditions. [9] Westergaard introduced the term "modulus of subgrade reaction" for the k value, and also introduced the term "radius of relative stiffness," ℓ , to describe the stiffness of a concrete slab relative to that of the subgrade:

$$\ell = \sqrt[4]{\frac{E h^3}{12 (1 - \mu^2) k}} \quad (\text{A-1})$$

where ℓ = radius of relative stiffness (units of length)

E = elastic modulus of concrete slab (force/length²)

h = concrete slab thickness (length)

μ = concrete Poisson's ratio

k = modulus of subgrade reaction (force/length³)

Westergaard suggested that the subgrade k value could be backcalculated from deflections of the slab surface rather than from load tests on the subgrade:

"By comparing the contour lines which have been obtained for the deflected surface by tests and by theory, respectively, numerical values of the elastic constants which are involved, especially a certain constant which measures the stiffness of the subgrade, may be determined in any given case." [10]

"It is true that tests of bearing pressures on soils have indicated a modulus, k which varies considerably depending on the area over which the pressure is distributed. Yet, so long as the loads are limited to a particular type, that of wheel loads on top of the pavement, it is reasonable to assume that some constant value of the modulus, k , determined empirically, will lead to a sufficiently accurate analysis of the deflections and stresses ... The modulus, k , enters in the formulas for the deflections of the pavements, and may be determined empirically, accordingly, for a given type of subgrade, by comparing the deflections found by tests of full-sized slabs with the deflections given by the formulas." [9]

To support the statement that load tests on soils produced bearing capacity estimates which depended on the load size, Westergaard cited the results of field tests reported by Bijls in 1923 [11], Goldbeck in 1925 [12], and Goldbeck and Bussard in 1925 [13].

Westergaard's proposed approach to backcalculating k from pavement measurements was to solve for the quantity $k\ell^2$ which his edge, corner, and interior deflection equations had in common. The equation defining radius of relative stiffness could be rearranged to solve for k from the solved quantity $k\ell^2$, a slab thickness h , and an assumed concrete modulus E .

Westergaard envisioned his equations as being useful for evaluating existing pavements in order to gain insight for design of new pavements. Westergaard did not, however, explicitly address determination of subgrade k values for use in new design. Thus, he did not shed light on the problem of reconciling k values from plate load tests with k values backcalculated from pavement deflections.

Westergaard also pointed out several important aspects in which the behavior of actual slabs and foundations might differ from that assumed in theory:

"In using the tables and diagrams it should be kept in mind that the analysis is based on the assumptions which were stated at the beginning of this discussion. By the nature of these assumptions certain influences were left out of consideration, especially the following: (1) variations of temperature, and other causes for tendency to change of volume; (2) the gradual diminishing of the thickness from the edge toward the interior [with respect to thickened-edge pavements]; (3) local soft or hard spots in the subgrade; (4) horizontal components of the reactions of the subgrade; and (5) the dynamic effect, expressed in terms of the inertia of the pavement and subgrade." [9]

With these remarks, Westergaard identified some of the major concerns in characterizing subgrade support which still persist, namely: slab curling and warping, nonuniformity of support, friction at the slab/foundation interface, and dynamic versus static loading, and encouraged further analysis of all of these influences. Westergaard suggested that the dynamic loading response "may possibly be expressed approximately in terms of an increased value of the modulus k ." [9]

ARLINGTON ROAD TESTS

In the early 1930s, the Bureau of Public Roads conducted extensive field tests at the Arlington Experiment Farm in Virginia to investigate several aspects of

concrete pavement behavior. These investigations were documented in a series of reports by Teller and Sutherland. [14, 15, 16, 17, 18]

One of the stated objectives of these field tests was to study "the effects of loads placed in various ways on pavement slabs on uniform thickness ... intended primarily as an experimental verification of the only rational theory of pavement slab stresses thus far advanced, i.e., the Westergaard analysis." [14] Another objective was to study "the effects of temperature conditions on the size, shape, and load-carrying ability of pavement slabs ... to provide information, not heretofore available, on the complex relations created by temperature and moisture variations, and the practical significance of these relations with respect to the design of the pavement slab as a load-carrying structure." [14]

Among the many valuable findings of the Arlington tests are those concerning (1) measurement of subgrade k values, (2) effects of seasonal moisture variation on k values, (3) effects of slab curling on corner k values, and (4) effect of subgrade "improvement" on k values. These findings are summarized below.

Measurement of Subgrade k Values

Because one of the major objectives of the Arlington Road Tests was to verify Westergaard's equations with experimental results, it was necessary for the Arlington researchers to develop some way to determine the subgrade k value. Bearing tests of soils had been conducted with rigid plates for many years prior to the Arlington Road Test, but the Arlington researchers did not feel that such tests were applicable to subgrade characterization for concrete pavement design, because of the conditions under which the tests were run and the large deformations produced.

"To make practical use of the analysis one must be able to assign a value to the modulus of the subgrade reaction for the particular soil structure with which [one] is concerned. At the time the investigation was undertaken no determinations of the value of such a soil coefficient had been made, so there was no background of experience in testing that would indicate either the probable range of values of the coefficient or a procedure by which values might be obtained. Therefore, it was necessary to devise a test procedure that would indicate how the soil of the subgrade beneath the test sections behaved when subjected to pressure intensities and vertical deformations of the same order as occur under pavement slabs in service." [18]

Teller and Sutherland acknowledged that ideal dense liquid behavior was not likely to be observed in real soils:

"The ideal subgrade assumed by Westergaard is perfectly elastic, has uniform properties at all points and its vertical deformation varies as a linear function of the vertical pressure exerted on its surface. Such a subgrade probably does not exist and the problem becomes one of how nearly the soil under a given pavement approaches the ideal and what stiffness coefficient [i.e., k value], if any, can reasonably be assigned to it for the purpose of applying the method of analysis to a particular problem." [18]

Three alternatives were considered for measuring k values:

1. Load-displacement tests using "rigid circular plates of relatively small size,"
2. Load-displacement tests using "slightly flexible rectangular or circular plates of relatively large dimensions," and
3. "Load-deflection tests on full-size pavement slabs in which the load-deflection data are obtained by measurement and used in the Westergaard deflection formulas to provide values for the soil stiffness coefficient or 'modulus of subgrade reaction.' " [18]

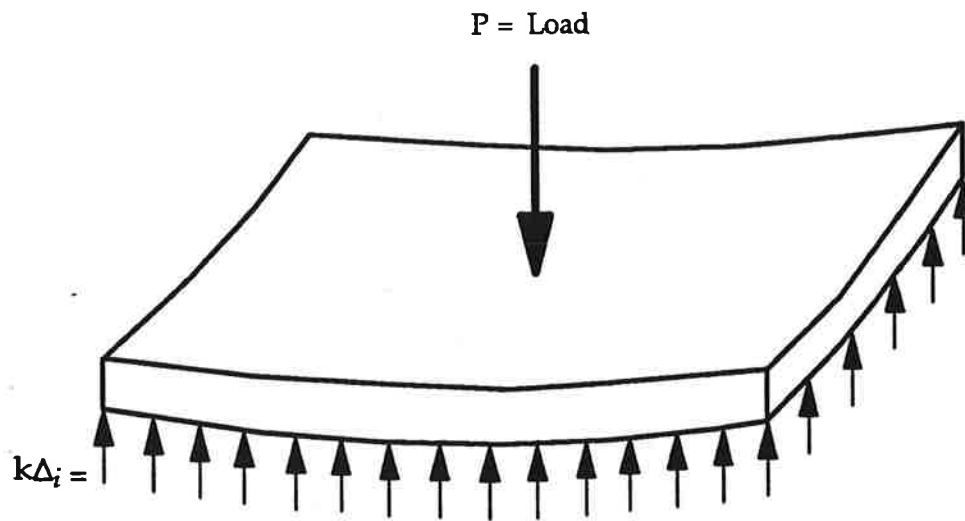
The Arlington researchers felt that testing with small rigid plates more practical than testing with large flexible plates (because it required lighter loads and fewer deflection measurements), but was not without limitations:

"The first [complication] is that the ability of a soil to sustain a given unit pressure varies within limits with the area over which the pressure is applied to the soil. This variation may be quite marked and this makes it necessary to determine the effect of size of plate in order to avoid error from using a bearing plate that is too small. The second complication is that the supporting ability of the soil varies with its moisture state and it is necessary, therefore, to take special precautions to insure that the soil on which the bearing plate is placed is in the same physical state and moisture condition as that which will obtain or does obtain under the pavement to be considered." [18]

The first method (rigid plate testing) and third method (full-size slab testing) were employed at Arlington to investigate necessary test procedures which would produce compatible results from the two methods. The second method (large flexible plate testing) was not employed at Arlington because "it has a certain theoretical appeal but offers considerable practical difficulty as a method of test." [18] Teller and Sutherland explained that when this method is used, the shape of the deflected plate must be measured precisely "in order to be able to estimate accurately the volumetric displacement of the soil that is effected by the application of the test load on the plate. The modulus of subgrade reaction is then computed by dividing the load (in pounds) by the volume of displaced soil (in cubic inches)." [18] These remarks allude to the fact that the subgrade k may be defined either as the ratio of applied pressure to uniform deflection or as the ratio of applied force to deflected volume. The volumetric definition of k , illustrated in Figure A-2, was later employed by the Corps of Engineers for interpretation of deflection measurements of full-size slabs.

The subgrade soil at the Arlington Test site was a uniform brown silt loam (AASHTO classification A-4). The subgrade in the area used for the plate bearing tests was prepared in the same manner as the area in which the experimental concrete slabs were cast. To maintain the moisture content in the tested subgrade at the same level as the subgrade beneath the slabs, the larger sizes of plates were cast in place of concrete, and concrete slabs 4 ft [1.2 m] square were cast on the subgrade and moved temporarily as needed to conduct bearing tests with the smaller steel plates. Four series of tests were conducted:

1. Circular plates of 8, 12, 16, 20, and 36 inches [203, 305, 406, 508, and 914 mm] diameter and a rectangular plate 48 inches [1219 mm] square were used with



$$\Sigma F = 0$$

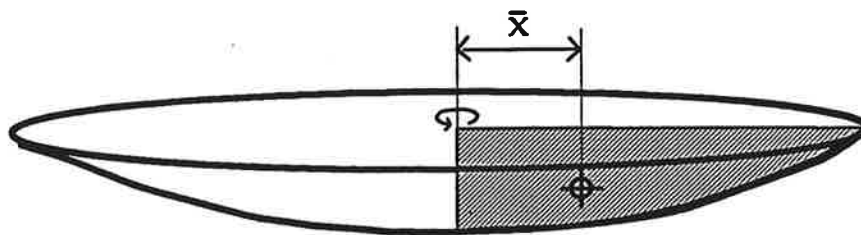
$$P = \Sigma k\Delta$$

$$= k \Sigma \Delta$$

$$= k V$$

$$k = P / V = \text{Force} / \text{Volume}$$

$$\bar{x} = \text{distance to centroid} = \frac{\Sigma A_i x_i}{\Sigma A_i}$$



$$\text{Volume} = \text{Area} \cdot 2\pi \cdot \bar{x}$$

Figure A-2. Schematic illustration and calculation of k from deflected volume.

loads sufficient to produce deflections in the range of 0.01 to 0.05 inch [0.254 to 1.27 mm], which was considered the range of concrete pavement slab deflections under truck wheel loads. This series of tests was conducted in two ways: with successively smaller plates at the same location, and with the different plate sizes at different locations. The purpose of this series of tests was to investigate the effect of plate size and to compare tests at one location with tests at different locations.

2. Circular plates of 2, 4, 6, 8, 12, 16, 20, 26, 36, 54, and 84 inches [51, 102, 152, 203, 305, 406, 508, 660, 914, 1372, and 2137 mm] were used to test at different locations, again producing deflections from 0.01 to 0.05 inch [0.254 to 1.27 mm]. The purpose of this series of tests was to explore further the effect of plate size.
3. Circular plates of the same sizes as in the second series of tests were used to produce deflections of about 0.25 inch [6.35 mm]. The purpose of this series of tests was to compare with the results from tests at lower deflection levels.
4. One circular 54-inch [1372-mm] plate was left in place at one location and used in tests in June and in January. The purpose of this series of tests was to study the effect of seasonal variation on the load-bearing ability of the soil.

Teller and Sutherland described the loading method used in the tests:

"For each size of bearing plate a series of 3 to 5 ascending load values was selected, such that the series would give a good spread of displacement values and the maximum would not produce a displacement greater than the desired limit. With the smallest load value selected for a plate of a

given size, the load was applied and removed several times. The number of applications was not constant but was determined by the character of the data, it being desired to reach a condition such that each succeeding application of a given load would produce the same vertical displacement of the bearing plate. This might be termed a state of approximate elastic equilibrium. The number of loadings required to develop this condition ... usually varied from about 5 to 10. When a satisfactory load-displacement relation had been determined for the lowest load value, the procedure was repeated with the next higher load level and so on until the displacement limit was reached." [18]

Figure A-3 is an example load-displacement plot for the repetitive loading procedure described above. The k value was determined by dividing the plate pressure at a given load level by the elastic deflection at equilibrium.

The load-deflection tests clearly showed the effects of plate size and displacement magnitude on k , as shown in Figure A-4 and summarized below:

"It appears that when making tests to determine the value of the soil stiffness coefficient k it is necessary to limit the deformation to a magnitude within the range of pavement deflection and that it is of great importance to use a bearing plate of adequate size." [18]

Teller and Sutherland concluded that plate bearing tests for k value should be conducted with rigid plates of fairly large diameter (48 to 60 inches [1219 to 1524 mm]), and displacements not exceeding 0.2 to 0.3 inch [5.1 to 7.6 mm].

1 in = 25.4 mm, 1 lb/ft² = 47.85 Pa

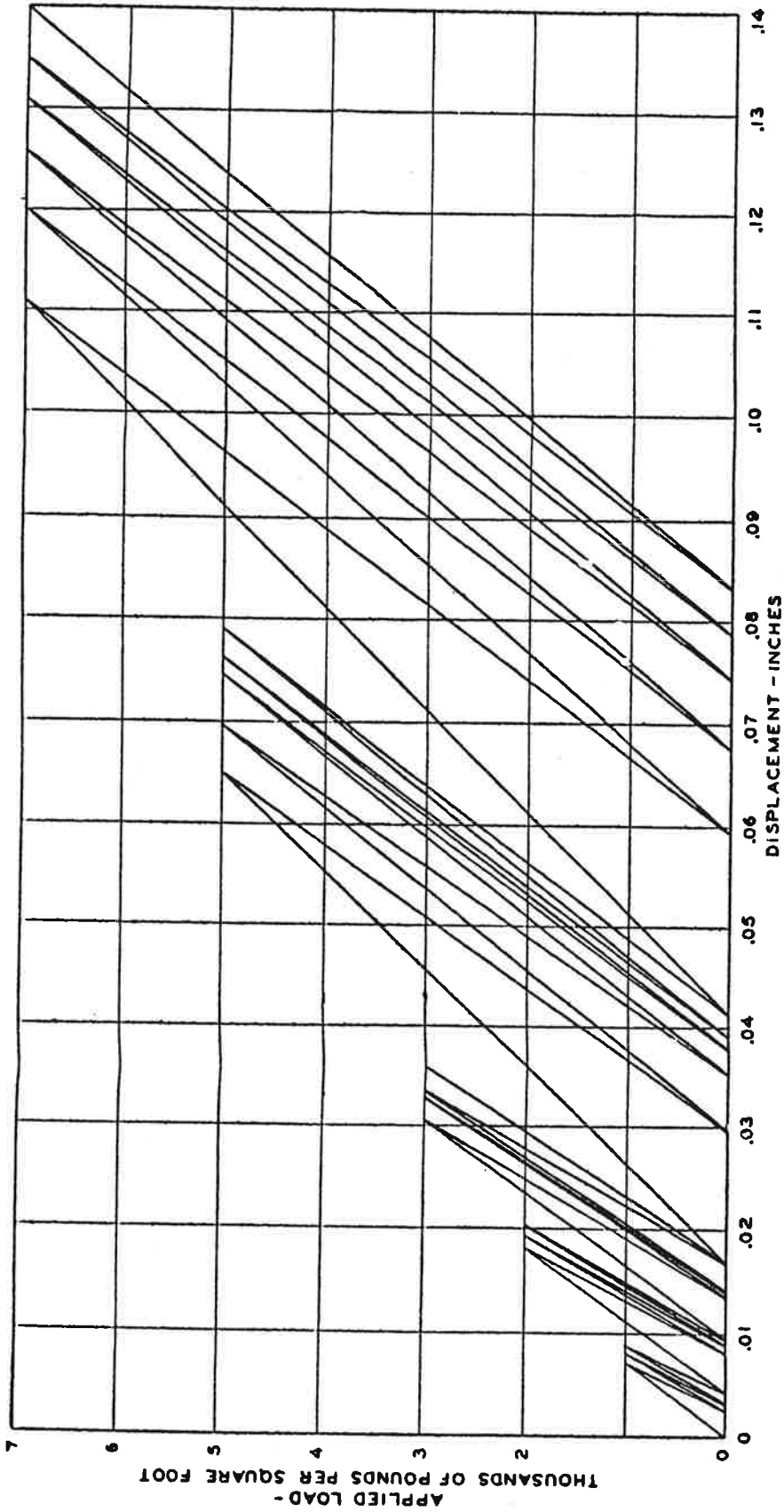


Figure A-3. Typical load-displacement data from Arlington plate tests. [18]

1 in = 25.4 mm, 1 lb/in³ = 0.27 kPa/mm

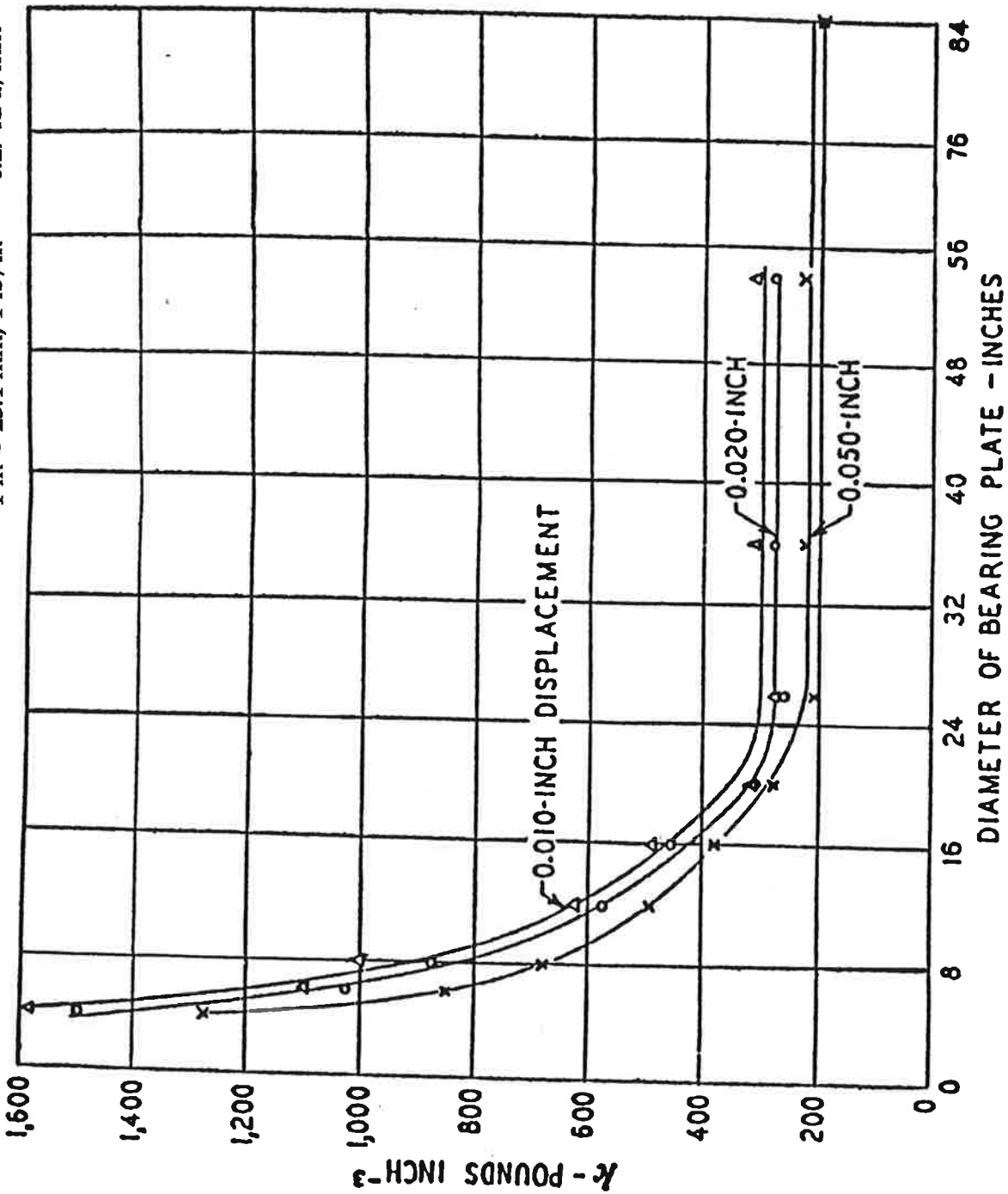


Figure A-4. Effect of load size and deflection magnitude on k . [18]

Teller and Sutherland also commented on the time-dependent nature of subgrade deformation: when a given load was applied to a bearing plate, displacement of the plate "may continue for a long time before a state of complete equilibrium is reached," i.e., before deflection ceased. In the Arlington tests, the deflections recorded for a given load level were those measured after the load had been maintained for five minutes, since it was not considered practical to wait until deflection had completely stopped. The load was then removed and five more minutes were allowed to elapse before another load was applied.

Deflection testing was also conducted on concrete slabs in the Arlington tests to experimentally verify the stresses and deflections predicted by Westergaard's equations. This verification included the first "backcalculation" of subgrade k values and slab E values from deflections measured on top of concrete slabs under interior, edge, and corner loading conditions. Radius of relative stiffness values were determined by matching slab deflection basin measurements to contours developed by Westergaard [9] for deflection versus distance from load. This required preparing two-dimensional diagrams of the deflection basins, and varying both the horizontal and vertical scales until the measured deflection basins matched the theoretical basins as closely as possible. The results of the backcalculation of k and E from interior, edge, and corner deflections are shown in Table A-1 and summarized below:

"For a given slab thickness, values of the radius of relative stiffness, l , are in good agreement for the three cases of loading [interior, edge, and corner]. For conditions that are comparable there is rather good agreement also between the values of the modulus of subgrade reaction, k , as determined by pavement deflection, for the interior and edge loadings but

Table A-1. Subgrade k values and concrete elastic moduli backcalculated from slab deflections at Arlington Road Test. [18]

Load Position	Season	Slab Thickness, in	Subgrade k value, psi/in	Concrete E, psi
Interior	Late summer	6	195	4,140,000
	Winter	7	238	5,750,000
	Summer	7	222	4,670,000
	Winter	8	260	5,500,000
	Late fall	8	203	5,490,000
	Summer	9	220	4,210,000
			MEAN:	223
Edge	Late summer	6	171	4,235,000
	Winter	7	212	5,125,000
	Winter	8	279	5,175,000
	Late fall	9	243	5,220,000
			MEAN:	226

Notes:

Plate bearing k values for 30-in [762 mm] plate, 0.05 in [1.27 mm] deflection: 166 psi/in [44.8 kPa/mm] in January to 233 psi/in [62.9 kPa/mm] in June.

Static concrete E from laboratory flexural tests on specimens cut from slabs: 4,500,000 psi [31005 MPa] for specimens dried 12 months in normal laboratory environment to 6,000,000 psi [41340 MPa] for specimens immersed in water for 10 months at laboratory temperature.

1 inch = 25.4 mm, 1 psi = 6.89 kPa, 1 psi/in = 0.27 kPa/mm

the value for the corner is consistently lower. This is believed to be the result of incomplete contact between the corner area and the subgrade and is in accord with the evidence of the strain data... The general level of values of k from the bearing plate tests is in reasonably good agreement with that determined from pavement deflections... The values of the modulus of elasticity for the concrete, E , as determined from the slab deflections are in the same general range as the values that were obtained from the tests of the laboratory specimens." [18]

Thus, the k values determined from repeated loads on a 30-in [762 mm] plate at a deflection at 0.05 in [1.27 mm] appeared to give k values which agreed well with those backcalculated from deflections induced by loads on top of concrete slabs.

Seasonal Variation in k Value

Using one plate size, the Arlington researchers also investigated the effect of seasonal variation in moisture content on k values measured by plate bearing tests. The results are illustrated in Figure A-5. The moisture content of the subgrade was 17 percent during the summer testing, and higher during the winter testing: 25 percent in the upper 6 inches [152 mm] of the subgrade, and 19 percent at depths of 6 to 12 inches [152 to 305 mm]. [18] At each displacement magnitude, the lower summer moisture content corresponded to a 40 to 50 percent increase in k value.

Effect of Displacement Level on K Value

Figure A-5 also illustrates the different k values obtained at different displacement levels. In June, for example, k values from 315 to 233 psi/in [85.1 to 62.9 kPa/mm] were obtained for displacements from 0.01 to 0.05 in [0.25 to 1.27 mm].

1 in = 25.4 mm, 1000 lb = 4.45 kN

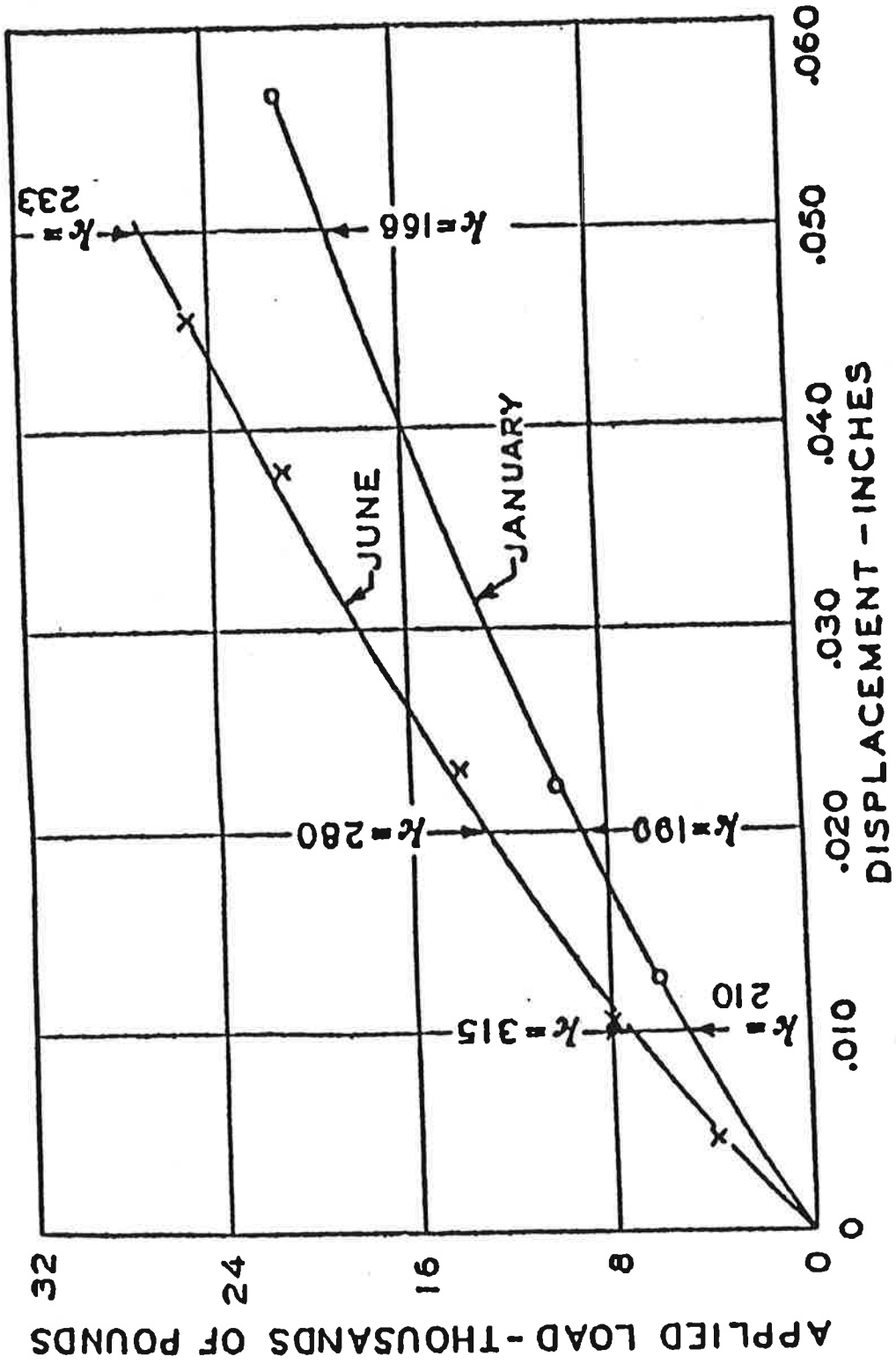


Figure A-5. Effect of seasonal variation and deformation level on k value. [18]

Effect of Slab Curling and Corner Support on Corner k Values

Deflections were measured at slab corners when the corners were curled up, flat, and curled down. The total vertical displacement of the corners was observed to "vary considerably with the degree of support afforded the loaded corner, being approximately three times as great for the upward warped corner as for the same corner brought into better contact with the subgrade by downward warping." Teller and Sutherland concluded:

"It is believed that ... because the measured apparent deflections of the slab corner contain displacements from causes other than flexure, such measurements are not suitable for use in determining the value of the several coefficients [l , k , E , etc.] previously discussed. One possible exception is the value of the radius of relative stiffness, l , which is determined more by coincidence of curve shapes than by absolute deflection magnitude. Because of this, values of l determined from corner loadings are in good agreement with values determined from interior and edge loadings for all four slab thicknesses." [18]

Effect of Subgrade Improvement on k Value

Teller and Sutherland described some rather surprising results concerning plate load tests on modified subgrade. In 1940, a concrete pavement was constructed at the same location where slabs used in Teller and Sutherland's original experiments had been. However, prior to the new construction, "the character of the subgrade had been altered by mixing sand with the original silty loam to a depth of several inches and recompacting." [18] Since plate load tests on the original subgrade had

shown that plate diameters in excess of 30 inches [762 mm] were sufficient to yield consistent k values, the modified subgrade was tested with a 36-inch [914 mm] plate.

The k value obtained was 400 psi/in [108 kPa/mm], whereas the k value of the original subgrade had been about 280 psi/in [75.6 kPa/mm] for summer conditions. Testing on the modified subgrade with a larger (54-inch [1372 mm]) plate yielded a smaller increase in k value (315 psi/in [85.1 kPa/mm]). After a concrete slab was constructed on the modified subgrade, the k value backcalculated from slab deflections was found to be 285 psi/in [76.9 kPa/mm], "considerably lower than that indicated by the bearing tests with the 36-inch [914 mm] diameter rigid plate but essentially the same as that found for the original unmodified subgrade under similar summer conditions." [18] Teller and Sutherland offered the following explanation:

"It is indicated that in modifying the character of the upper layer of the subgrade ... its load supporting ability within a given deformation limit was considerably increased so long as the given unit load was applied over a relatively small area. When the loaded area was relatively large, as with the slab deflection test, on the other hand, the influence of the strengthened upper layer on the load support offered by the subgrade as a whole tended to disappear." [18]

Effect of Loads and Temperature on Total Slab Stress

A summary of the findings of the Arlington experiments was written by Kelley in 1939. [19] Kelley pointed out that the stresses produced in concrete slabs by the combined effects of wheel loads and temperature variation could be much greater than the stresses predicted by Westergaard's equations for wheel loads only, and that

for short slabs (e.g., less than 17 ft [5.2 m] for $k = 100$ psi/in [27 kPa/mm] and less than 13 ft [4.0 m] for $k = 300$ psi/in [81 kPa/mm]), temperature curling stresses actually increase with increasing k value:

"Variations in the value of the subgrade modulus have no significant effect on the [temperature curling] stresses in long slabs. However, for short slabs increases in the value of the subgrade modulus result in considerable increases in the computed stresses... This effect of the subgrade modulus on temperature stresses is the reverse of its effect on stresses due to wheel loads where low values of the modulus give higher stresses than do high values." [19]

These observations are reasonable if one imagines that the stiffer the foundation is, the less a curled slab can settle into the foundation, thus the greater proportion of the slab area will be unsupported by the foundation, and thus the higher the slab stresses will be. Nonetheless, the idea of total slab stress increasing with k value is somewhat difficult to accept if one is accustomed to thinking of k value only in terms of its effect on stresses due to traffic loads.

Kelley felt that a default k value of 100 psi/in [27 kPa/mm] was a somewhat conservative value which still provided a tradeoff between load and curling stresses. If the actual k value of a subgrade was higher than the assumed value, for example, the stress equations would overestimate the load stress and underestimate the curling stress. However, consideration of curling stresses has not been a part of concrete pavement design practice in the fifty or more years after Kelley's recommendations were published, although curling stresses certainly have been significant to the performance of concrete pavements.

CORPS OF ENGINEERS FIELD STUDIES

In 1941, the Corps of Engineers (as it is now called) conducted static and dynamic load tests on concrete slabs constructed at Wright Field in Ohio. [20, 21, 22] One of the objectives of the Wright Field slab tests was to develop a standard procedure for determining subgrade k values. The need for such a procedure was summarized by Sale in 1977:

"Except to state that the subgrade modulus '... may be determined empirically -- for a given subgrade by comparing the deflections found by tests of full-sized slabs with the deflections given by the formulas...'

Dr. Westergaard never suggested a test method for determining the k value. This lack of definition has through the years caused Corps' researchers and, we believe, many others considerable concern." [23]

The experiments the Corps conducted at Wright Field to develop a k value test were described by Sale and Hutchinson in 1959 [22]:

"The test slabs were instrumented with deflection and strain gages so that the failure loads could readily be related to the Westergaard theory.

Through the entire range of increment loads leading to the development of the first structural break in the pavement slabs, a check was maintained on the volumetric displacement of the subgrade beneath the slab. From this determination the modulus of subgrade reaction could be established. A series of plate loading tests were made on each subgrade condition in order to determine the size of plate which would yield a k value that most

closely checked the value obtained from the volumetric subgrade displacement under the test slabs. Circular plates ranging in diameter from 12 to 72 inches [305 to 1829 mm] were used in this study and almost without exception tests made with a 30-inch [762 mm] diameter plate gave results that were in close agreement with the subgrade displacement determination. As would be expected smaller plate sizes gave higher values and larger plate sizes gave smaller values. Thus was born the basic procedure for establishing a design k-value with a 30-inch [762 mm] diameter plate bearing test that is still used in Corps of Engineers pavement design with only minor modification." [22]

A detailed description of the development of the Corps' standard plate bearing test method was provided by Phillippe in a 1948 ASTM symposium on bearing capacity of soils. [24] Phillippe reported that the plate load data and slab deflection data analyzed by the Corps "indicate reasonable correlation between the k values determined by the 30-in-diameter [762 mm] plate at 0.05 in [1.27 mm] deflection and the static loading of full scale concrete pavement slabs." The Corps subsequently modified its test procedure to (1) determine k at a pressure of 10 psi [68.9 kPa] rather than a deflection of 0.05 in [1.27 mm], (2) use stacked plates to minimize plate bending, and apply a correction for plate bending when necessary, and (3) to assess "soaked" k values based on laboratory tests on saturated and unsaturated subgrade samples. [25]

The Corps carried out additional field tests of concrete pavements at Lockbourne, Maxwell, McDill, and other airfields. [24, 26, 27] The k value results obtained in these later tests were consistent with those obtained at Wright Field:

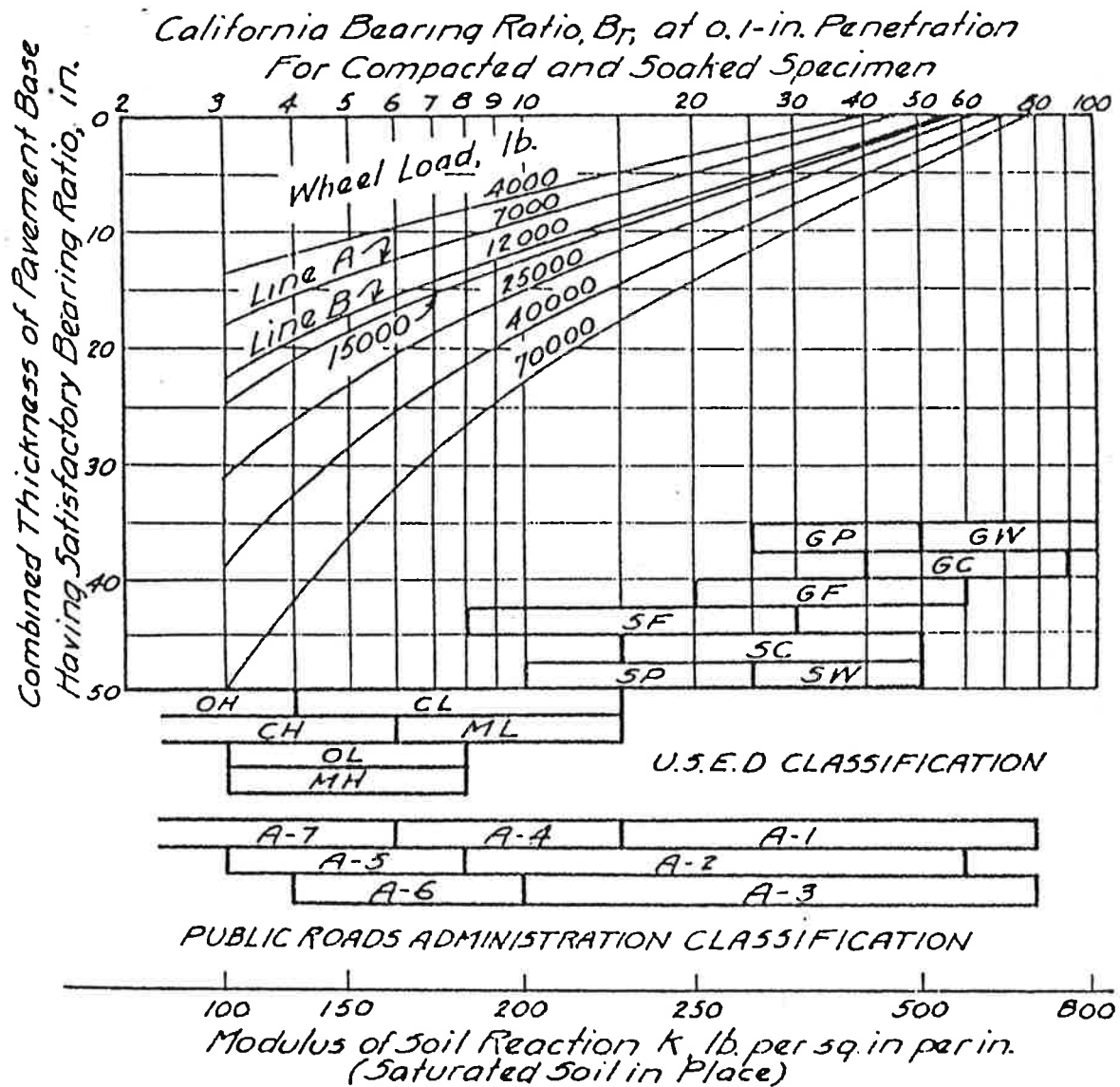
"Responding to the continual growth of military aircraft during the 1940's and 1950's and the attendant increase in pavement thickness, the Corps has repeatedly questioned and subjected to test the continued applicability of the standard 30-in [762 mm] plate bearing test.

"Surely the geometry of a Model T Ford automobile on a 5- or 6-in [127 or 152 mm] concrete slab in 1926 would bear little resemblance to a 360,000-lb [1602 kN] C-5A 12-wheel loading gear on a 20-in [508 mm] concrete slab today. Yet the Corps, in every major airfield pavement test program carried out since 1941 has found the procedures for determining the subgrade modulus developed in conjunction with the Wright Field Slab Tests to be essentially representative of the values obtained by the load-deflection tests of full-size slabs or the so-called volumetric k.

"The only exception to this pattern is the high k value obtained on moderate base course thicknesses which generally must be adjusted downward to match full-size slab performance." [23]

Correlation of K Value and CBR and Soil Classification

In 1942, Middlebrooks and Bertram [28] published a paper summarizing many aspects of the Corps of Engineers' subgrade studies, including perhaps the first published correlation of k value to California Bearing Ratio (CBR) and to the Unified and Public Roads (now AASHTO) soil classification groups. These correlations are illustrated in Figure A-6, and summarized below.



1 in = 25.4 mm, 1 psi/in = 0.27 kPa/mm

Figure A-6. Correlation of k value, CBR, and soil classification. [28]

"You will note that the k values range from 100 [27 kPa/mm] for the fat clay to approximately 800 [216 kPa/mm] for an excellent well-graded gravel. These values are considered only approximate, although to date some very good checks have been obtained. However, they are not considered close enough for use in construction in this country, where there is sufficient time available for a more accurate determination of the k values." [28]

An important detail of the Corps of Engineers' k value test method on which these correlations are based is the selection of 0.05 in [1.27 mm] as the deflection at which k is defined. The Corps' plate bearing test procedure does not involve repeated loading and unloading, as was done at the Arlington Road Test, so it is reasonable to ask whether the k value obtained from the Corps' test procedure is an "elastic" k, or whether it includes both elastic and plastic deformation. It is a significant question because Figure A-6 formed the basis for correlation charts and tables which, with some modifications, were later incorporated in the U. S. Army's technical manuals [29, 30] and the Portland Cement Association's design manuals for highway and airport concrete pavements [31, 32], and which have been widely used ever since. An example of an early PCA table relating Bureau of Public Roads and Unified soil classes to k values is shown in Figure A-7.

Phillippe [24] and Middlebrooks and Bertram [28] state that the deflection value of 0.05 in [1.27 mm] was selected because many tests indicated that this deflection corresponded to k values which agreed with the k values obtained from deflection testing on full-size slabs. If one presumes that k values calculated from slab deflections represent elastic response of the subgrade, then one may conclude that the k value obtained from the Corps' definition (at a deflection of 0.05 in

Major divisions	Soils groups and typical description	Subgrade group symbol	Approximate range of <i>k</i> -values for each soil group
Gravelly and sandy soils	Well-graded gravel-sand-clay. Excellent binder. Sand-clay mixtures. Excellent binder.	A-1	400-700 or greater
	Gravel with fines, very silty gravel, poorly graded gravel-sand-clay and sand-clay mixtures. Poor binder. Friable.	A-1	250-575
	Poorly graded clayey gravels, gravel-sand-clay and sand-clay mixtures. Inferior binder. Plastic.	A-2, Friable	300-700 or greater
	Well-graded gravel, gravel-sand mixtures, and sands. Little or no fines.	A-2, Plastic	175-325
	Poorly graded gravel, gravel-sand mixtures and sands. Little or no fines.	A-3	325-700 or greater
		A-3	200-325
Fine-grained soils in which silt sizes predominate.	Predominantly silty soils with moderate to small amounts of coarse material and small amounts of plastic clay. Poorly graded silty soils which contain mica and diatoms and which have elastic properties	A-4	100-300
		A-5	50-175*
Very fine-grained organic and inorganic soils in which clay fraction governs.	Clay soils with moderate to negligible amounts of coarse materials. Includes well-graded inorganic silt-clay, sand-silt-clay and sand-clay soils.	A-6	50-225
	Elastic clay soils with moderate to negligible amounts of coarse materials. Usually poorly graded or contains organic or other materials which make them elastic.	A-7	50-225

* Some soils of volcanic origin may have *k*-values greater than those shown for this group.

Major divisions	Soil groups and typical description	Subgrade group symbols	Approximate range of <i>k</i> -values for each soil group
Gravel and gravelly soils	Well-graded gravel and gravel-sand mixtures. Little or no fines.	GW	500-700 or greater
	Well-graded gravel-sand-clay mixtures. Excellent binder. Poorly graded gravels and gravel-sand mixtures. Little or no fines.	GC	400-700 or greater
	Gravel with fines, very silty gravel, clayey gravel, poorly graded gravel-sand-clay mixtures.	GP	300-500
		GF	250-500
Sands and sandy soils	Well-graded sands and gravelly sands. Little or no fines.	SW	250-575
	Well-graded sand-clay mixtures. Excellent binder.	SC	250-575
	Poorly graded sands. Little or no fines.	SP	200-325
	Sand with fines, very silty sands, clayey sands, poorly graded sand-clay mixtures.	SF	175-325
Fine-grained soils having low to medium compressibility	Silts (inorganic) and very fine sands, mo, rock flour, silty or clayey fine sands with slight plasticity. Clays (inorganic) of low to medium plasticity, sandy clays, silty clays, lean clays.	ML	150-300
		CL	125-225
	Organic silts and organic silts of low plasticity.	OL	100-175
Fine-grained soils having high compressibility	Micaceous or diatomaceous fine sandy and silty soils, elastic soils.	MH	50-175
	Clays (inorganic) of high plasticity, fat clays.	CH	50-150
	Organic clays of medium to high plasticity.	OH	50-125

G = gravel
S = sand
M = mo, very fine sand, silt, rock flour
C = clay
O = organic
W = well-graded
P = poorly graded
L = low to medium compressibility
H = high compressibility
F = fines, material smaller than 0.1 mm. diameter

Figure A-7. Bureau of Public Roads and Unified soil classes versus *k* values. [82]

[1.27 mm] is the equivalent of an elastic k , and thus that the correlations shown in Figure A-6 are correlations of CBR and soil classification to an elastic k value.

EFFECT OF BASE LAYERS ON K

In the 1940s, numerous reports appeared in the literature concerning plate load tests on subgrades and on base layers. One of many examples is the report by Campen and Smith of plate load tests at several airports in Nebraska and Iowa. [33] The results were summarized in tables which showed increase in load-bearing value of the subgrade per inch of superimposed thickness of base material. Another example is the report by Hittle and Goetz on the effect of soil type, base type, base thickness, and seasonal moisture variation on the load-carrying capacity of various base-subgrade combinations. [34] McLeod presented similar results from several years of testing at several Canadian airports, including plate load tests on natural subgrades, granular bases, and bituminous surfaces. [35] These and other studies of the time illustrate a developing trend to consider base layers as an effective means of improving subgrade k values, and to consider this improvement as a function of base thickness and base material.

The Corps of Engineers also apparently changed its position on the effect of base layers on k value during this time. As Ahlvin describes in his report on the historical development of the Corps' pavement design procedures [36], airfield pavements were constructed directly on natural subgrades throughout the 1940s, but base materials came into use in the early 1950s to combat pumping. However, the Corps also began to attribute an improved k value to the base. "Limited early experience," Ahlvin states, "had been interpreted to indicate that subbase or base under rigid pavement had no structural advantage," a conclusion which is consistent

with Sale's description of the results of the Wright Field Tests. In the 1950s, however, the Corps modified its design practice to require plate bearing tests on top of bases. This led eventually to development of curves for top-of-base k value:

"As the use of base courses continued, manual guidance directed use of the plate-bearing test on top of the emplaced base for determination of the k-value. This practice continued into the 1970s.

"However, late in the 1950s there was a need for guidance, for evaluation purposes, in assessing the contribution of base courses to improve the subgrade k-value without requiring plate tests. Accordingly curves were developed ... which related k at the surface of the base to base thickness and subgrade k. These have been included in engineer manual doctrine as an alternate to direct plate testing." [36]

Ahlvin's historical review does not mention any attempts by the Corps to validate the base k value curves by deflection testing on top of concrete pavements. Had this been attempted, the results obtained earlier at the Arlington and Wright field tests might have been reaffirmed and the erroneous concept of top-of-base k value might not have been perpetuated.

ASTM PLATE BEARING TEST METHODS

The first standard ASTM tests methods for plate bearing tests on soils were published in 1952. Two tests, based largely on the Corps of Engineers procedure, were published: D 1195, Repetitive Static Plate Load Test, and D 1196, Nonrepetitive

Static Plate Load Test. These two tests have changed very little since they were originally published. The steps in the repetitive testing procedure are described briefly below for illustration. Details of the test procedures are given in Appendix B.

1. Set the bearing plate level in a thin bed of a mixture of sand and plaster of Paris, or plaster of Paris alone, or fine sand.
2. Center the bearing plate of the selected diameter under the jack assembly. Set the remaining plates of smaller diameter concentric with and on top of the bearing plate.
3. After the equipment has been arranged, seat the plate by the quick application and release of a load sufficient to produce a deflection of not less than 0.01 in [0.254 mm].
4. Apply a load sufficient to produce a deflection of about 0.04 in [1 mm], start a stopwatch, and maintain the load until the rate of change of deflection is no more than 0.001 in [0.0254 mm] per minute for three successive minutes.
5. Release the load and observe the rebound deflection until the rate of recovery is less than 0.001 in [0.0254] per minute for three successive minutes.
6. Apply and release the same load in this manner six times.
7. Increase the load to a level sufficient to produce a deflection of about 0.2 in [5 mm], and proceed as before.
8. Increase the load to a level sufficient to produce a deflection of about 0.4 in [10 mm], and proceed as before.
9. Plot the corrected deflection at which the rate of change of deflection is exactly 0.001 in [0.0254 mm] per minute versus the number of repetitions of the corrected load.

10. Similar graphs may be prepared in which corrected residual deflection and rebound deflection are plotted versus the number of repetitions of each corrected load.

Further details on these plate bearing test methods are given in Appendix B. Interestingly, neither test method gives any guidance on calculation of the subgrade k value from the load and deflection data obtained. Calculation of k value is covered in the Corps of Engineers test method, and in the AASHTO test methods T221 and T222, which were not standardized until the 1960s.

AASHTO ROAD TEST

This major field test was conducted by the Highway Research Board between 1958 and 1960, near Ottawa, Illinois. The AASHTO Road Test is documented in great detail in a series of Highway Research Board reports and many related documents. [37, 38, 39, 40, 41, 42, 43, 44]

Subbase and Embankment Material Properties Studied

Detailed investigations of base and subgrade properties and their variation throughout the seasons were conducted at the road test. Plate load, CBR, moisture content, and density tests were made on the subbase and the embankment.

Figures A-8 and A-9 illustrate the seasonal trends observed in subgrade moisture content, dry density, CBR, and plate load k_E (described further below). The data shown in Figure A-8 were collected from trenches cut in the flexible pavement tangent of Loop 1, the untrafficked loop. Figure A-9 shows similar data collected from the Loop 1 rigid tangent. Trends of increasing CBR and k_E with decreasing moisture content are noticeable, particularly for 1959.

1 lb/ft³ = 16.02 kg/m³, 1 psi/in = 0.27 kPa/mm

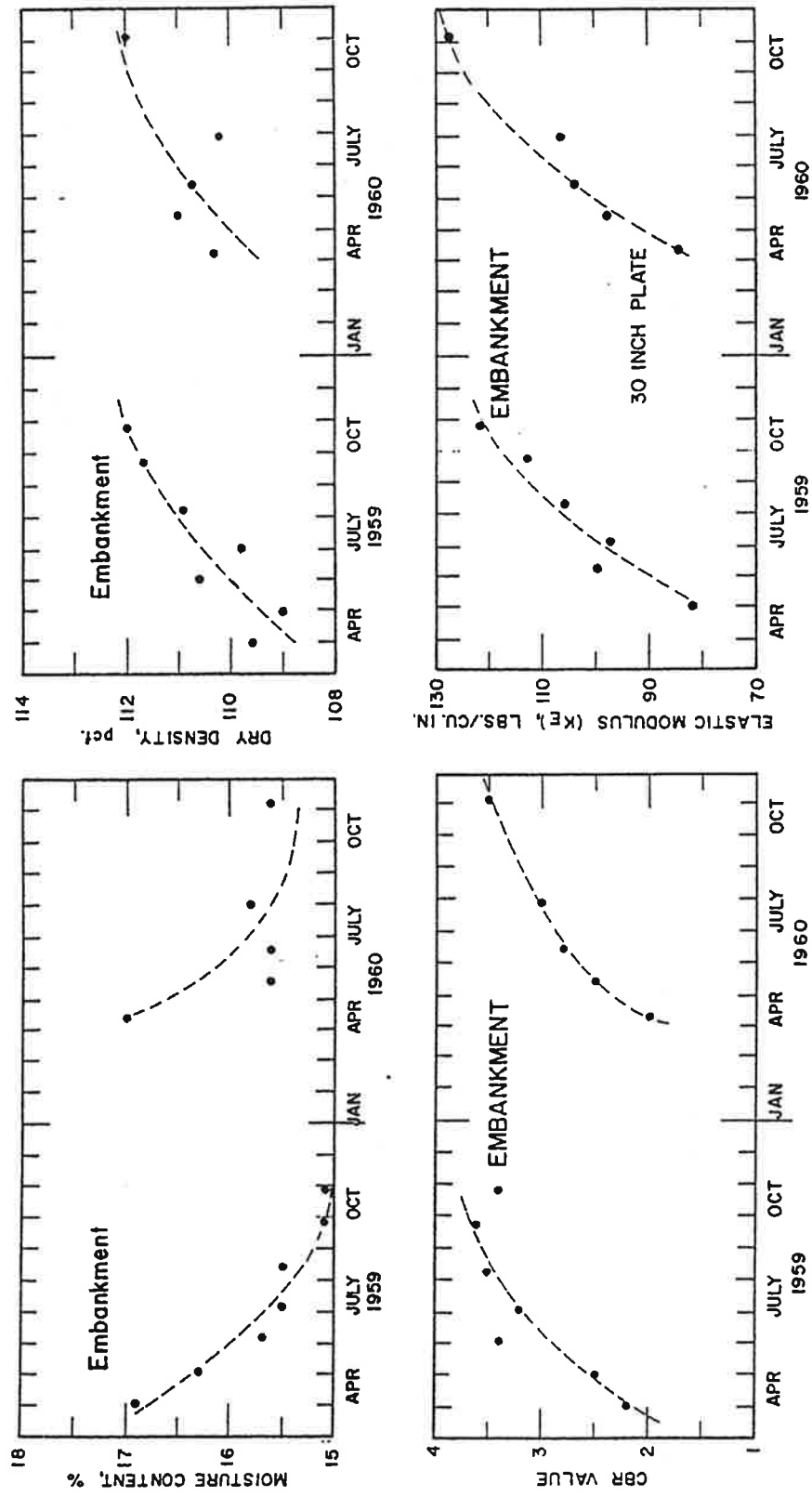


Figure A-8. Seasonal variation in moisture content, dry density, CBR, and k_E AASHO Road Test Loop 1 flexible tangent data. [41]

1 lb/ft³ = 16.02 kg/m³, 1 psi/in = 0.27 kPa/mm

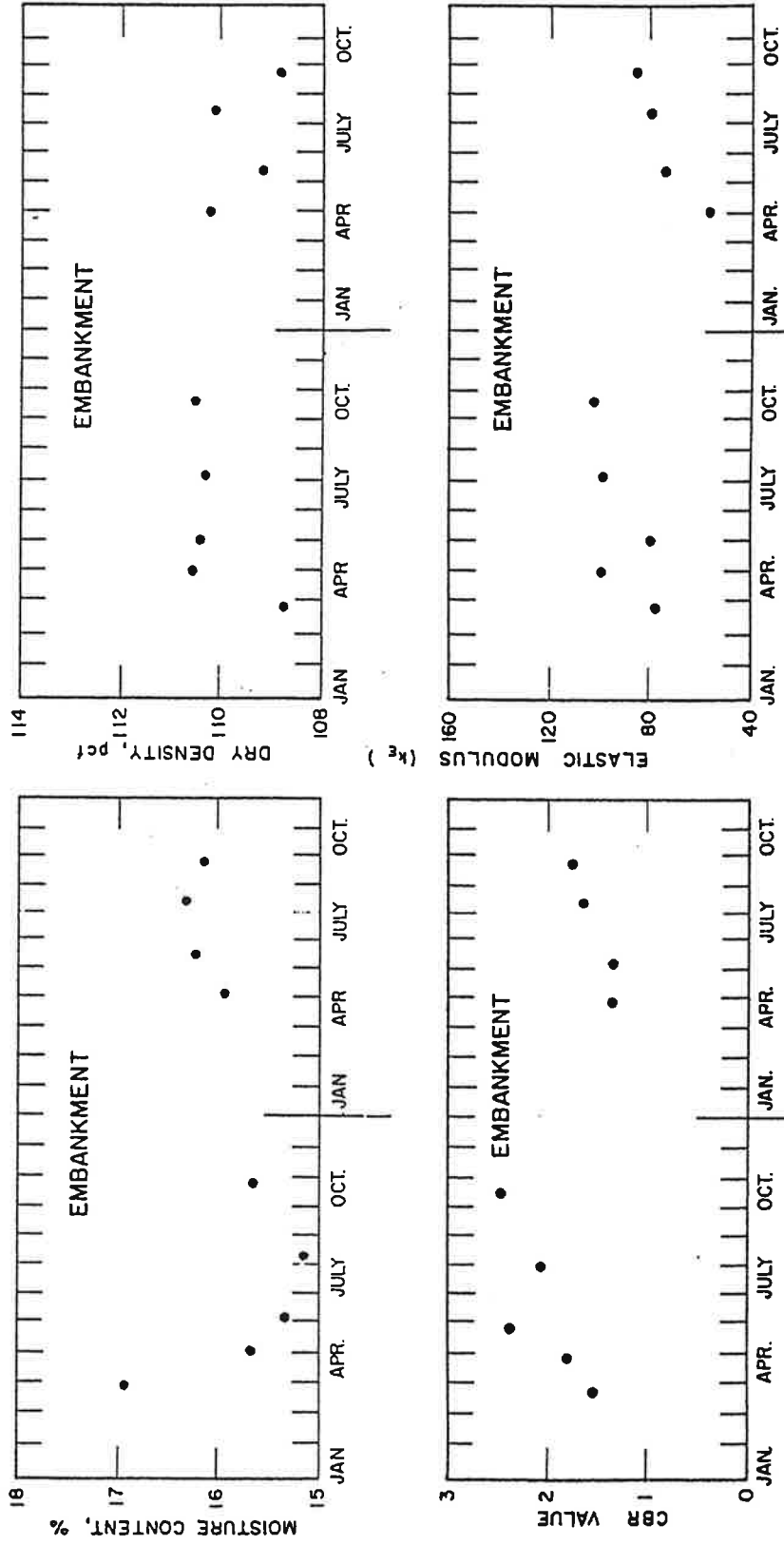


Figure A-9. Seasonal variation in moisture content, dry density, CBR, and k_E AASHO Road Test Loop 1 rigid tangent data. [41]

Figure A-10 illustrates the relationships of k_E to dry density, moisture content, and percent saturation, based on data from trenches cut in the main traffic loops. Although no relationship between k_E and dry density is evident, k_E shows some tendency to decrease with increasing moisture content. A clearer trend of decreasing k_E with increasing percent saturation (which represents a combination of dry density and moisture content) is evident. The same is true for CBR versus percent saturation.

Plate Bearing Test Procedure

At the time of the Road Test, AASHO did not have standard test methods for plate bearing tests, and the test procedure used did not conform to the ASTM or Corps of Engineers standards. The procedure, which was similar to that used at the Arlington Road Test, involved the following steps: [41]

1. The test area was covered with fine silica sand and leveled by rotating the plate. Sand was not used for testing on pavement surfaces when the pavement surface was level.
2. The loading equipment, shown in Figure A-11, was set in place.
3. A seating pressure of 2 psi [13.8 kPa] was applied and released. Dial gages were set to zero.
4. The first increment of pressure (5 psi [34.5 kPa] for the 30-inch [762 mm] load plate) was applied and held 15 seconds, and the dial gage was read.
5. The load was released and the dial gage read at the end of 15 seconds.
6. The load was reapplied and released in the same manner three times.
7. Steps 4 through 6 were repeated for the second and third increments of load (10 and 15 psi [68.9 and 103.3 kPa] for the 30-inch [762 mm] load plate).
8. Gross and elastic deflections were computed from the dial gage readings.

1 lb/ft³ = 16.02 kg/m³, 1 psi/in = 0.27 kPa/mm

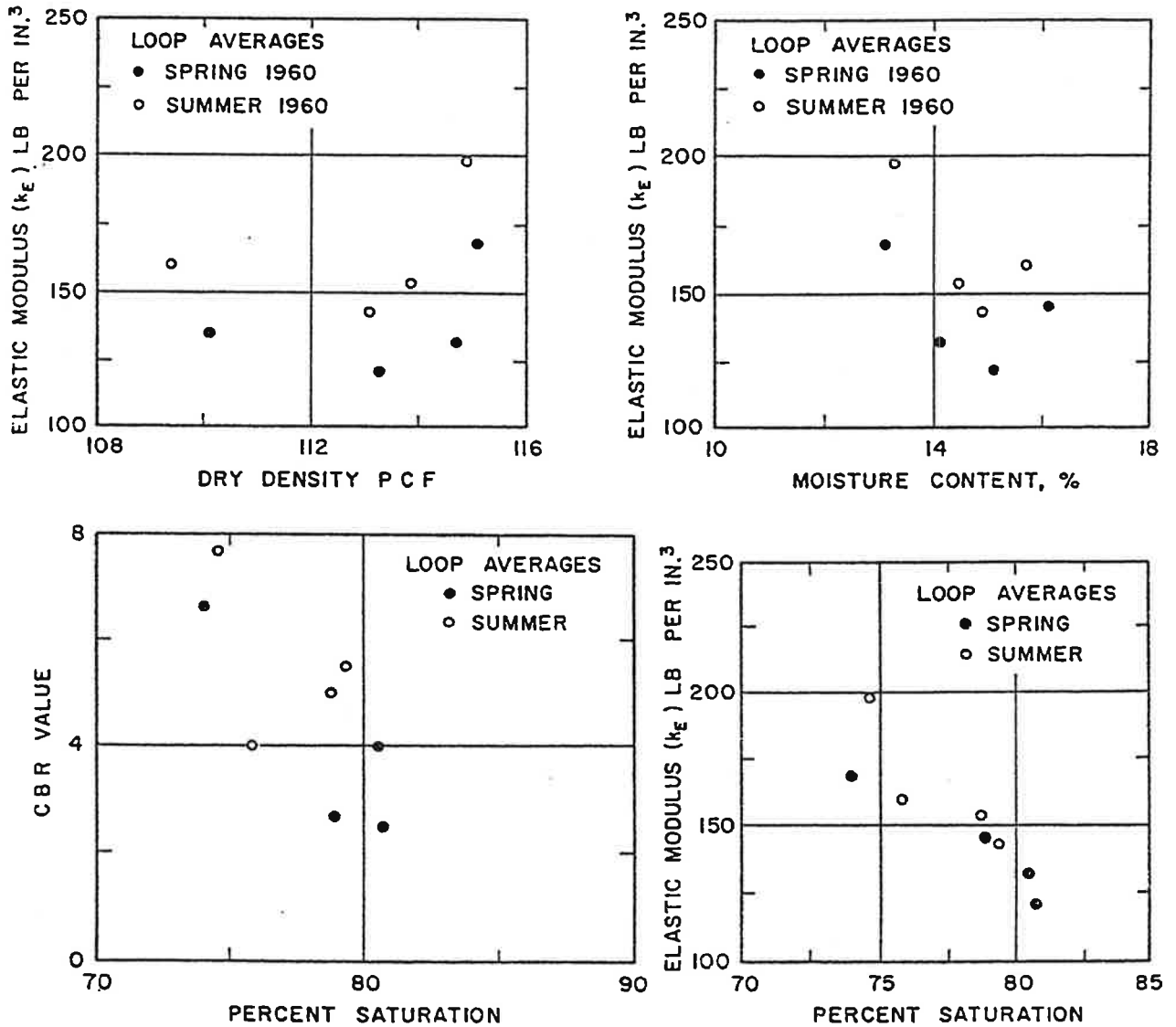


Figure A-10. Effect of moisture and density on k_E and CBR, AASHO Road Test main loop data. [41]

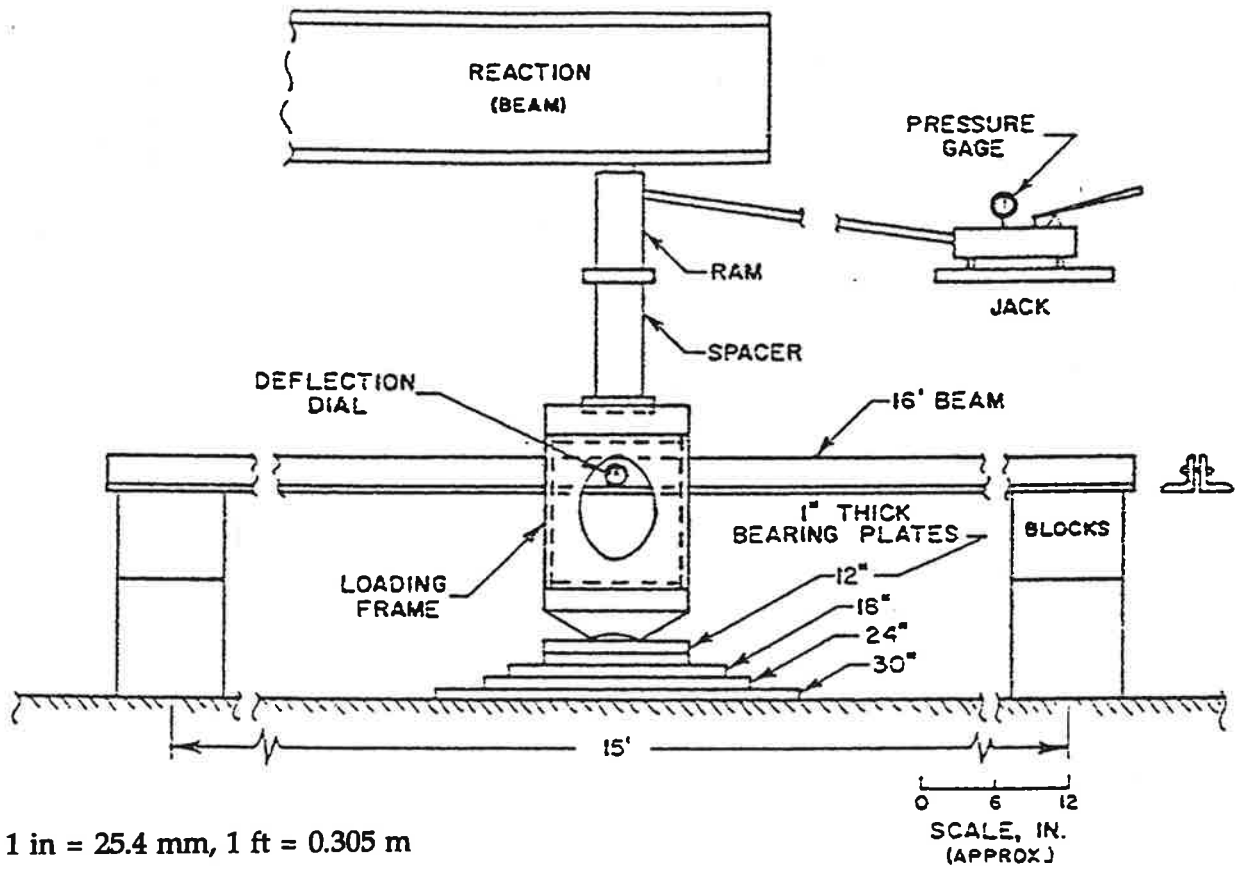


Figure A-11. Plate load test apparatus used at AASHO Road Test. [41]

Elastic K Value and Gross K Value

The following description of calculation of k values from the plate load test data was given:

"Values of k_E were computed as follows: (a) Elastic k-value: k_E = the unit load divided by the elastic deformation at each application of the incremental load. The reported k_E was an average of all nine of these computations; (b) Gross k-value, k_G = the unit load divided by the maximum gross deflection. The reported k_G was an average of all three of these computations." [41]

A schematic illustration of the load-deflection results obtained from the plate load tests is shown in Figure A-12. The following explanation was given for the k_G calculation:

"Because in rigid pavement design the modulus k_G is more commonly used than the elastic modulus k_E , data obtained from the trench studies in Loop 1 (in both flexible and rigid pavement sections) were used to develop a correlation between k_E and k_G ." [41]

As shown in Figure A-13, the average ratio of k_E to k_G was 1.77. The remark quoted above is curious, because no confirmation has been found in the prior literature that gross k values determined in the manner employed at the AASHO Road Test were commonly used in design. On the contrary, the elastic k value was recommended by the Bureau of Public Roads after the Arlington Road Tests, and the

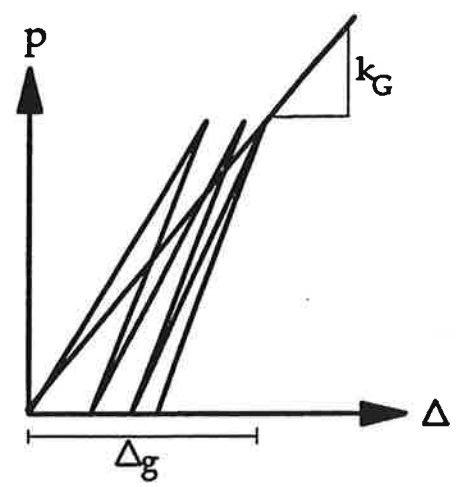
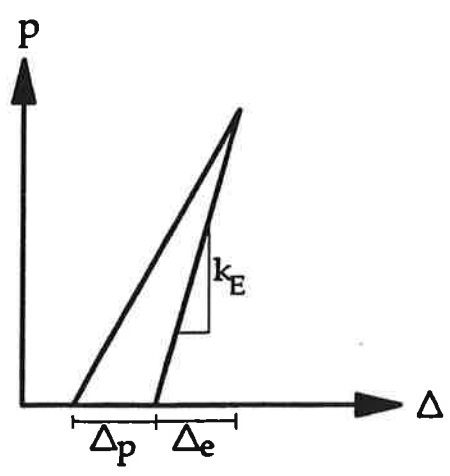
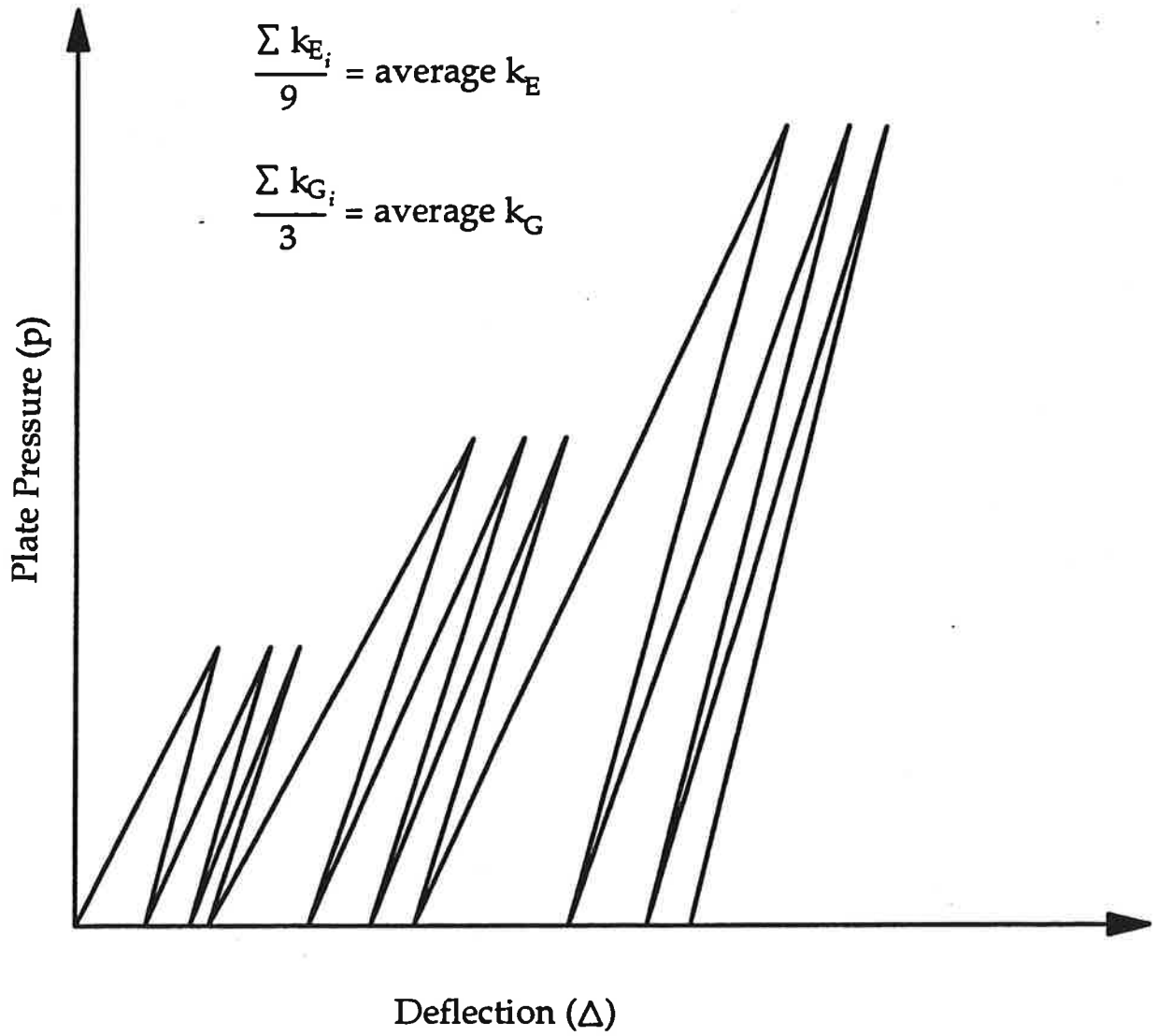


Figure A-12. Schematic illustration of AASHO Road Test plate load test results.

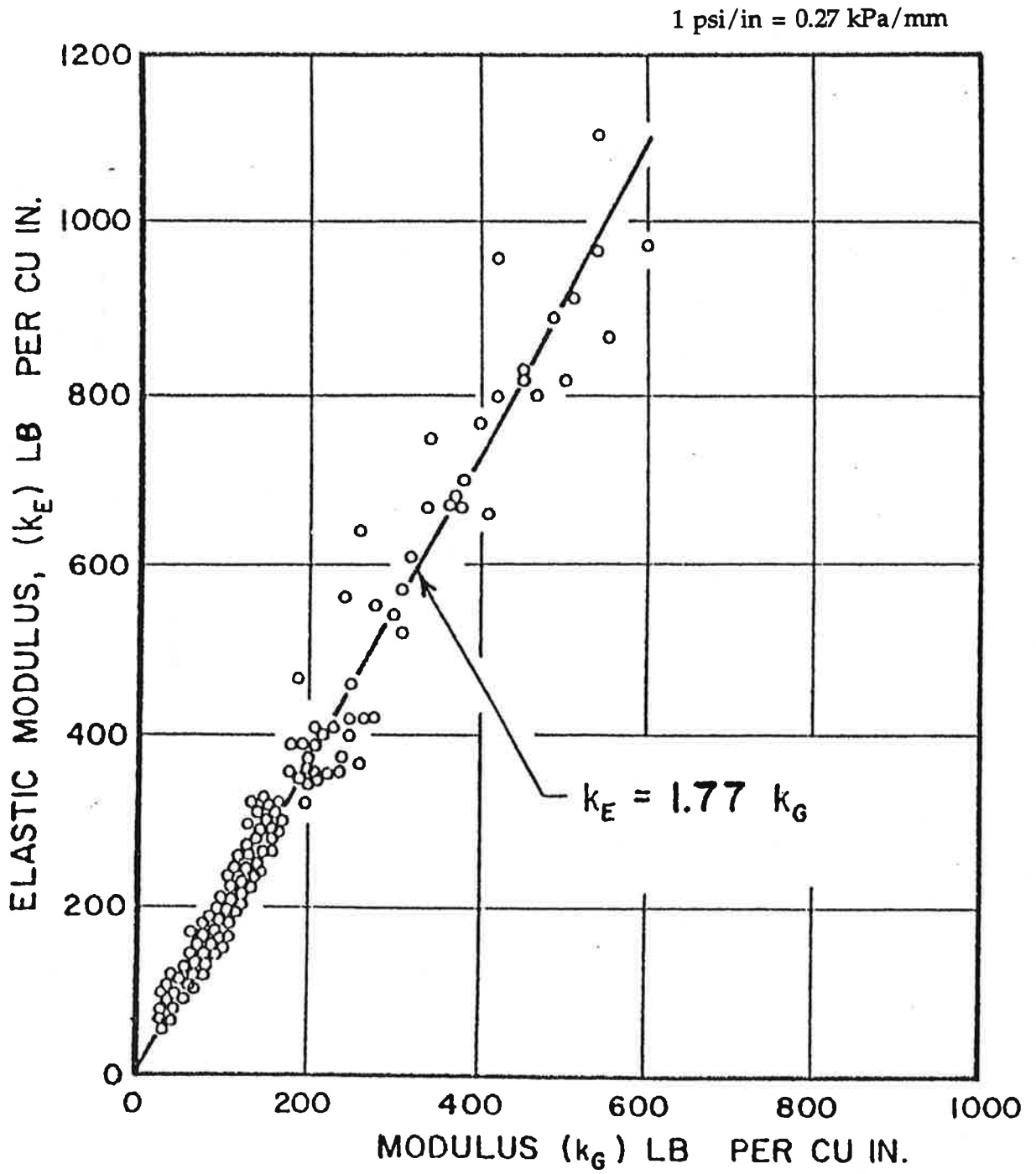


Figure A-13. Correlation of k_E and k_G , AASHO Road Test data. [41]

k values obtained from the Corps of Engineers test method can also be presumed to represent the elastic k value. However, because the Corps of Engineers method for determining k value is a nonrepetitive test, one might presume that the AASHO Road Test researchers felt that the gross k was more representative of the k obtained in a nonrepetitive test than the elastic k. This presumption is reinforced by the recommendations for k given by the AASHO Committee on Design in 1962:

"The modulus of subgrade reaction is the gross k_G determined in the Road Test, which is the value commonly used in design. It may be determined by test following the procedure specified in ASTM Designation: D 1196-57, using a 30-in [762 mm] diameter plate. It has been common practice to estimate the modulus of subgrade reaction." [45]

In April and May of 1960, trenches were cut in several sections of pavement in the main trafficked loops 3 through 6 to test the subbase and embankment. The sections in which the trenches were cut had reached terminal serviceability. The k_E values obtained are shown in Table A-2.

A k value of 60 psi/in [16.2 kPa/mm] was used to represent AASHO Road Test conditions in the development of the AASHO rigid pavement design equation. [45] This value, as Table A-2 shows, is equivalent to the mean springtime gross k value from tests on top of the subbase. It is almost as conservative a value as could possibly have been picked to represent the Road Test conditions. The only more conservative value would have been the springtime gross k value of 49 psi/in [13.2 kPa/mm] on top of the subgrade. Why the subbase k_G was selected rather than the subgrade k_G is not documented.

Table A-2. AASHO Road Test k values from spring trenching program. [39]

Layer	Inner Wheelpath k_E , psi/in	Outer Wheelpath k_E	Average k_E	k_G
Subbase	107	109	108	61
Embankment	85	87	86	49

Notes: k_G values obtained by dividing k_E values by 1.77
 1 psi/in = 0.27 kPa/mm

In 1962, the Corps of Engineers conducted load tests on top of the existing slabs at the AASHO Road Test site and backcalculated k values from the deflection basins measured. [46] According to Hudson, the value of 60 psi/in [16.2 kPa/mm] was in reasonably good agreement with k values from measurements made on full-sized slabs. [47] According to Vesic and Saxena, the volumetric k values calculated by the Corps ranged from 25 to 97 psi/in [6.75 to 26.2 kPa/mm]. [48]

PORTLAND CEMENT ASSOCIATION

In the 1960s, the Portland Cement Association (PCA) conducted a series of laboratory experiments with full-sized concrete slabs. These experiments included plate load tests on prepared subgrade soils, untreated gravel and crushed stone bases, cement-treated subbases, and soil-cement pavements. [49, 50, 51] Example k value results from tests on untreated granular bases and cement-treated bases are shown in Figure A-14.

The plate tests on top of the granular bases yielded slightly higher k values than the subgrade plate tests, but the plate tests on the cement-treated bases yielded

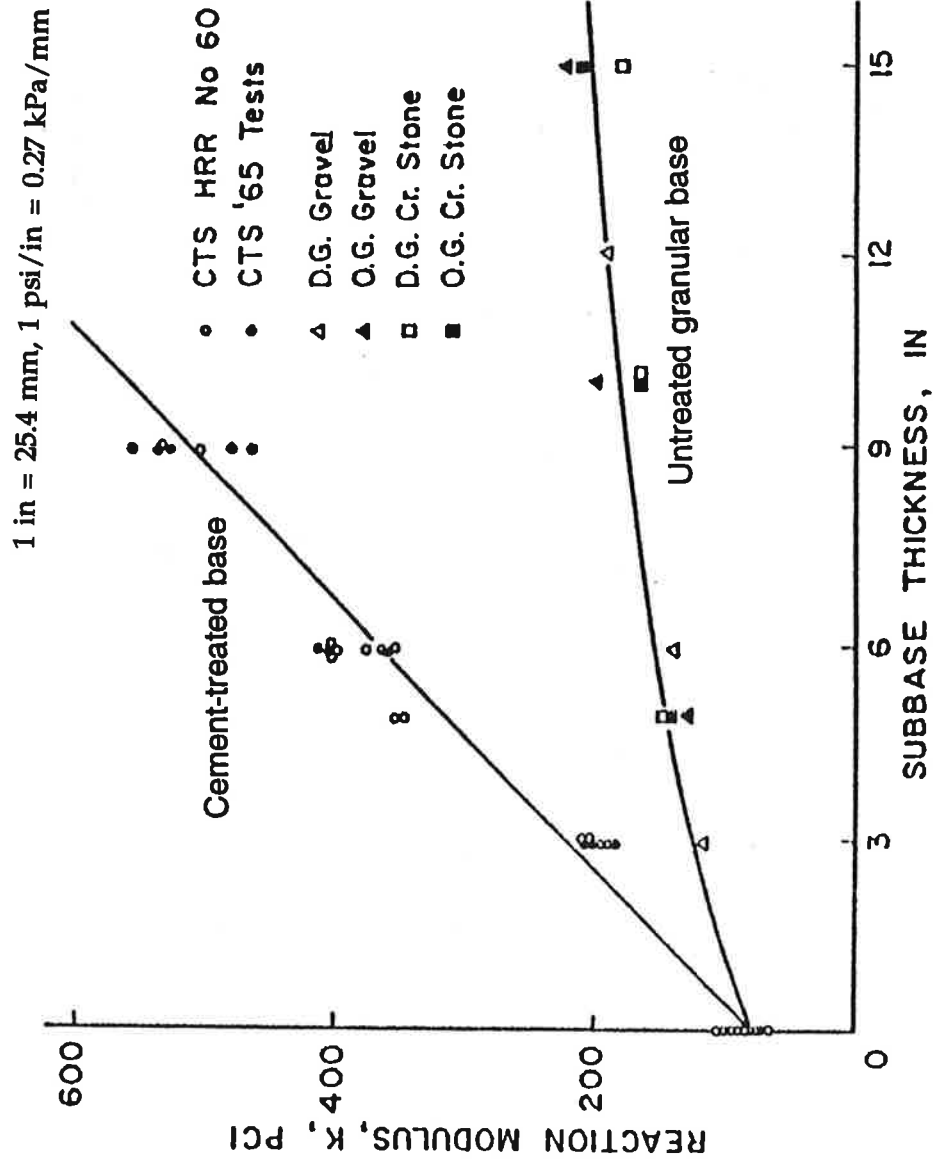


Figure A-14. Results of PCA plate tests on granular and cement-treated bases. [50]

considerably higher k values, which increased linearly with cement-treated base thickness. Subsequent load tests on concrete slabs constructed on the cement-treated bases showed a decrease in maximum edge and interior deflections with increasing base thickness:

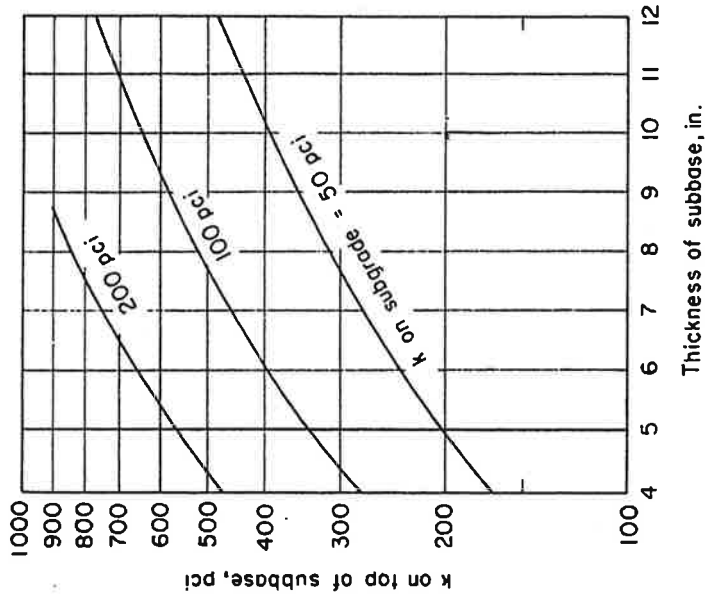
"Although it is known that small changes in k are not of consequence in thickness design, the large increases achieved by the use of cement-treated material over those normally attained on granular materials are significant, and subsequent data from load tests on slabs demonstrate the degree to which load-carrying ability is increased." [50]

The PCA used these results to develop curves for top-of-base k values for granular and cement-treated bases, which were incorporated into PCA's concrete pavement design procedures and published in 1966. The base k value curves which appeared in PCA's 1973 design manual for concrete airport pavements [52] are shown in Figure A-15. The correlations between soil type, soil tests, and k values presented in PCA's design manual are shown in Figure A-16.

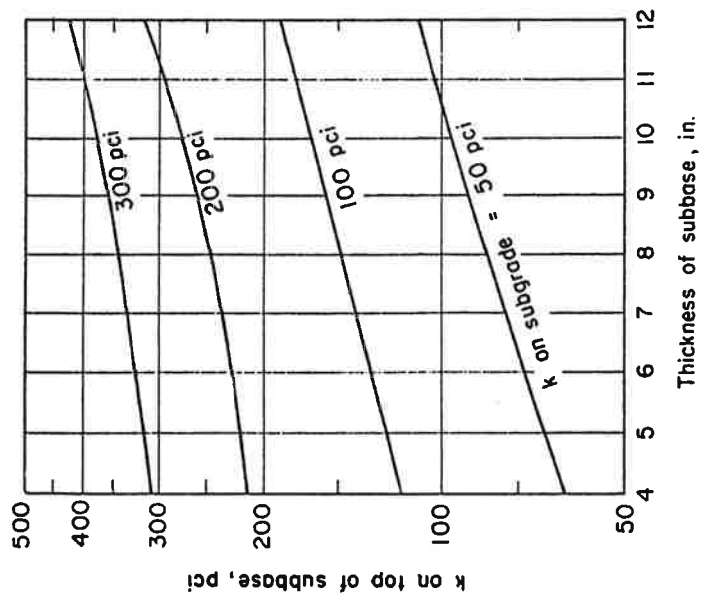
The PCA's 1973 design manual also provided insight into the AASHO Road Test k_E and k_G :

"The dense-liquid subgrade assumption results in computed stresses that are somewhat higher than measured stresses. This is true when the k_g value is used -- gross k determined from a nonrepetitive plate-load test such as ASTM D 1196. In the past, most designs have been based on the k_g value. The elastic k_e value, determined from repetitive plate-load tests

1 in = 25.4 mm, 1 psi/in = 0.27 kPa/mm

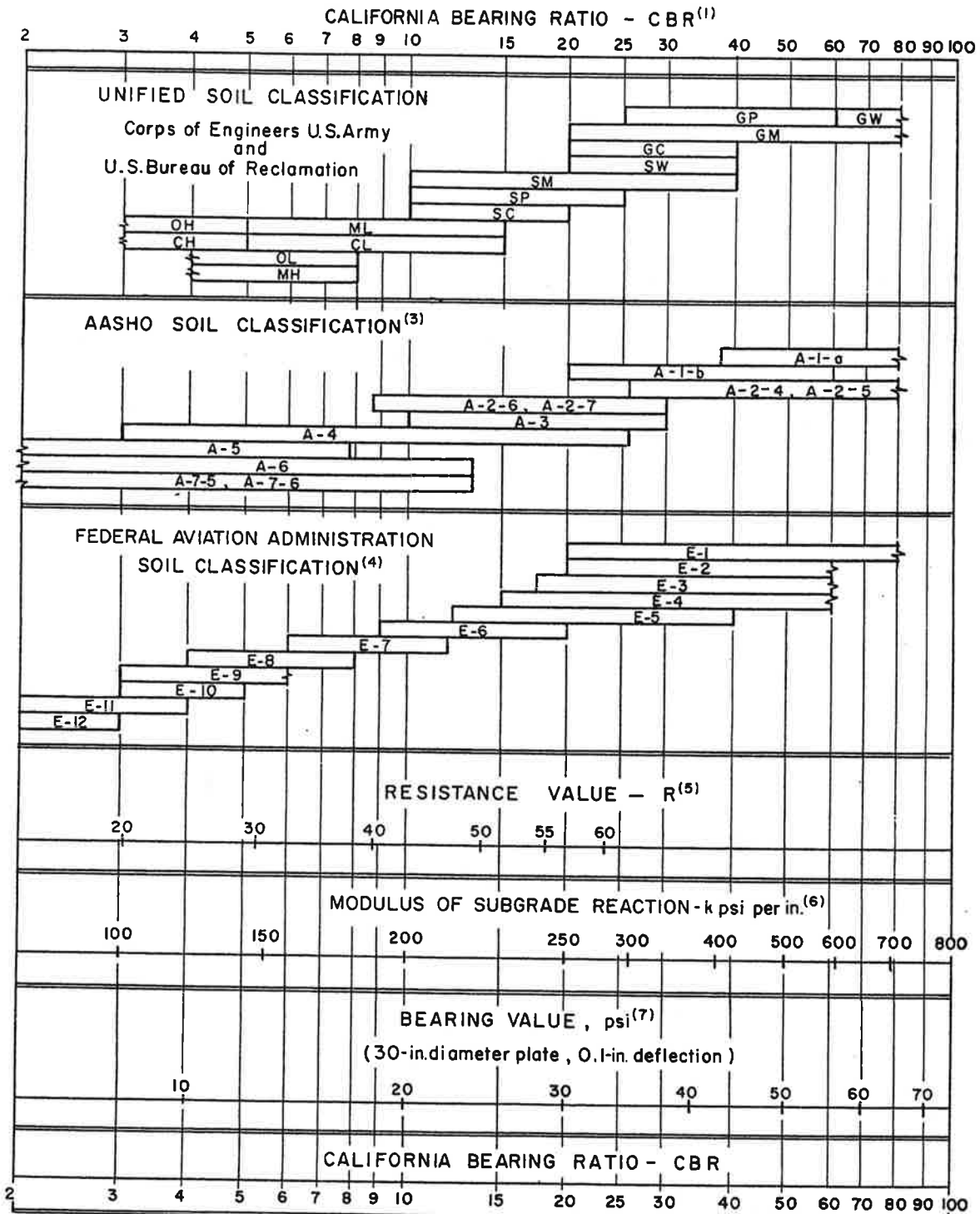


Effect of granular subbase thickness on k value.



Effect of cement-treated subbase thickness on k value.

Figure A-15. Base k curves from 1973 PCA airport pavement design manual. [52]



1 psi/in = 0.27 kPa/mm, 1 psi = 6.89 kPa, 1 in = 25.4 mm

- (1) For the basic idea, see O. J. Porter, "Foundations for Flexible Pavements," *Highway Research Board Proceedings of the Twenty-second Annual Meeting*, 1942, Vol. 22, pages 100-136.
- (2) "Characteristics of Soil Groups Pertaining to Roads and Airfields," Appendix B, *The Unified Soil Classification System*, U.S. Army Corps of Engineers, Technical Memorandum 3-357, 1953.
- (3) "Classification of Highway Subgrade Materials," *Highway Research Board Proceedings of the Twenty-fifth Annual Meeting*, 1945, Vol. 25, pages 376-392.
- (4) *Airport Paving*, U.S. Department of Commerce, Federal Aviation Agency, May 1948, pages 11-16. Estimated using values given in *FAA Design Manual for Airport Pavements*.
- (5) F. N. Hveem, "A New Approach for Pavement Design," *Engineering News-Record*, Vol. 141, No. 2, July 8, 1948, pages 134-139. *R* is factor used in California Stabilometer Method of Design.
- (6) See T. A. Middlebrooks and G. E. Bertram, "Soil Tests for Design of Runway Pavements," *Highway Research Board Proceedings of the Twenty-second Annual Meeting*, 1942, Vol. 22, page 152. *k* is factor used in Westergaard's analysis for design of concrete pavement.
- (7) See item (6), page 184.

Figure A-16. Correlations between k, soil type, and other tests. [52]

such as ASTM D 1195, is a higher value, since most of the inelastic deformation is eliminated in the repetitive test. At the AASHO Road Test,, a ratio of k_e to k_g of 1.77 was established for granular bases and clay subgrades. Use of such a k_e value would reduce theoretical stresses for aircraft loads by approximately 10 percent.. Although the more conservative k_g value is suggested for design purposes in this manual, it is recognized that the accumulation of information on the relation of k_e and k_g to design and performance of pavements will be valuable." [52]

The 1973 PCA manual also sheds light on the shift in defining plate load k values from those obtained at 0.05 in [1.27 mm] deflection to those obtained at 10 psi [68.9 kPa] pressure:

"The displacement of the bearing plate used in determining k should approximate the deflection of pavement slabs under expected wheel loads. The load-deformation ratio at a displacement of 0.05 in [1.27 mm] is generally used in determining k . However, the Corps of Engineers determines k from the deformation obtained under a 10 psi [68.9 kPa] load. When stabilized subbases are tested, the loading equipment may not be heavy enough to obtain a deflection of 0.05 in [1.27 mm]. Even if it were, the resulting pressure on the subbase may far exceed the pressures exerted under the slab by aircraft loads and would thus not represent service conditions. As a result, a maximum pressure of 10 psi [68.9 kPa] is recommended for plate loading tests on stabilized subbases." [52]

Base Effect on Radius of Relative Stiffness

The most intriguing aspect of the PCA's guidelines on effect of base layers on slab behavior is the procedure offered in an appendix for determining an adjusted ℓ value when a stiff base is present. The radius of relative stiffness or ℓ for a slab on grade was defined in Equation A-1. Note that the slab modulus and slab thickness are in the numerator and the subgrade k value is in the denominator. According to the PCA manual's recommendation to increase k when a base is present, the radius of relative stiffness would decrease. The alternate procedure suggests that the opposite result, an increase in ℓ , may be more realistic:

"Conventional methods of computing pavement response to loads, either by the dense-liquid subgrade assumption or the elastic-solid subgrade assumption, assume that the subbase and subgrade reaction is evaluated by a single modulus, k or E . By this assumption, the radius of relative stiffness, ℓ , is decreased when a subbase layer is used since the subbase and subgrade support is greater than that for the subgrade alone. This concept has satisfactorily given the approximate pavement response under past conditions of load configuration and pavement thickness.

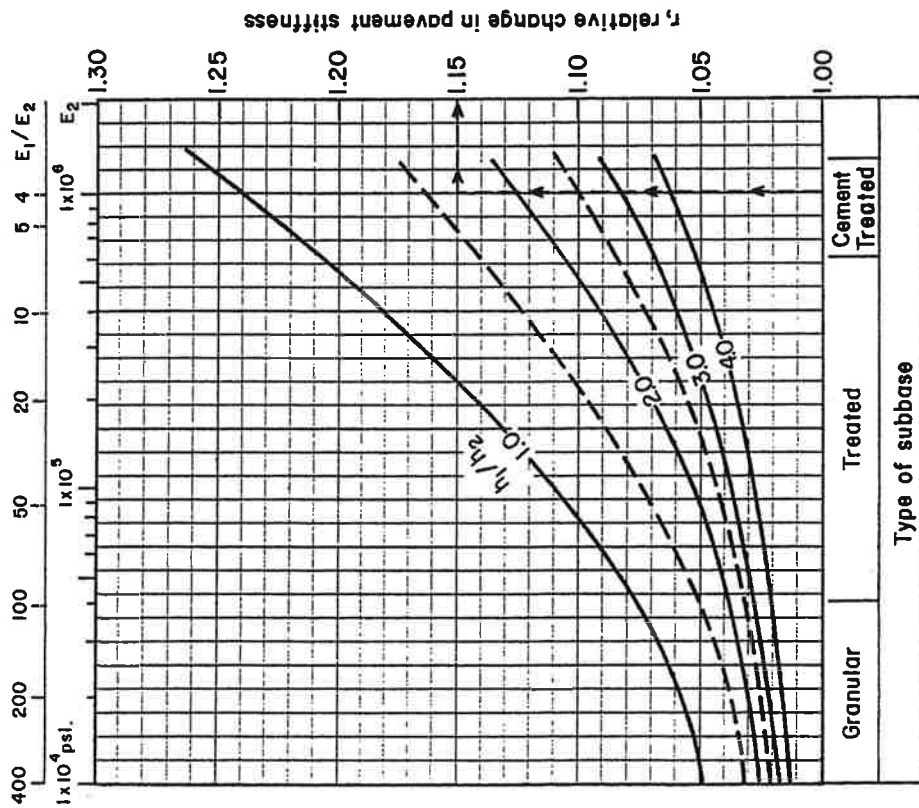
"When a subbase is used, especially a strong subbase, it is understood intuitively that the load-spreading capability of the pavement is increased -- in effect, that the radius of relative stiffness is increased... As a result, an adjustment in the design procedure has been developed and is recommended for use in heavy-duty pavement design." [52]

The appendix suggests that the two approaches to defining ℓ (combining the base with the k versus combining the base with the slab), although diametrically opposed in concept, produce reasonably similar results for thinner pavements, weak bases, and small load sizes. However, the latter approach was considered more appropriate for thicker pavements, stiffer bases, and larger load sizes (i.e., multiwheel aircraft gear configurations). The adjusted ℓ is calculated from the concrete-to-base stiffness ratio (E_1/E_2), the concrete-to-base thickness ratio (h_1/h_2), and the ℓ calculated for the concrete slab and subgrade k alone (from Equation A-1), using the chart shown in Figure A-17. The chart was derived from elastic layer theory and correlation to the PCA's subgrade and plate load test data.

Backcalculation of K from PCA Test Data

The load tests run on concrete slabs in the PCA experiments showed decreases in deflection with increasing thickness of cement-treated base, which was interpreted as being the result of an increase in the k value. These experimental results would then appear to be contrary to the statements quoted above concerning the effect of the base on increasing ℓ . However, the PCA studies did not report that any k values were backcalculated from the slab deflections to determine whether the top-of-base k values were confirmed.

This can be done using the deflection data reported in Reference 50, because elastic moduli are also reported for the concrete slabs and cement-treated bases. Three interface conditions were studied: full bond (denoted by B) achieved with a sand-cement grout, an SS-1 emulsion treatment (S), and no bond (N), attempted with a sheet of 4-mil [0.1 mm] polyethylene. The ratios of maximum deflections for the B versus the S and N cases indicate that the sections with unbonded (N) interfaces were



Boeing 747, gear load = 166,500 lb.
 Concrete slab, h_1 = 12 in., E_1 = 4×10^6 psi
 Cement-treated subbase, h_2 = 7 in., E_2 = 1×10^6 psi
 Clay subgrade, k_3 = 100 pci
 ℓ (no subbase) = 49.27 in.
 r , for h_1/h_2 = 1.7 = 1.15
 ℓ' = $r\ell$ = 1.15×49.27 = 56.7 in.

1 psi = 6.89 kPa, 1 lb = 4.45 kN,
 1 psi/in = 0.27 kPa/mm, 1 in = 25.4 mm

Figure A-17. PCA's alternate procedure for effect of base on ℓ . [52]

actually not unbonded, but had high degrees of friction producing deflections not much higher than the bonded interface. This explains the conclusion in Reference 50 that interface treatment was not a significant factor in load-bearing capacity.

The data for four test sections with bonded interfaces are provided in Table A-3. The k values were obtained from plate tests on the subgrade and cement-treated base. The concrete and base elastic moduli were obtained from beam tests.

Table A-3. Sections in PCA tests of slabs with cement-treated bases. [50]

Section	h_c in	h_{CTB} in	E_c million psi	E_{CTB} million psi	k_{sub} psi/in	k_{CTB} psi/in
5B6	5	6	5.1	1.3	79	435
5B9	5	9	5.1	1.5	70	580
7B6	7	6	5.3	1.1	71	380
7B9	7	9	5.1	1.4	93	535

Note: 1 in = 25.4 mm, 1 million psi = 6895 MPa, 1 psi/in = 0.27 kPa/mm

Using backcalculation equations developed by Croveti [53] and other equations developed in this study, presented later in this Appendix, k values were backcalculated from the maximum interior deflections for the four sections. The load radius a_r was assumed to be 8 in [203 mm], based on diagrams of the test setup, and the k values were adjusted for the effect of finite slab size. The load magnitude P was 9000 lbs [40 kN]. The results are shown in Table A-4. The k values backcalculated from the slab deflections are much more similar to those obtained from plate tests on the subgrade than to those obtained from plate tests on the CTB.

Table A-4. Backcalculation results for PCA test slabs.

Section	Δ_0 , in	l , in	Backcalculated k, lb/in ³	k from plate test on subgrade, lb/in ³	k from plate test on CTB, lb/in ³
5B6	0.0085	44.95	89	79	435
5B9	0.0065	58.70	91	70	580
7B6	0.0045	41.24	185	71	380
7B9	0.0040	55.16	154	93	535

Note: 1 in = 25.4 mm, 1 psi/in = 0.27 kPa/mm

This does not mean, however, that a cement-treated base has no effect on stresses in the concrete slab. A cement-treated base may significantly reduce stress in the concrete slab, especially if a high degree of friction exists between the slab and base.

1972 AASHO INTERIM GUIDE

In the evolution of the AASHTO rigid pavement design methodology following the AASHO Road Test, a series of modifications was made to the process of selecting a k value for design. The 1972 AASHTO Interim Guide recommended the use of the subgrade gross k value in the main section of the manual. [54] However, an alternate procedure to determine the design k value, termed a composite k value on top of the subbase, was also given. According to this procedure, the subbase stiffness and the modulus of subgrade reaction are used in a nomograph, developed using elastic layer theory, to determine the composite k value on top of the subbase. This seems to be a discrepancy, because the AASHO Road Test's granular subbase k value ($k_G = 60$ psi/in [16.2 kPa/mm]) was already incorporated in the rigid pavement design equation. The 1972 Guide suggested that an adjustment to the k value might be warranted to reflect loss of support:

"The composite k value . . . is used in pavement thickness determinations. Although there are no specific procedures for reducing support value to account for losses due to pumping, erosion, consolidation, etc., a design agency should consider such reduction based on its own experience." [54]

This too appears to be a discrepancy, because loss of support was already incorporated into the AASHTO model: the rigid pavement design equation was developed from the performance data for the AASHTO Road Test's concrete pavement sections with granular bases, and these pavements experienced substantial pumping and loss of support beneath the slabs. [41]

CORRELATION OF K TO SOIL TYPE AND MOISTURE

The concrete pavement design procedure developed in the 1977 Zero-Maintenance study [55, 56] recommended that a soil's k value in various seasons be determined from its AASHTO classification and the degree of saturation in the upper 1 to 5 ft [0.3 to 1.5 m] of soil. Recommended k values for fine-grained soils at various degrees of saturation are shown in Figure A-18. Recommended k values for coarse-grained soils are shown in Figure A-19, except A-1 and A-3 soils, for which values of 400 and 215 psi/in [108 and 58 kPa/mm] respectively were recommended.

A-2 materials are divided into "gravelly" and "sandy" soils, with more than 50 percent and less than 50 percent respectively retained on the No. 10 sieve. A k value of 500 psi/in [135 kPa/mm] was recommended for periods when the subgrade was frozen. The k values shown in Figures A-18 and A-19 were obtained using correlations between resilient modulus, static elastic modulus, and degree of saturation developed from an extensive field and laboratory study of Illinois soils. [57]

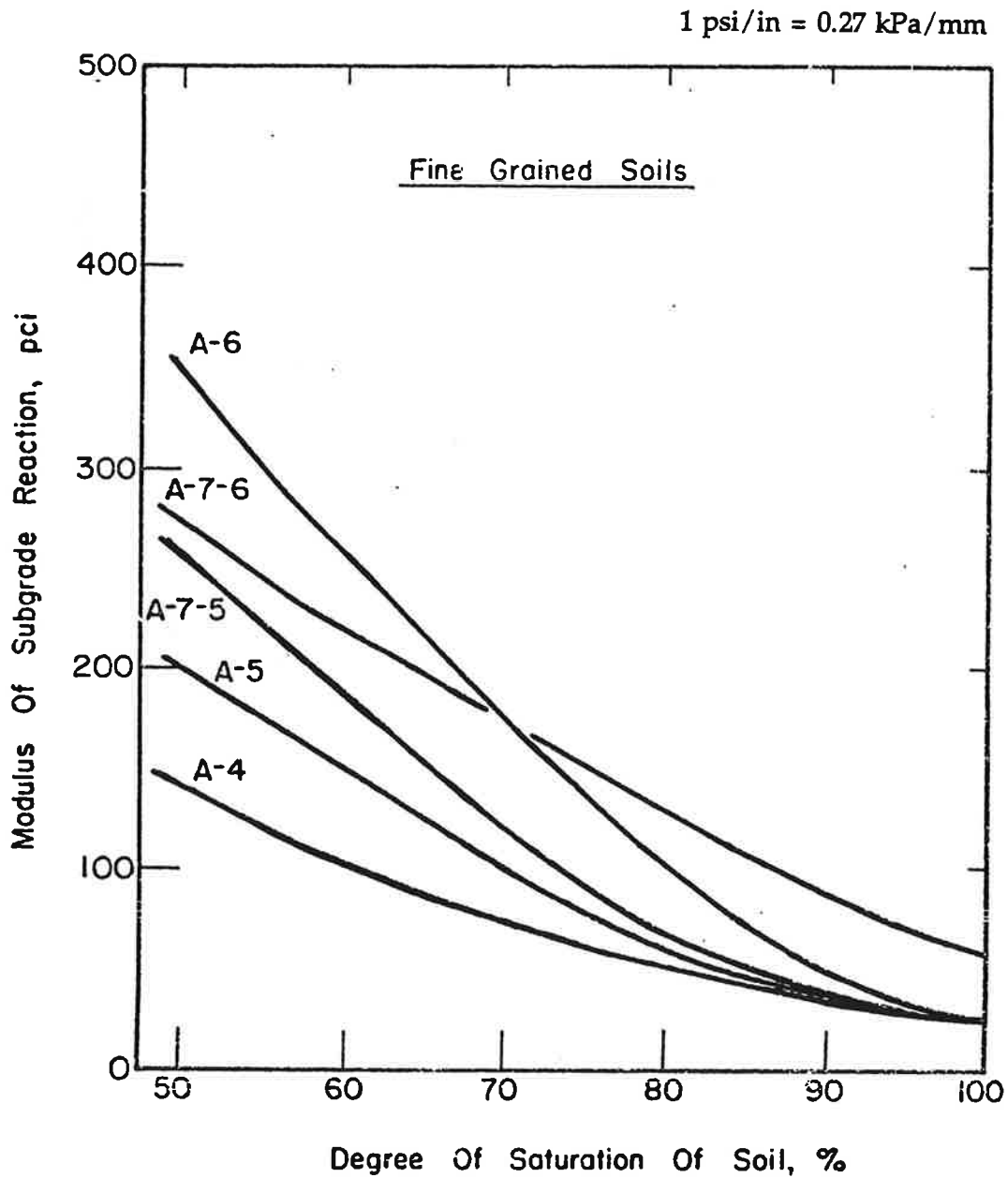


Figure A-18. k values for fine-grained AASHTO soil classes and degrees of saturation. [56]

1 psi/in = 0.27 kPa/mm

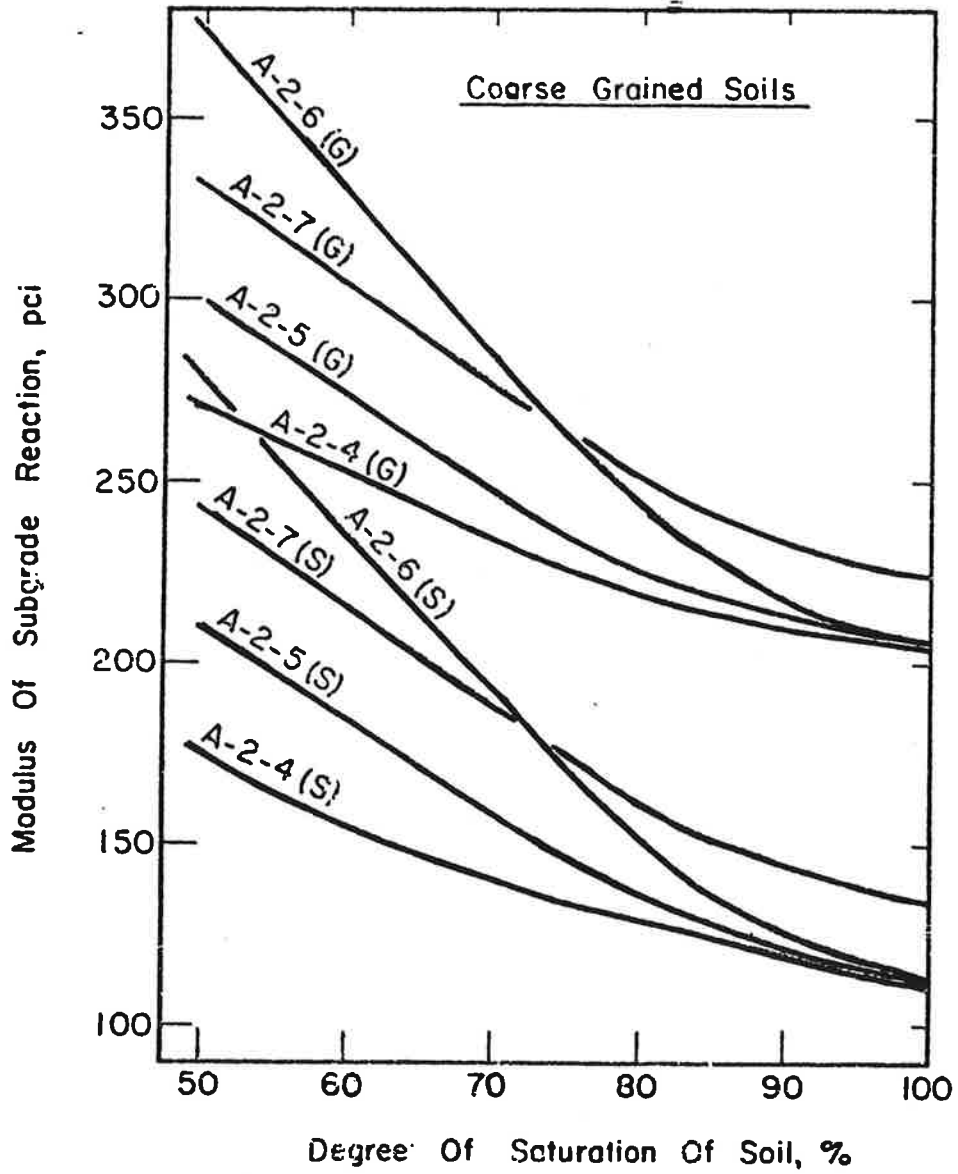


Figure A-19. k values for coarse-grained AASHTO soil classes and degrees of saturation. [56]

1986 AASHTO GUIDE K VALUE METHODS

The 1986 version of the AASHTO Guide [58] contained five modifications to the k value guidelines in the 1972 Interim Guide:

1. An equation was provided for k value for an unprotected subgrade,
2. A new nomograph for composite (top-of-base) k was provided,
3. An adjustment for depth to a rigid foundation was introduced;
4. A seasonal adjustment procedure for k was provided; and
5. A loss-of-support adjustment was introduced.

K Value Equation for Unprotected Subgrade

A simple linear relationship between subgrade k value and the resilient modulus (M_R) of the subgrade soil was presented in the 1986 AASHTO Guide:

$$k = \frac{M_R}{19.4} \quad (\text{A-2})$$

The development of this equation was documented in the Guide's Appendix HH. [59]

Laboratory M_R versus In Situ E_s

Equation A-6 is described in Appendix HH as a "theoretical relationship between k-values from a plate bearing test and elastic modulus of the roadbed soil." [59] The 1986 Guide makes no distinction between the laboratory-measured resilient modulus of a soil sample (M_R) and the in situ elastic modulus of a subgrade soil mass (E_s). In fact, the laboratory resilient modulus M_R and the in situ elastic modulus E are likely to be very different. One reason for this is that the vertical

deviator stresses used to characterize M_R in the laboratory test are higher (e.g., about 6 psi [41 kPa]) than the vertical deviator stresses typically experienced by an in situ subgrade soil under a concrete pavement and granular base (e.g., 1 to 2 psi [7 to 14 kPa] beneath the load and even less away from the load).

The laboratory resilient modulus probably differs from the field elastic modulus for other reasons as well, as several studies have shown. For example, in 1947 Palmer compared subgrade elastic moduli values determined from field plate bearing tests and from laboratory triaxial tests, using data from three airfields. [60] The purpose of this comparison was to "indicate the degree of practicability of using a value for the modulus as obtained by a laboratory triaxial shear test rather than a value for the modulus as computed by a plate-load test on the subgrade." The subgrades at the three sites were predominantly silt (AASHTO classification A-4) with some clay (A-7) at one site. Palmer's data are shown in Figure A-20. The field subgrade support values in pounds, on the left vertical axis, can be converted to field E values in pounds per square inch [1 psi = 6.89 kPa] using Equation A-7, substituting in $a = 15$ inches [381 mm] and $\Delta = 0.2$ inch [5 mm]:

$$E = \frac{\frac{\pi}{2} (1 - \mu^2) p a}{\Delta} = \frac{1.178 p a}{\Delta} = \frac{P}{8} \quad (\text{A-3})$$

where Δ = deflection under rigid plate

p = plate pressure

a = load radius

E = modulus of elasticity of soil

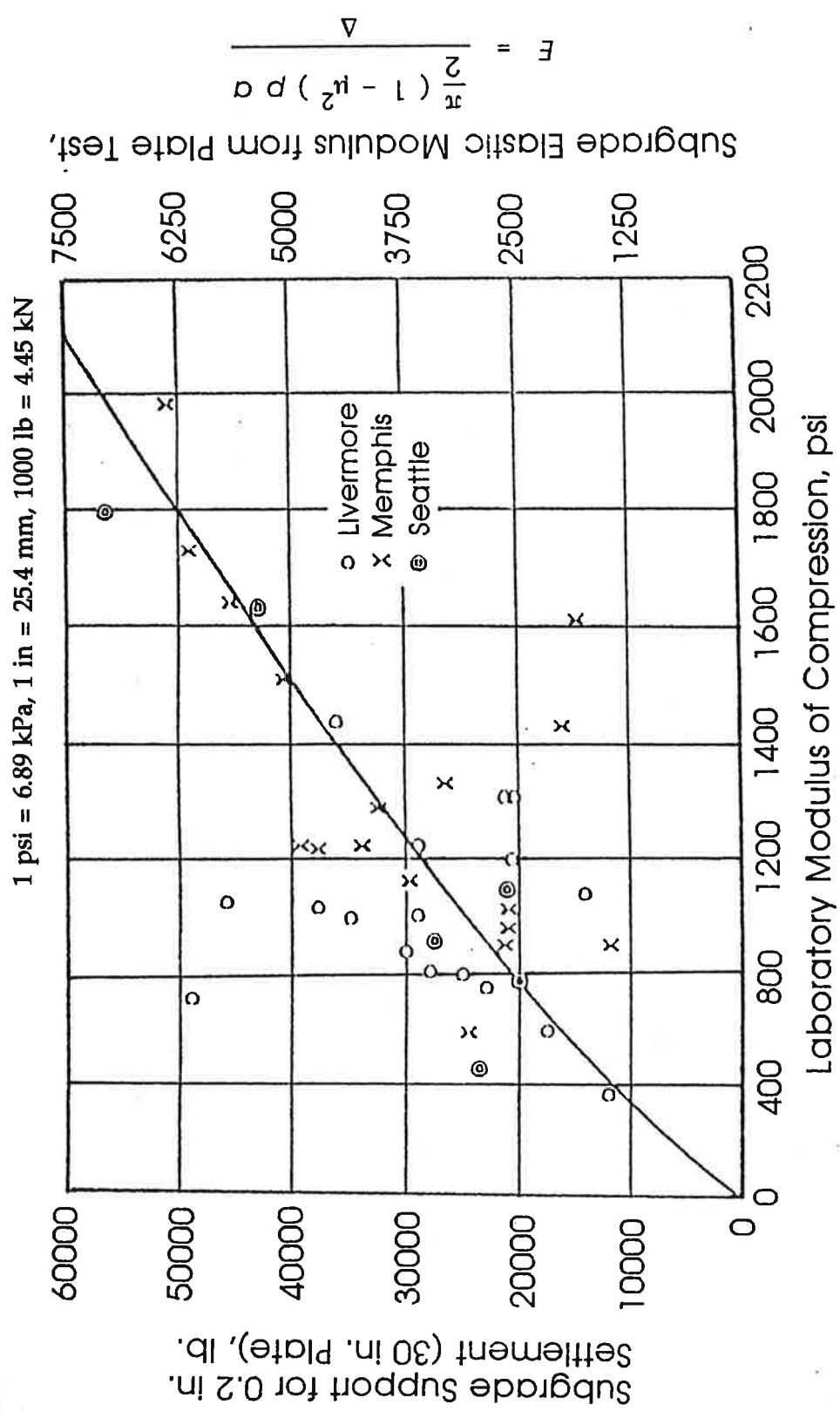


Figure A-20. Comparison of field subgrade bearing values and laboratory triaxial test results, from Palmer. [60] (Bearing values on left axis, equivalent E values superimposed on right axis).

Note that this equation is for rigid plate loading; even though the tests were conducted with steel plates, Palmer actually used the equation for flexible plate loading, which would produce E values about 27 percent higher. Using Equation A-7, an axis for field E was superimposed on the right vertical axis of Figure A-18. The slope of the curve is about 3.5 to 1. It is also worth noting also that the plate loads applied to produce 0.2-in [5 mm] deflections correspond to plate pressures of about 15 to 75 psi [103 to 517 kPa], certainly equal or greater to those applied in the lab. Palmer gave the following interpretation of these results:

"One of two possible conclusions must follow: either [Equation A-7], derivable from the theory of elasticity, cannot apply even to cohesive soils, or the laboratory-determined E is not the proper value to use [in Equation A-7]. The author believes that the latter conclusion is the correct one for the reason that the field modulus E is almost invariably higher than the laboratory E, and for very sandy soils the laboratory E is so low as to preclude the notion that the sandy soil can have any considerable bearing value, which it nevertheless has, as plate-loading tests prove... This all tends to point definitely to the advisability of carrying the laboratory to the field and making tests on the subgrade *in place*, rather than to take small samples to the laboratory... The latter procedure could be used, however, if and when a good correlation between laboratory data obtained with small samples and the in-place field tests has been well established." [60]

A discussion of Palmer's results by Sprague, Bell, and Schwartz cited other findings that elastic moduli from laboratory tests were not representative of in situ elastic moduli [61]:

"It is unfortunate that the term 'undisturbed' in relation to soil samples can have only the meaning, 'least disturbed.' Rutledge [62] has shown that for cohesive soils, the degree of disturbance markedly affects the stress-strain relationship and maximum compressive strength. He states that the modulus of elasticity of a clay in nature will not be less than that obtained from triaxial compression tests, but it may be greater by an amount which cannot be predicted from the results of laboratory tests. Independent observations by Peck [63] have corroborated these findings." [61]

Elastic Layer Simulation of Plate Load Test

The relationship suggested between k and resilient modulus in Appendix HH of the 1986 AASHTO Guide is actually the following relationship between k and elastic modulus E , derived using an elastic layer computer program:

$$k = \frac{E}{19.4} \quad (\text{A-4})$$

In a real plate load test on a natural subgrade material, the shear stress at the edge of a flexible load plate is equal to the applied pressure (e.g., 10 psi [69 kPa]). The shear stress at the edge of a rigid load plate is considerably higher. If this shear stress exceeds the shear strength of the soil, the plate will punch down into the soil and relatively little deflection will occur outside the load plate. To the extent that this happens, the real soil's response approaches that of an ideal Winkler foundation,

in which the "independent springs" making up the foundation respond individually to load and do not transfer loads to adjacent springs. However, as Figure A-21 illustrates, an elastic layer program is not capable of reproducing the type of discontinuous deflected shape of the subgrade surface which would really occur in plate tests on most natural soils of relatively low shear strength.

Equation A-8 was developed by modeling a circular load with a radius of 15 inches [381 mm] and a pressure of 10 psi [69 kPa] on an elastic half-space, with Poisson's ratio $\mu = 0.45$ and E ranging from 1000 to 50,000 psi [6890 kPa to 344 MPa]. Because an elastic layer program cannot model rigid plate loading, k was not computed as pressure divided by deflection:

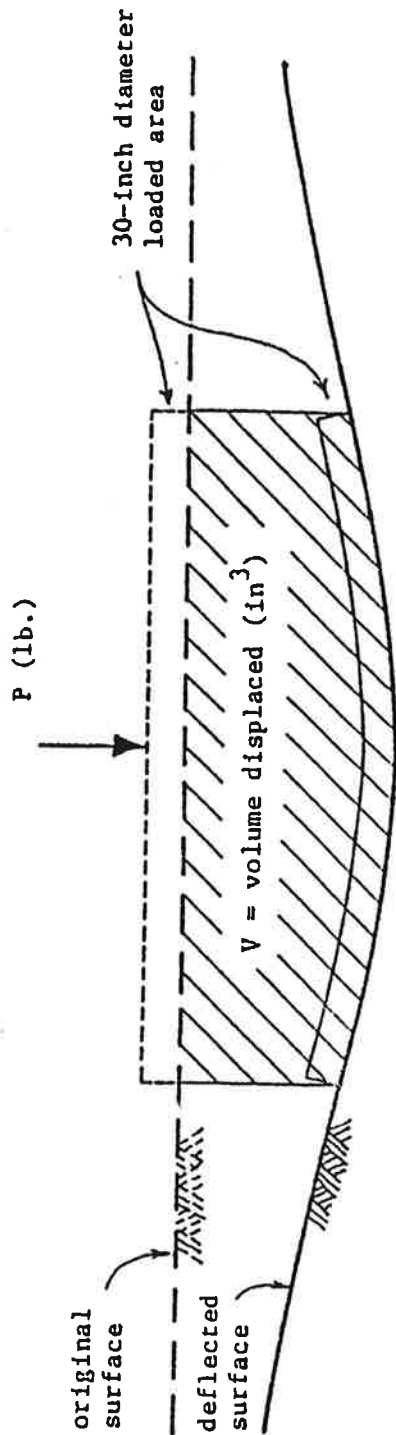
$$k = \frac{P}{\Delta} \quad (\text{A-5})$$

but rather as plate load P divided by deflected volume V:

$$k = \frac{P}{V} \quad (\text{A-6})$$

These two equations for k are equivalent only when the total deflected volume V is equal to the plate deflection times the contact area. It is important to note that in the derivation of Equation A-8, the k value corresponding to each input E value was computed by dividing the plate load P by only the deflected volume V within the radius of the load plate, as shown in Figure A-21. Modelling the soil as an elastic solid produces a smooth continuous curve from the center of loading to an infinite distance away. The deflected volume within the radius of the load plate as calculated from this smooth deflection curve is only a portion of the total volume deflected by the applied load.

Equation: $k = \frac{P}{V}$



Elastic Moduli (psi): 1,000; 2,000; 5,000

10,000; 20,000; 50,000

Poisson's Ratio: 0.45

Depth: Semi-infinite

1 in = 25.4 mm, 1 psi = 6.89 kPa

Figure A-21. Elastic layer simulation of plate load test, from AASHTO Guide Appendix HH. [59]

Backcalculated k for Slab on Elastic Solid

To demonstrate the general relationship between k and E beneath a concrete slab with no base, k values were backcalculated for this study from deflections calculated using an elastic layer program (BISAR) for a concrete slab resting on an elastic foundation. A range of subgrade E values from 1,000 to 50,000 psi [6890 kPa to 344 MPa] was used.

The concrete slab was modelled as 9 inches [229 mm] thick with an elastic modulus of 5 million psi [34450 MPa] and a Poisson's ratio of 0.15. The load was modelled with a radius of 5.9 inches [150 mm] and a magnitude of 9000 pounds [40 kN]. Although the load size and load level differ from those used in Appendix HH, these differences do not significantly affect the results of the backcalculation, because deflections of a concrete slab are very insensitive to load radius, and according to elastic theory, k is independent of the load magnitude. The slab/subgrade interface was modelled two ways, unbonded and bonded, but since the subgrade Poisson's ratio (0.45) was very close to 0.50, the results are nearly the same. The k values were backcalculated from the calculated deflections at 0, 12, 24, and 36 inches [0, 305, 610, and 914 mm] from the load center, according to the procedure given in Part III of the 1993 AASHTO Guide [64], described later in this Appendix. The results are compared with the 1986 AASHTO Guide's equation in Figure A-22.

The Guide's equation produces k values substantially higher than the backcalculated k values. Indeed, even if the input elastic moduli were reduced by a factor of 3 or 4 to approximate laboratory resilient moduli, the k values computed by Equation A-8 would still exceed the backcalculated k values.

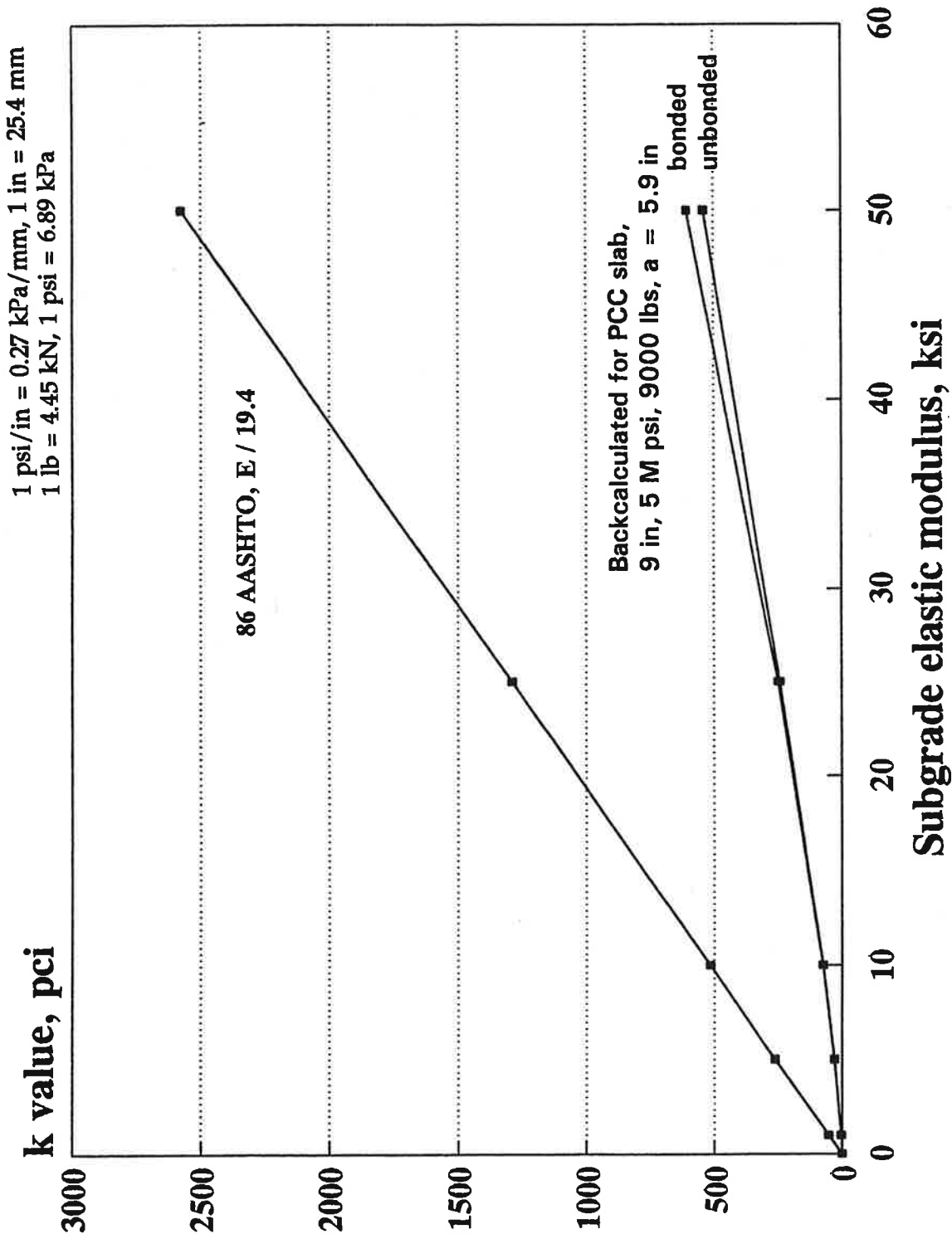


Figure A-22. Comparison of AASHTO k value equation and backcalculated k values for unprotected subgrades.

This example should not be taken as representing a precise relationship between subgrade E and k , for the following reasons:

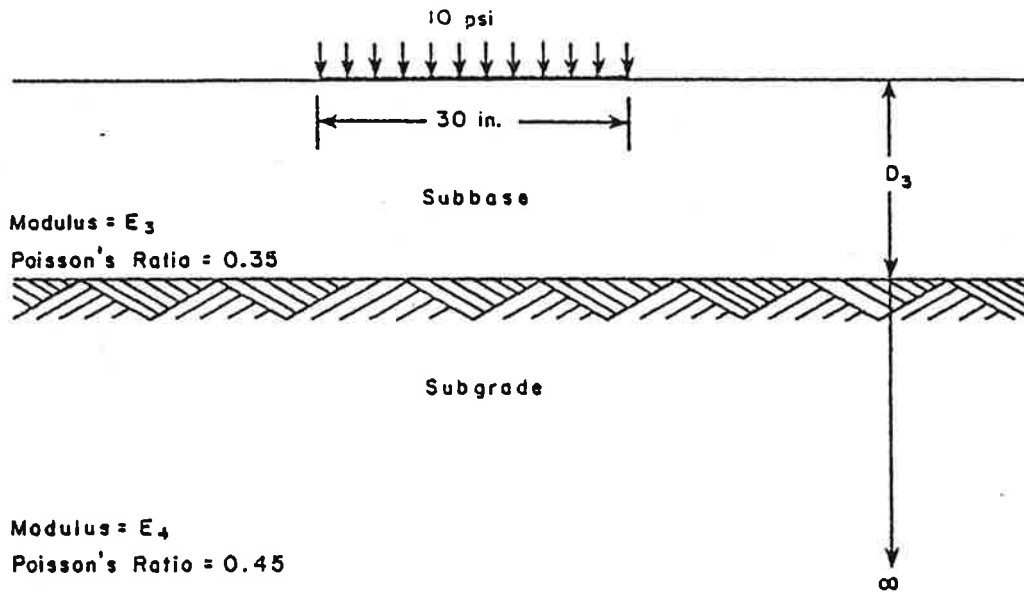
1. In any type of test (on a subgrade, on a slab, etc.) the relationship between E and k is a function of the load radius,
2. The relationship of E and k beneath a concrete slab is a function of the slab's thickness and elastic modulus,
3. The relationship of E and k for equal deflections is not the same as the relationship of E and k for equal bending stresses in a concrete slab, and
4. The deflection basins calculated by BISAR in this example would only be representative of an infinite and linearly elastic subgrade and a horizontally infinite concrete slab; real conditions of finite subgrade depth, nonlinear subgrade response, and finite slab size would alter measured deflections.

The conclusion drawn from this analysis is that the AASHTO Guide's equation for k for an unprotected subgrade yields unrealistically high k values.

Composite K Nomograph for Base and Subgrade

The 1986 AASHTO Guide presented a nomograph for determining a composite k as a function of subgrade resilient modulus and the thickness and elastic modulus of a base layer. The development of this nomograph was documented in the Guide's Appendix LL. [59] Again, the subgrade resilient modulus was presumed equal to the subgrade elastic modulus. The nomograph was developed in the same manner as the equation for subgrade k : by simulating plate load tests with an elastic layer computer program. The inputs used are shown in Figure A-23, from Appendix LL.

1 in = 25.4 mm, 1 psi = 6.89 kPa



Levels of Variables for Subbase Analysis

Level Number	1	2	3	4	5	6	7
D_3 (in.)	0	3	6	9	12	15	18
$\text{Log } E_3^*$	4.0	4.35	4.70	5.05	5.40	5.75	6.10
E_4 (psi)	600	3600	6600	9600	12,600	15,600	

* Equi-spaced $\text{Log}_{10} E_3$ values were taken to cover a wide range of E_3

Figure A-23. Inputs to 1986 AASHTO Guide composite k analysis. [59]

The base/subgrade interface was modelled as bonded. The plate load test was simulated as a 10 psi [69 kPa], 30-inch-diameter [762 mm] load on the top of the base.

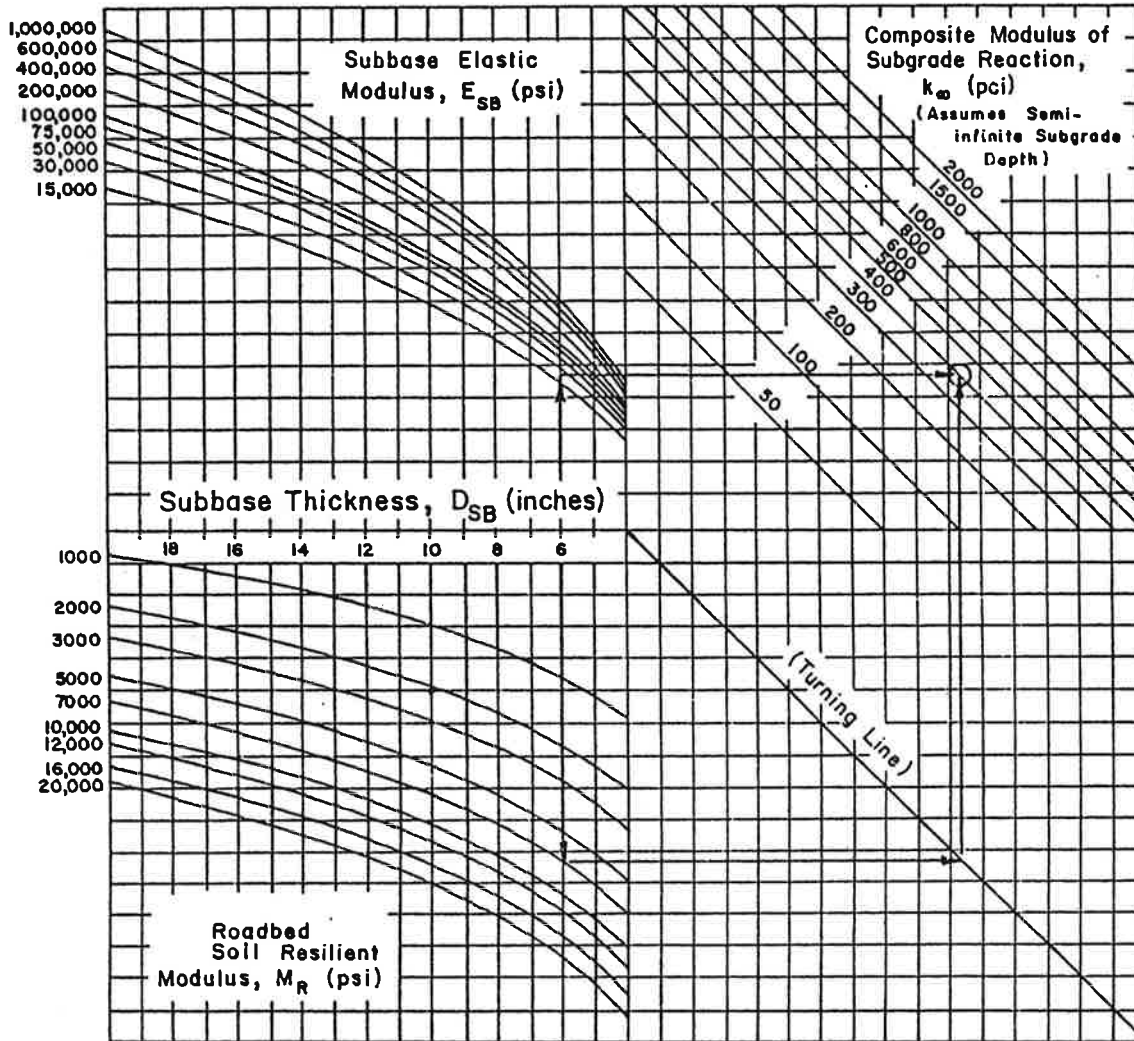
For each subgrade E, base E, and base thickness, a k value was calculated as the plate pressure of 10 psi [59 kPa] divided by the maximum deflection under the plate. Appendix LL does not explain why these k values were not calculated using the volumetric approach to compensate for flexible plate loading, as was done to compute the k values for an unprotected subgrade.

According to Appendix LL, the complete set of top-of-base k values computed for base thicknesses from 0 to 18 inches [457 mm] was used to develop the composite k nomograph, shown in Figure A-24, which appeared as Figure 3.3 in Part II of the 1986 AASHTO Guide. As an example, Appendix LL presents a table of k values obtained for the ranges of base and subgrade moduli considered and a base thickness of 6 inches [152 mm]. These k values are illustrated in the chart at the top of Figure A-25. Although the composite k nomograph was supposedly developed from these values and k values calculated similarly for other base thicknesses, the example k values given in Appendix LL differ significantly from those obtained using the nomograph, as shown in Table A-5 for a subgrade E of 15,600 psi [107.5 MPa] and base thickness of 6 inches [152 mm].

Another anomaly of the AASHTO composite k nomograph is that, although it yields very high k values for base layers, in some cases these k values are lower than the k values that would be assigned to the subgrade if the base were not present. For example, according to Equation A-8, a subgrade with an E of 10 ksi [6.9 MPa] has a k value of $10,000 / 19.4 = 515$ psi/in [135 kPa/mm]. According to Appendix LL, adding a 6-inch [152 mm] base which also has an E of 10 ksi [6.9 MPa] produces a composite k of only 390 psi/in [105], or 25 percent lower. The nomograph gives a composite k of about 450 psi/in [121.5], or 13 percent lower.

Example:

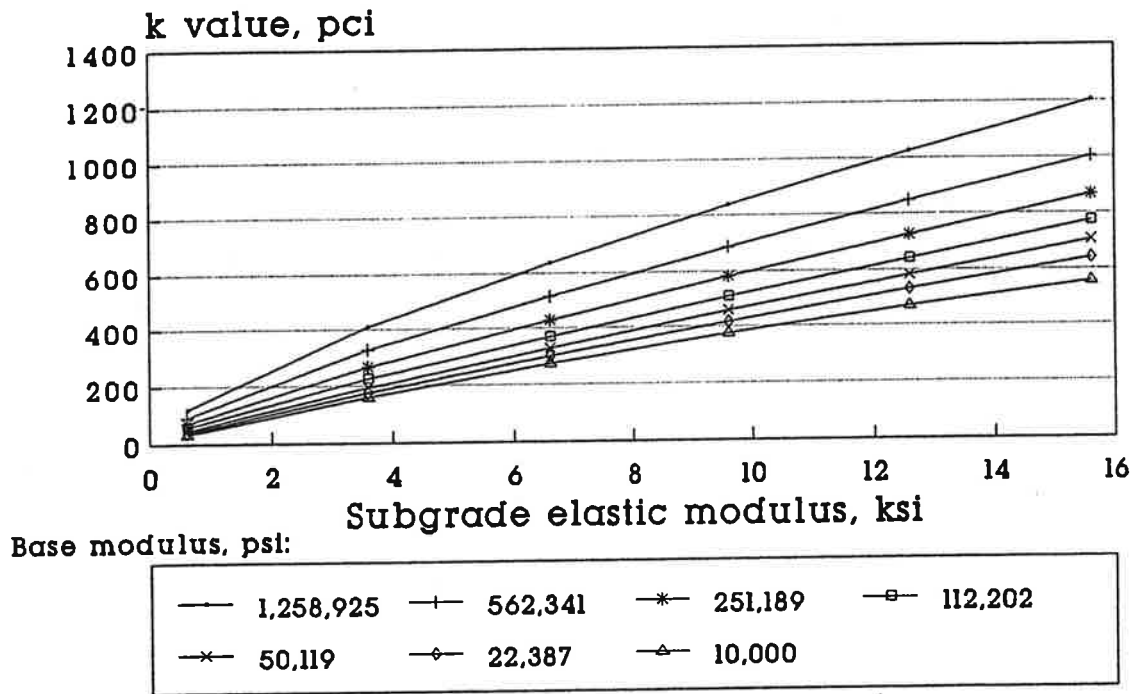
- $D_{SB} = 6$ inches
- $E_{SB} = 20,000$ psi
- $M_R = 7,000$ psi
- Solution: $k_{\infty} = 400$ pci



1 in = 25.4 mm, 1 psi = 6.89 kPa, 1 psi/in = 0.27 kPa/mm

Figure A-24. Composite k nomograph (1986 AASHTO Guide, Figure 3.3 [58]).

**k values for 6-inch base
from 1986 AASHTO Guide Appendix LL**



1 in = 25.4 mm, 1 psi = 6.89 kPa, 1 psi/in = 0.27 kPa/mm

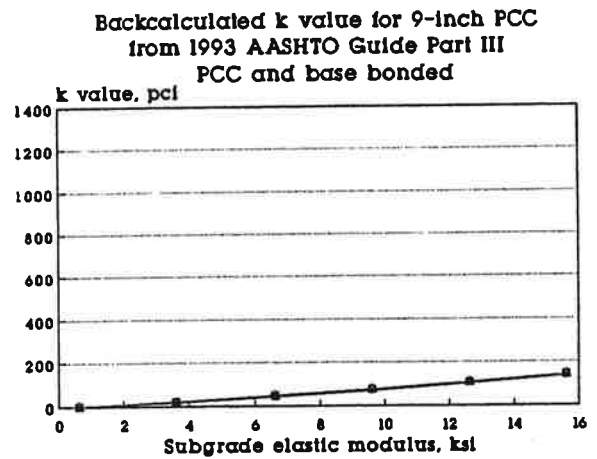
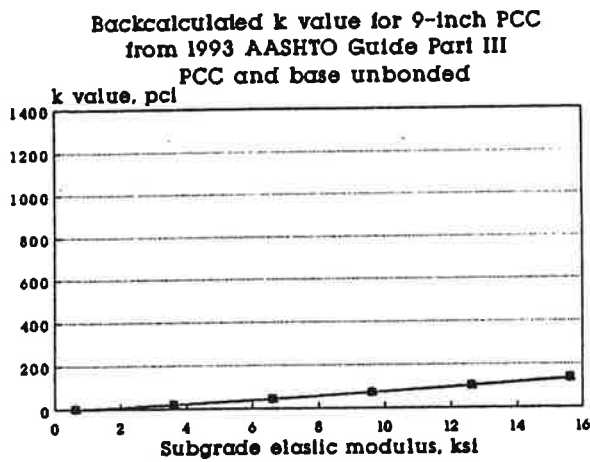


Figure A-25. Comparison of k values from 1986 AASHTO Guide Appendix LL and k values backcalculated from concrete slab deflections.

Consider another example: according to the k equation, a subgrade with an E of 15.6 ksi [107.5 MPa] has a k value of $15,600 / 19.4 = 804$ psi/in [217 kPa/mm]. As Table A-5 shows, a 6-inch [152 mm] base with a modulus up to about 125 ksi [861 MPa] would have a lower k value according to Appendix LL, and a 6-inch [152 mm] base with a modulus up to about 40 ksi [276 MPa] would have a lower k value according to the nomograph.

Table A-5. Comparison of composite k values from Appendix LL and nomograph.

Base E, ksi	k, pci, from Appendix LL	k, pci, from Nomograph
10	556	600
22	640	750
50	704	825
112	771	975
251	865	1100
562	1003	1200
1258	1202	1400

1 ksi = 6.89 MPa, 1 pci = 0.27 kPa/mm

In this study, another elastic layer analysis was conducted to assess whether or not the composite k nomograph yielded reasonable k values. Deflections were calculated in BISAR for a 9-inch [229 mm] concrete slab (elastic modulus of 4 million psi [27560 MPa]) resting on a 6-inch [152 mm] base, for each of combination of base and subgrade modulus listed in Appendix LL. The base/subgrade interface was modelled as bonded, as was done to develop the composite k nomograph, and the slab/base interface was modelled two ways, bonded and unbonded. The load was

modelled with a magnitude of 9000 pounds [40 kN] and a radius of 5.9 inches [150 mm]. The calculated deflections were used to backcalculate k values using the method described in Part III of the 1993 AASHTO Guide. The results are shown in the two charts at the bottom of Figure A-25.

The elastic layer simulation of the plate load test on the base produces substantially higher k values than those backcalculated from deflections computed by elastic layer theory for a concrete slab resting on the same base and subgrade. For example, for a subgrade E of 15.6 ksi [107.5 MPa] and a 6-inch [152 mm] base, base E values from 10 ksi [69 MPa] to 1.26 million psi [8680 MPa] produce k values ranging from 556 to 1202 psi/in [150 to 324 kPa/mm]. In contrast, the k value backcalculated from BISAR-computed slab deflections, for the same subgrade and base, is about 140 psi/in [38 kPa/mm], regardless of the base modulus.

Comparison of the two charts for backcalculated k at the bottom of Figure A-25 shows that the backcalculated k values are not affected by the slab/base interface bonding. However, when the slab and base are modelled as bonded, the slab bending stresses are much lower and the apparent elastic modulus of the slab (backcalculated as a function of the slab thickness alone) is much higher than when the slab and base are modelled as unbonded.

An example which illustrates all of the inconsistencies pointed out above is shown in Figure A-26. In the first case, a 9-inch [229 mm] slab ($E = 4$ million psi [27560 MPa]) is modelled in BISAR on a 15.6 ksi [107.5 MPa] subgrade. The AASHTO equation gives this subgrade a k value of 804 psi [217 kPa/mm]. The backcalculated k value is only 138 psi/in [37]. The backcalculated concrete modulus is 3.76 million psi [25925 MPa], and the calculated maximum tensile stress at the bottom of the concrete slab is 138 psi [951 kPa] for a 9000-pound [40 kN] load.

1 in = 25.4 mm, 1 psi = 6.89 kPa, 1 psi/in = 0.27 kPa/mm

PCC	9 in, 4 M psi
subgrade	15.6 ksi

PCC	9 in, 4 M psi
base	6 in, 50 ksi
subgrade	15.6 ksi

PCC	9 in, 4 M psi
base	6 in, 1.26 M psi
subgrade	15.6 ksi

1986 AASHTO Guide

k = 804 pci

k = 825 pci

k = 1400 pci

Backcalculated from BISAR deflections

k = 138 pci

k = 143 pci

k = 136 pci

Epcc = 3.76 M psi

Epcc = 3.98 M psi

Epcc = 7.28 M psi

Calculated by BISAR for 9000-pound load

PCC stress = 138 psi

PCC stress = 128 psi

PCC stress = 51 psi

Figure A-26. Example of subgrade and base effects on k value and slab response.

In the second case, a 6-inch [152 mm] base with an E of 50 ksi [344 MPa] is modelled between the slab and subgrade. Both the slab/base and base/subgrade interfaces are modelled as bonded. The AASHTO nomograph gives a composite k of 825 psi/in [223 kPa/mm], only slightly higher than the k of the subgrade alone. The backcalculated k, however, is about the same as before: 143 psi/in [985 kPa]. The backcalculated concrete modulus is slightly higher, 3.98 million psi [27420 MPa], and the slab stress under a 9000-pound [40 kN] load is slightly lower, 128 psi [882 kPa].

In the third case, the base is modelled with an E of 1.26 million psi [8680 MPa]. The AASHTO nomograph gives this base a composite k of 1400 psi/in [378 kPa/mm]. The backcalculated k is still about the same as before, 136 psi [937 kPa]. However, the high modulus of the base and the full bond between the slab and base result in an increase in the apparent elastic modulus of the slab (backcalculated for a thickness of 9 inches [229 mm]) to 7.28 million psi [50200 MPa], and a decrease in the slab stress to 51 psi [351 kPa].

This example was conducted using the BISAR elastic layer program, and should be considered primarily qualitative and only approximately quantitative. The actual deflections, stresses, and backcalculated k and E values which would be obtained for real concrete slabs of finite dimensions would be somewhat different. Nevertheless, the results do serve to demonstrate the following conclusions:

1. The 1986 AASHTO Guide equation for k values ($k = E / 19.4$) for unprotected subgrades produces unreasonably high values,
2. The 1986 AASHTO Guide's nomograph for composite k values for base/subgrade combinations yields values which are unreasonably high and also inconsistent with the values given by the equation for unprotected subgrades, and

3. According to elastic layer theory, base layers of typical thicknesses for highway design have no significant effect on calculated concrete slab deflections (and thus on k values backcalculated from those deflections). but relatively stiff bonded bases can significantly increase apparent slab stiffnesses and significantly decrease slab bending stresses.

Adjustment for Depth to Rigid Foundation

The nomograph introduced in the 1986 AASHTO Guide for increasing the k value when a rigid foundation is present at a depth of less than 10 feet [3 m] is shown in Figure A-27. The basis for this nomograph is not documented in the 1986 Guide or its Volume 2 Appendices. It may have been developed using elastic layer theory, in a manner similar to the unprotected subgrade k equation and composite k nomograph.

The 1986 Guide does not provide any guidance on modification of the k value when a substantial thickness of fill material is placed above the subgrade. The composite k nomograph is not adequate for this purpose because the maximum base thickness on the nomograph is 20 inches [508 mm]. A new nomograph, presented in Appendix B, has been developed in this study to modify the subgrade k value for the depth to a rigid layer and also for type and thickness of fill.

Seasonal Adjustment to K Value

The 1986 Guide's procedure for seasonal adjustment to the k value is documented in the Guide's Appendix HH. An effective k value for use in design is determined by: (1) assigning appropriate k values to the different seasons, (2) using the rigid pavement design equation to determine the "relative damage" done in each

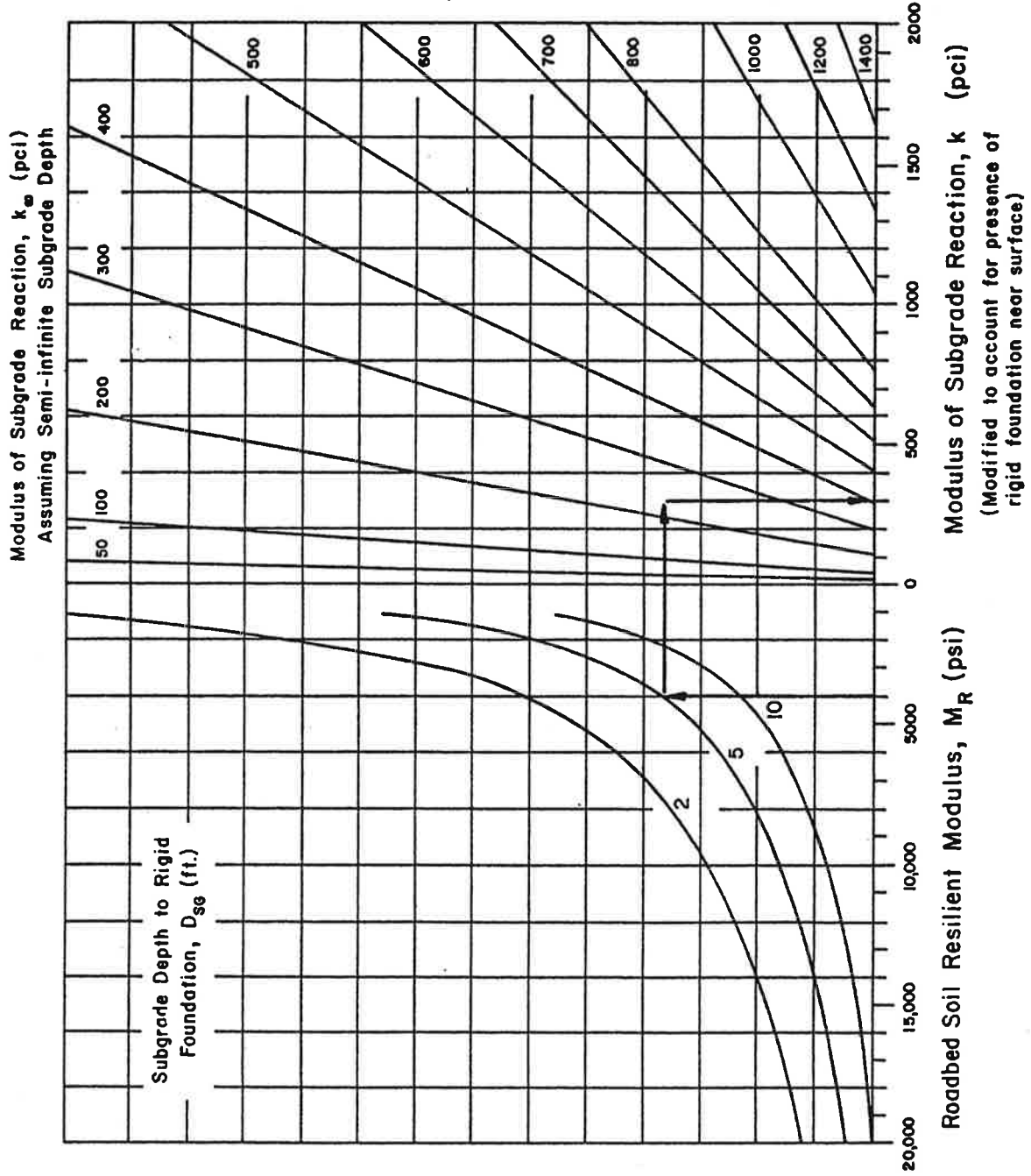


Figure A-27. Adjustment to k for rigid foundation within 10 ft [3 m], from 1986 AASHTO Guide. [58]

season, (3) computing the average annual damage as the sum of the seasonal damage amounts divided by the number of seasons considered, (4) finding a single k value which when used with the design equation will produce the same damage as the total annual damage.

According to the 1986 Guide, the relative damage factor must be determined as a function of the slab thickness because, of the variables in the rigid pavement design equation which could not be isolated from k (namely thickness, concrete modulus, and terminal serviceability), the equation was most sensitive to slab thickness. The nomograph developed for this equation is shown in Figure A-28. Its use requires selection of an initial trial slab thickness. In fact, many example cases examined using this nomograph and wide ranges of thickness and other inputs indicate that for a given set of seasonal k values, thickness has almost no effect.

Otherwise, this "relative damage" approach to determining a seasonally weighted average annual k value, seems to be reasonable in concept. The 1986 Guide does contain one significant discrepancy, however, in the application of this concept. Although the Guide recommends that a seasonally adjusted k value be used for design, the rigid pavement design equation was not derived using a seasonally adjusted k value for the AASHO Road Test site, but rather using the same springtime gross subbase k value of 60 psi/in [16 kPa/mm] which was used in the 1972 Guide. The flexible pavement design equation in the 1986 Guide was also derived using the same subgrade resilient modulus value which had been used for the AASHO Road Test soil (3000 psi [20.7 MPa]) in the past, rather than a seasonally weighted average annual resilient modulus.

In this study, a proposed revision to the rigid pavement design equation was developed for use in the AASHTO design procedure, as described in Appendix E.

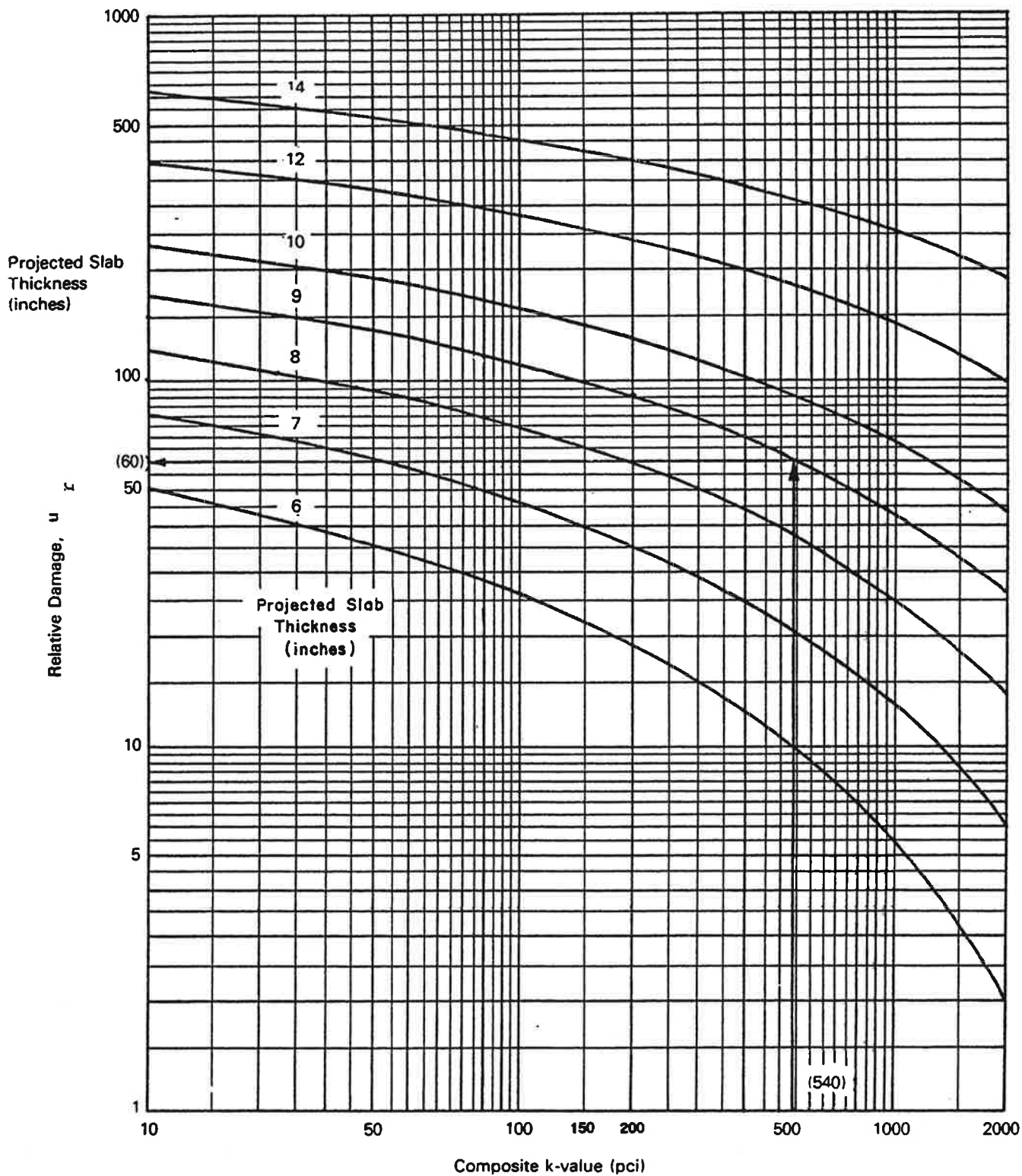


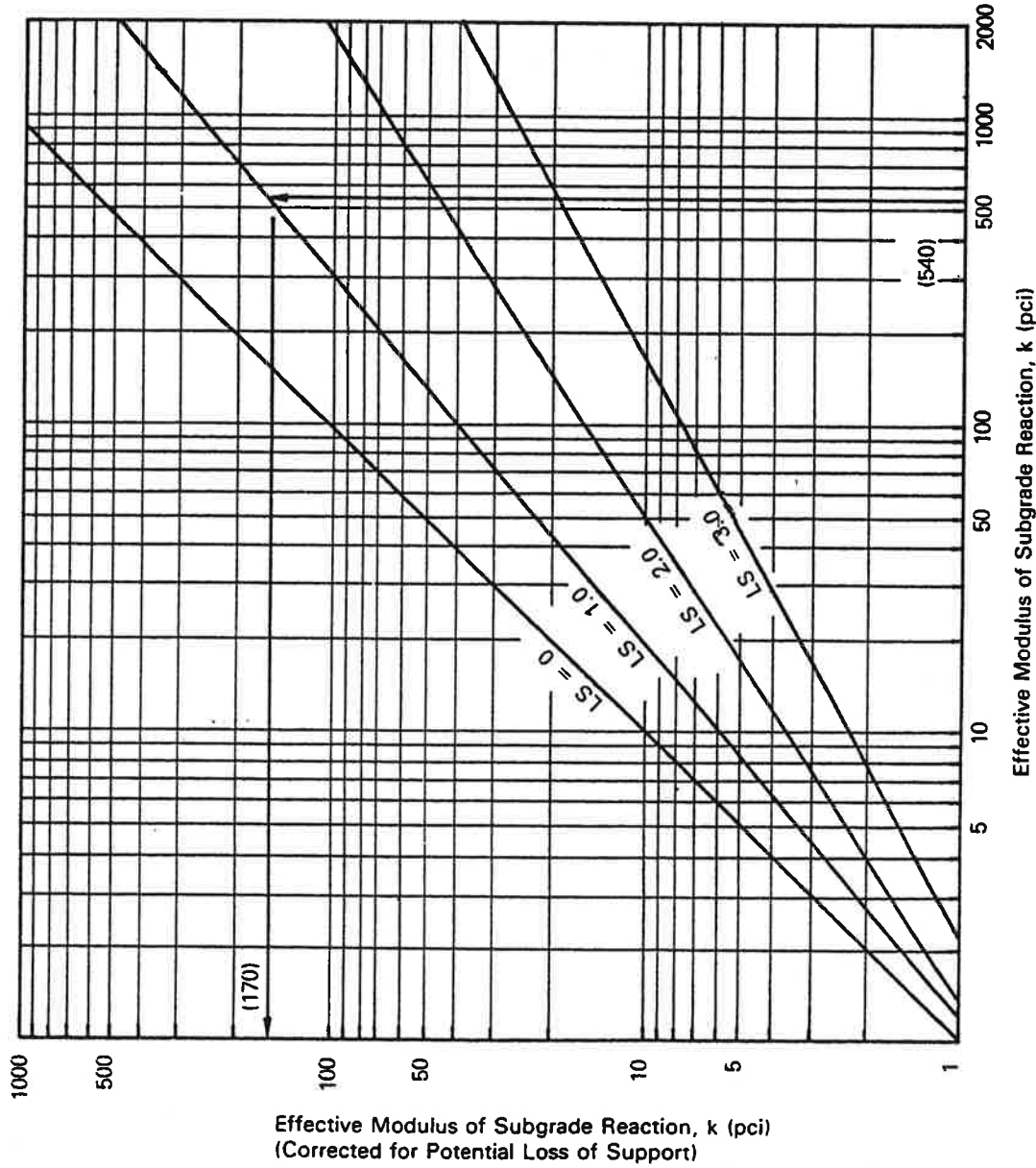
Figure A-28. Relative damage nomograph from 1986 AASHTO Guide. [58]

Using the proposed revised design equation and the seasonal k value data reported for the AASHO Road Test, the relative damage concept was applied to determine a seasonally adjusted k value for the AASHO Road Test site. This seasonally adjusted k value is the reference k value to which the new design equation is calibrated. It should be noted that it would not be appropriate to substitute this seasonally adjusted k value into the 1986 Guide's equation, as it was developed from a different damage model.

Loss of Support Adjustment to K Value

The nomograph introduced in the 1986 AASHTO Guide for reducing the k value for potential loss of support due to base erodibility is shown in Figure A-29. The development of the nomograph is described in the 1986 Guide's Appendix LL, although it is actually referenced to a 1979 manual for continuously reinforced pavement design by McCullough and Elkins. [65]

The nomograph for the loss of support adjustment was developed using the SLAB-49 discrete element program to compute slab responses to joint loading with no voids and with voids of three different sizes modelled under the joint. As shown in Figure A-29, various base types are assigned a range in the loss-of-support factor (LS) based on their relative erodibility. The LS factors correspond to the void sizes modelled, and thus presumably to the void sizes which those base types will develop for any design life, cumulative traffic, or combination of other design variables such as slab thickness or joint load transfer. The SLAB-49 program was used to determine the lower full-support k value which would produce the same slab response to loading as the input k value with a given void size. Thus, the effect of the LS factor is to reduce the k value if the base is an erodible material or if no base is present.



Type of Material	Loss of Support (LS)
Cement Treated Granular Base (E = 1,000,000 to 2,000,000 psi)	0.0 to 1.0
Cement Aggregate Mixtures (E = 500,000 to 1,000,000 psi)	0.0 to 1.0
Asphalt Treated Base (E = 350,000 to 1,000,000 psi)	0.0 to 1.0
Bituminous Stabilized Mixtures (E = 40,000 to 300,000 psi)	0.0 to 1.0
Lime Stabilized (E = 20,000 to 70,000 psi)	1.0 to 3.0
Unbound Granular Materials (E = 15,000 to 45,000 psi)	1.0 to 3.0
Fine Grained or Natural Subgrade Materials (E = 3,000 to 40,000 psi)	2.0 to 3.0

Note: E in this table refers to the general symbol for elastic or resilient modulus of the material.

Figure A-29. Loss of support nomograph from 1986 AASHTO Guide. [58]

Although this loss-of-support adjustment factor may be well suited for the CRCP design procedure for which it was developed, it is not at all compatible with the AASHTO design procedure. As mentioned before, the AASHTO rigid pavement performance model was developed from the performance data of the granular base rigid pavement sections at the AASHO Road Test. These pavements experienced substantial loss of support due to pumping. The degree of loss of support was quantified by a "pumping index" of cubic inches of pumped material per inch of pavement length. Many sections had a PI of over 100, equivalent to 2.6 cubic yards [2 m³] of material pumped from beneath 100 ft [30.5 m] of pavement. The pumping index was found to be inversely proportional to slab thickness and directly proportional to axle load level. For some sections, voids extending more than 5 ft [1.5 m] beneath the slab edge are shown in photographs in the Road Test report. [41] The pavement sections without any granular base experienced worse pumping, but the performance data from these sections were not used in the development of the performance model. It is clear from the AASHO Road Test report that the basic performance model for the Road Test site represents the performance of pavements which experienced substantial loss of support:

"Inasmuch as the great majority of the sections which failed pumped severely prior to failure, many of these sections would have survived the two years of traffic had the subbase material been stabilized effectively to resist erosion by water." [41]

As with the seasonal adjustment, the loss-of-support adjustment introduced in the 1986 Guide is inconsistent with the k value of 60 psi/in [16 kPa/mm] embedded

in the rigid pavement design equation. According to the loss of support nomograph, the granular base at the AASHO Road Test site would be assigned an LS of 1.0 to 3.0, which would reduce the k value to between 6 and 22 psi/in [1.6 and 6 kPa/mm]. A more consistent approach for use with the 1986 design equation would have been to recommend an LS of 0 (no adjustment to k) for a granular base, a positive LS (increase in k) to a stabilized base, and a negative LS (decrease in k) for fine-grained material.

The loss of support procedure presented in the 1986 Guide is based on an assumption that the effect of base type on performance can be accounted for by modifying the design k value. This is necessary because the 1986 design equation has no inputs for base properties such as thickness, stiffness, or erodibility. An alternate approach, taken in this study, is to develop a performance equation which explicitly considers the effects of base type (i.e., erodibility), stiffness, thickness, and slab/base friction on predicted loss of serviceability due to cracking and also predicted faulting. This approach is described in detail in Appendix E.

Summary of 1986 AASHTO Guide K Value Methods

The following conclusions are drawn concerning the k value methods presented in the 1986 Guide:

1. **Equation for k value for an unprotected subgrade:** The equation ($k = M_R/19.4$, where laboratory resilient modulus M_R is assumed in the Guide to be equal to the in-place elastic modulus E of the subgrade), developed from elastic layer simulation of plate testing on an elastic half-space, produces unrealistically high k values.

2. **Nomograph for composite (top-of-base) k:** This nomograph, also developed from elastic layer simulation of plate tests on base/subgrade combinations, produces unrealistically high k values.
3. **Adjustment to k for rigid foundation within 10 ft [3 m] depth:** It is difficult to assess the adequacy of the nomograph for this adjustment without documentation on its development. Analyses have been conducted to replace this nomograph with one which would adjust k not only for a rigid foundation but also for fill thicknesses greater than 1 ft [0.3 m].
4. **Seasonal adjustment procedure for k:** The AASHTO Guide provides a reasonable method for determining a design k value which represents the range of k values expected in various seasons, weighted with respect to the relative damage done to the pavement in those seasons. The relative damage is calculated using the AASHTO rigid pavement design equation. The one inconsistency of the seasonal adjustment procedure is that the design equation itself is not calibrated to a seasonal average k for the AASHO Road Test site, but rather the springtime k value. Also, if the rigid pavement design equation is replaced, the seasonal adjustment procedure should be modified accordingly.
5. **Loss of support adjustment to the k value:** This nomograph, developed using discrete element analysis of various sizes of voids under a concrete pavement joint, produces dramatic reductions in k

value for erodible bases. This loss of support adjustment is a major discrepancy in the design procedure, as mentioned before, because the performance prediction model is based on the AASHO Road Test pavements which had granular bases and experience substantial loss of support.

K VALUE BACKCALCULATION METHODS

Methods for backcalculation of elastic moduli for multilayered pavement systems from measured deflections first appeared in the 1970s, starting with Scrivner's graphical solution for elastic moduli in a two-layer pavement system in 1973. [66] Most of the available backcalculation computer programs are based on multilayer elastic theory, and thus cannot produce a backcalculated k value for the subgrade. Procedures have also been developed over the last fifteen or more years for backcalculating k values for concrete pavements. Three approaches are reviewed in this section: solutions based on the AREA concept, other approaches to backcalculating a radius of relative stiffness, and the Iowa Road Rater method which correlates Road Rater deflection basin parameters directly to static k values.

All of the methods summarized here except the Iowa Road Rater method are two-layer solutions: they solve for a subgrade k and an elastic modulus of the concrete slab. If a base layer is present, its primary effect on the backcalculation solution is an increase in the apparent modulus of the concrete slab; the effect of a base on the backcalculated k value is usually insignificant. Additional comments on the effect of base layers and other limitations of existing backcalculation procedures are given later in this Appendix.

AREA Concept for Backcalculation

The AREA concept was proposed by Hoffman and Thompson in 1981 for use in backcalculating surface and subgrade elastic moduli for flexible pavements. [67]

The AREA, given by the equation below, is used to characterize the deflection basin:

$$AREA = 6 * \left[1 + 2 \left(\frac{d_{12}}{d_0} \right) + 2 \left(\frac{d_{24}}{d_0} \right) + \left(\frac{d_{36}}{d_0} \right) \right] \quad (A-7)$$

where d_0 = maximum deflection at center of loading plate

d_i = deflections at 12, 24, and 36 in [305, 610, 914 mm] from the center

AREA has units of length, rather than area, since each of the deflections is normalized by d_0 in order to remove the effect of different load levels and to restrict the range of values obtained. AREA and d_0 are thus independent parameters, from which two layer moduli (surface and foundation) may be determined. Hoffman and Thompson developed a nomograph for backcalculation of flexible pavement surface and subgrade moduli from d_0 and AREA. The term "AREA" is generally taken to mean AREA as defined by the above equation, i.e., for four sensors at 12-inch [305 mm] spacing. Other AREA parameters may be defined for more spacings or other sensors if desired.

Hoffman and Thompson also studied flexible pavement deflections under static loading (measured by a Benkelman Beam), vibratory loading (measured by a Road Rater), and impulse loading (measured by a Falling Weight Deflectometer). Among their conclusions was one that deflections under static loading could be anywhere from 2 to 10 times greater than deflections under dynamic loading. [67]

ILLI-SLAB Solutions

The AREA concept was subsequently applied to backcalculation of PCC slab elastic modulus values and subgrade k values for many airport and highway projects. [68] The ILLI-SLAB finite element program was used to compute a matrix of maximum deflections and AREA solutions by varying the k value and E for a given slab thickness and slab size. A family of curves was then plotted against AREA and d_0 axes. Individual midslab deflection basins (AREA and d_0) measured with a Falling Weight Deflectometer (FWD) could then be plotted on the matrix, and the slab E and foundation k value interpolated. In 1985, Foxworthy adapted this backcalculation scheme to a computerized solution. [69]

An attractive feature of the ILLI-SLAB-based AREA solutions was that the effect of finite slab size was incorporated in the solution. However, the backcalculated k values obtained from the FWD were typically about twice as high as the static k values which would be expected for the same soils in standard plate bearing tests. Foxworthy's research included FWD deflection testing at several U.S. Air Force bases, and comparison of the backcalculation results obtained with results of plate load tests and laboratory tests of concrete samples. Foxworthy observed that k values backcalculated from FWD deflections exceeded static k values from plate load tests by a mean ratio of 2.7 (ranging from 1.6 to 4.4), as shown in Figure A-30.

ILLI-BACK Solution

Further investigation of the AREA concept by Barenberg and Petros [70] and by Ioannides [71] produced a forward solution procedure to replace the iterative and graphical procedures used previously. This solution is based on the fact that a unique relationship exists between AREA, defined for a given load radius and sensor

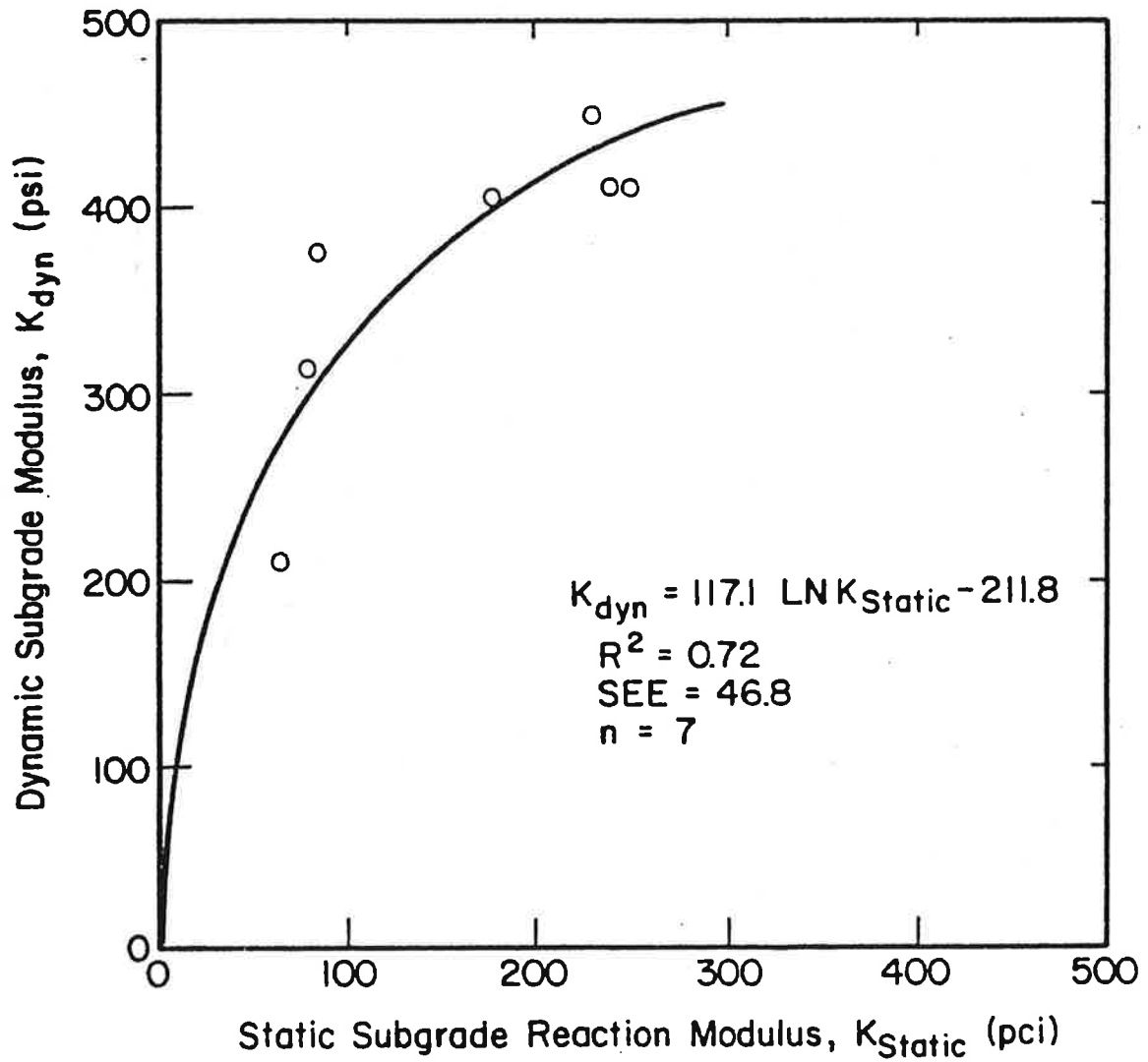


Figure A-30. Relationship of backcalculated k value to static k value. [69]

arrangement, and the dense liquid radius of relative stiffness (l) of the pavement system, in which the subgrade is characterized by a k value. Once the radius of relative stiffness is known, the subgrade k value may be backcalculated from the deflection measured at the load center or any other position using plate theory deflection equations presented by Westergaard [72] and Losberg [73]. In 1989, Ioannides, Barenberg, and Lary [74] demonstrated the application of this closed-form approach using the computer program ILLIBACK.

This solution method was much faster than the graphical methods used before, but it has some drawbacks. The solution for k is based on plate theory equations for deflection of an infinite slab. The deflection of an actual highway pavement slab (12 ft [3.7 m] wide, perhaps only 15 ft [4.6 m] long) may be quite different than that predicted from theory for infinite slabs. Also, as with the ILLI-SLAB solution, the k values backcalculated from FWD data are higher than static k values. The backcalculated concrete modulus will also be higher than the actual concrete modulus if a base layer is present.

1993 AASHTO Guide

Equations for backcalculation of concrete elastic moduli and subgrade k values for concrete and composite pavements were developed by Hall [75] and incorporated in the overlay design procedures in the 1993 AASHTO Guide. [64] This two-layer solution method is also based on deflection of an infinite slab. The procedure is described in detail in Appendix B.

The subgrade k value and concrete E value for a bare concrete pavement may be obtained from Figures A-30 and A-31 respectively. These charts may also be used to determine the subgrade k and concrete E for an existing AC-overlaid PCC

1 in = 25.4 mm, 1 mil = 25.4 μ m,
 1 pound = 4.45 N, 1 psi/in = 0.27 kPa/mm

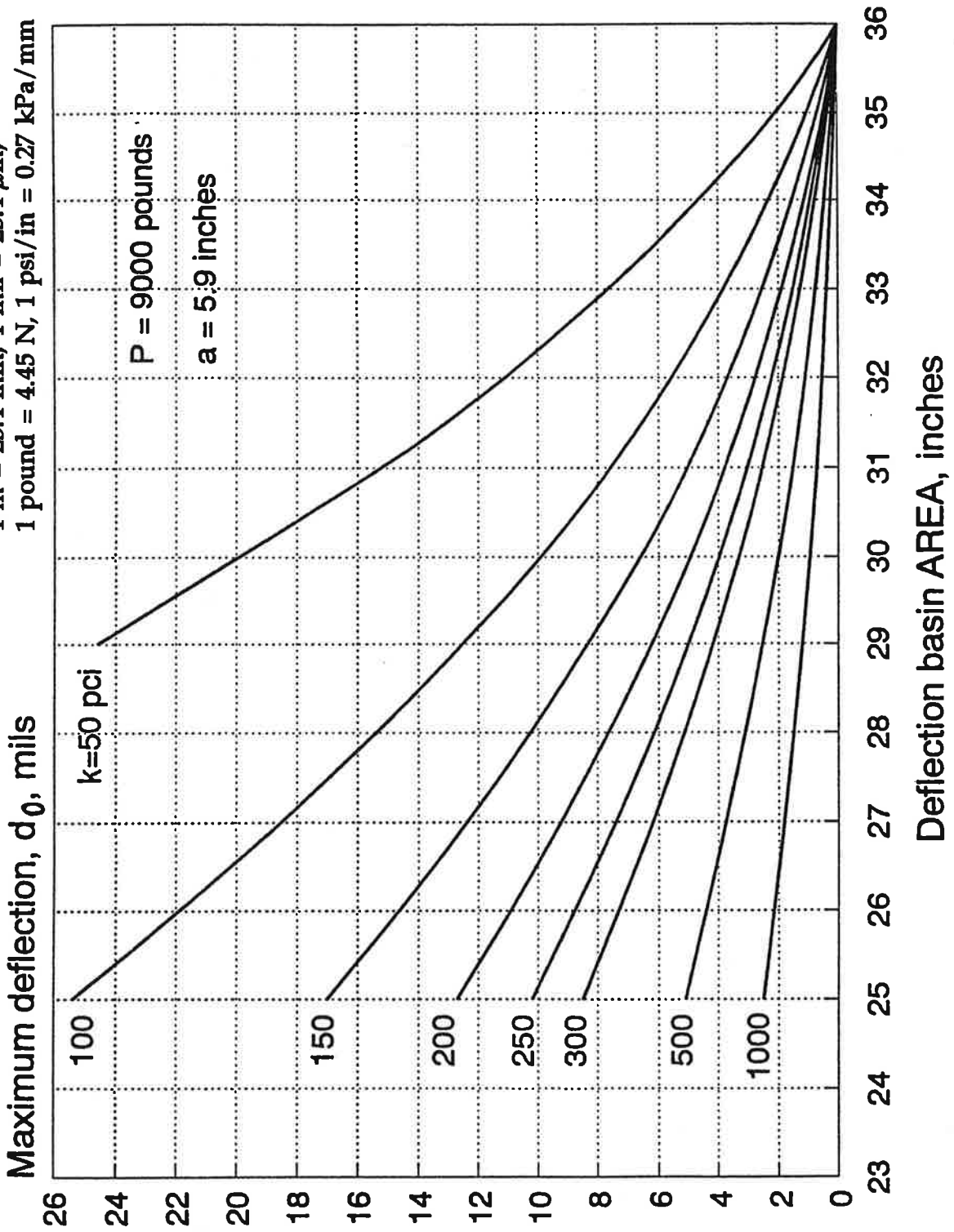


Figure A-31. Backcalculated k value determination from d_0 and AREA. [64]

1 in = 25.4 mm, 1 psi = 6.89 kPa,
 1 psi/in = 0.27 kPa/mm

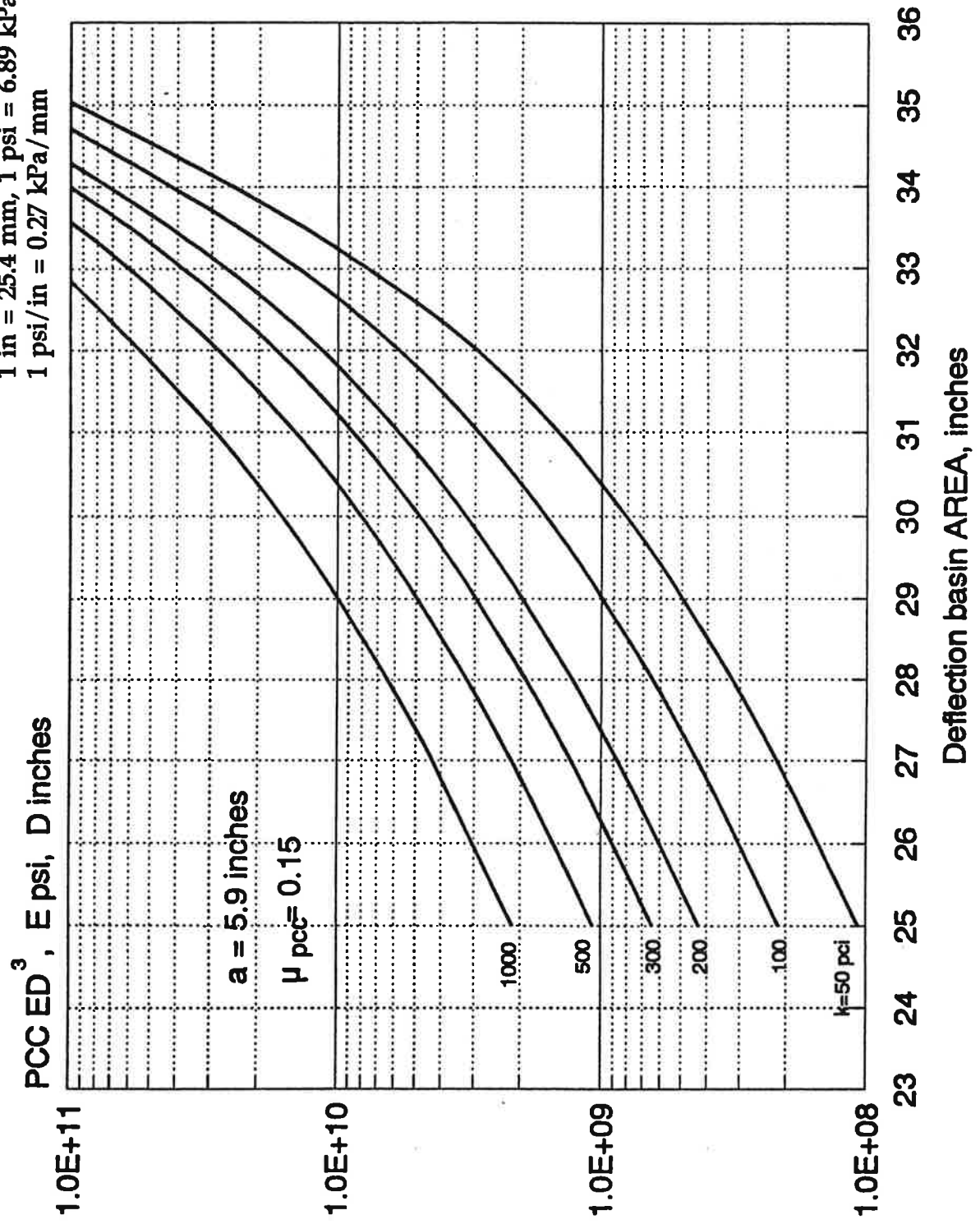


Figure A-32. Concrete E determination from k value, AREA, and slab thickness. [64]

pavements if the AREA and the k value are calculated with a maximum deflection d_0 which has been corrected for compression in the AC surface, as described in Appendix B.

The k value backcalculated with the 1993 Guide equations from deflections measured by an FWD or similar dynamic loading device are expected to be higher than the k values which would be obtained from a static load test on the subgrade or on the slab. The 1993 Guide recommended that these backcalculated k values be divided by two to approximate static k values for use in design.

Iowa Road Rater Method

In the 1980s, the Iowa Department of Transportation developed a method for determining springtime static k values from Road Rater deflection measurements. [76] The method was developed over several years by comparing springtime Road Rater deflection data from concrete pavements of various thicknesses and types of subgrades with static plate load k value data for subgrades of the same type. Details of the procedure are presented in Appendix B.

The k value obtained in this procedure is considered a static k value, i.e., what would be obtained in a static plate load test on the subgrade, and is also considered representative of springtime conditions only.

Other Advancements in k Backcalculation Methods

Recent research has produced several advances in the usefulness, efficiency, and accuracy of k value backcalculation methods. Among these are the following:

- **AREA backcalculation method for SHRP data:** Backcalculation equations similar to those presented in the 1993 AASHTO Guide have been developed for the six-sensor arrangement used to test SHRP LTPP experimental pavement sections. [77]
- **Equations for k and E for any sensor:** For an ℓ determined from some AREA definition or other method, the subgrade k and concrete E may be calculated from any sensor deflection. [77]
- **Solution for ℓ for any sensor arrangement:** Equations have also been developed for calculating ℓ from any two deflections measured away from the center of the load. This permits analysis of deflection data not collected using one of the standard AREA-based sensor arrangements (see Appendix B).
- **Solution for edge and corner k values:** Equations have been developed for backcalculating k at the edge or corner of a slab, using the measured edge or corner deflection and either an assumed slab E or an ℓ backcalculated in the slab interior by the AREA method. [53]
- **Slab size effects:** If L/ℓ , the ratio of least slab dimension (length or width in inches) to radius of relative stiffness, is less than about 8, incorrect k and E values may be backcalculated unless a slab size correction is applied. Equations have recently been developed to adjust the measured d_0 and calculated ℓ to account for finite slab size. [53]

- **Adjustments for embankment height and depth to rigid layer:** Although a granular base layer, typically 4 to 6 inches [102 to 152 mm] thick, has no significant effect on the k value, a substantial thickness (e.g., 1 or more ft [0.3 m]) of fill may yield a higher k value than that which would be assigned to the subgrade soil. In this study a nomograph was developed for adjusting the subgrade k when the pavement is built on fill material. This nomograph also provides an adjustment to the k value if a rigid layer (e.g., bedrock or very stiff clay) is located at a relatively shallow depth below the existing grade.
- **Slab and base elastic moduli:** The slab modulus backcalculated from these two-layer methods may be significantly higher than the actual concrete elastic modulus if a base is present. This is particularly true if the base is stabilized and a high degree of friction exists between the slab and base. The backcalculated slab modulus may be decomposed into moduli for the slab and base, assuming the two layers act as plates. This is done using the parallel axis theorem to solve for the two layer moduli which produce the same bending stiffness as the backcalculated modulus of the composite section. Procedures which have been developed for this purpose to date require an assumed interface condition (full slip or full friction) and an assumed ratio of the two layer moduli. [83]

Limitation of Plate Theory Backcalculation Methods

Most of the k value backcalculation methods developed to date (not including the Iowa Road Rater method, which is a direct correlation of deflection to k value) are based on plate theory, assuming pure bending of the concrete slab. A base layer, if it is considered, is also considered to exhibit plate behavior. In future work on k

value backcalculation methods for concrete pavements, three-dimensional finite element analysis is recommended to model the behavior of the slab and base as elastic layers on a k foundation. The effects on backcalculated k value of slab size, joint load transfer, base thickness and stiffness, slab/base interface friction, and slab deformation due to temperature or moisture gradients could also be examined more realistically using 3D finite element analysis.

BACKCALCULATION FIELD RESULTS

This section presents some backcalculation results from field testing which provide insight into subgrade k values and the factors which influence them.

Backcalculated versus Static k: AASHO Road Test Loop 1

Loop 1 of the AASHO Road Test was not trafficked during the experiment conducted between 1958 and 1960. It was used for strain measurements under vibratory loading and for materials sampling. Unlike the trafficked loops, Loop 1 was not incorporated into I-80 when the AASHO Road Test was completed, and still exists alongside I-80. The concrete pavement tangent of Loop 1 consists of two 12-ft-wide lanes of 15-ft [4.6 m] unreinforced concrete and 40-ft [12.2 m] reinforced concrete sections, with and without a 6-in [152 mm] granular base, and varying in slab thickness from 2.5 to 12.5 inches [63.5 to 317.5 mm].

Loop 1 was tested with a Falling Weight Deflectometer in May 1992 by the University of Illinois and the Illinois Department of Transportation. Slabs were tested at interior, outer edge, transverse joint, and corner locations. At every point tested, a sequence of five load drops was applied, with target loads of 12, 12, 5, 8 and 12 kips [53, 53, 22, 36, and 53 kN]. Many 2.5-in [63.5 mm] slabs were not tested because they had one or more cracks, or because trenches had been cut in them for soil sampling.

Effect of Temperature Gradient. Air, pavement surface, and pavement middepth temperatures were measured at the beginning and end of outer lane testing and again at the beginning and end of inner lane testing. The pavement surface temperatures were 7 to 20 °F [4 to 11°C] higher than those measured in holes drilled into the slabs, although likely variation in the depth of measurement makes it difficult to quantify the temperature gradients accurately. To assess whether or not the positive temperature gradients through the slabs affected the backcalculated k values, a plot of load versus maximum deflection (at the load plate center) was made for every interior basin, as recommended by Croveti. [53] If the maximum deflection plots on a straight line with respect to three or more load levels and the intercept of this line is close to zero, it is safe to assume that the interior of the slab is in full contact with the base or subgrade. All but a few of the nearly two hundred basins measured passed this test, so it was concluded that temperature curling would not influence the backcalculation results. This also suggests that the supporting base and subgrade are sufficiently soft that the slab edges were able to settle in when the slabs curled downward, so that the interiors of the slabs did not lose contact.

Joint Load Transfer. Deflections were measured across transverse joints at several slabs in the inner lane. The load transfer, computed as the unloaded side deflection as a percentage of the loaded side deflection, was about 75 to 90 percent. This load transfer level is reasonable, considering that the joints are dowelled and the Loop 1 was not subjected to truck traffic during or after the Road Test.

Backcalculation Results. The Loop 1 deflection data were analyzed in great detail. Careful efforts were made to account for the effects of temperature, load transfer, slab size, and concrete compressibility. The results are shown in Table A-6.

Table A-6. AASHO Road Test Loop 1 rigid pavement backcalculation results.

Slab Thickness (in)	Mean Backcalculated k (psi/in)	Mean Concrete E (million psi)
5.0	111	7.42
9.5	142	5.44
12.5	192	6.26
Overall Mean:	148	6.37

Note: 1 in = 25.4 mm, 1 psi/in = 0.27 kPa/mm, 1 million psi = 6890 MPa

Backcalculated k versus static k: The mean backcalculated k of 148 psi/in [40 kPa/mm], when divided by 2, yields an estimated static k of 74 psi/in [20 kPa/mm], which is within the range of 63 to 105 psi/in [17 to 28 kPa/mm] obtained from plate load tests on the subgrade, and within the 25 to 92 psi/in [7 to 25 kPa/mm] range of volumetric k values backcalculated by the Corps of Engineers from static load tests on top of the slabs. The mean backcalculated concrete E of 6.37 million psi [43890 MPa] is also very similar to the value of 6.25 million psi [43062 MPa] obtained from dynamic tests on beam samples.

Effect of Slab Thickness. Extensive efforts were made to account for finite slab dimensions, using a matrix of finite element runs for each slab thickness. The backcalculation results still show a slight trend of increasing k with increasing slab thickness. Stress-dependent subgrade behavior was ruled out as the cause for this phenomenon because for a given slab thickness, the backcalculated k values were consistent over a wide range of load levels.

It is not common to notice whether or not thickness variation affects backcalculated k values because most testing projects involve only one slab thickness at a given location. The AASHO Road Test site offers a rather rare opportunity to test a range of slab thicknesses of the same concrete, on the same subgrade. If slab thickness does affect backcalculated k values, even after corrections are made for temperature, load transfer, slab size, and concrete compressibility, one explanation is that the real behavior of the soil departs to some extent from theory. If the subgrade at the AASHO Road Test site were a true dense liquid, the backcalculated k value should be constant for all slab thicknesses. If, at the other extreme, the subgrade were a true elastic solid, elastic theory indicates (as Vesic and Saxena have shown) that the backcalculated k value should decrease with increasing slab thickness. [48] In fact just the opposite occurs.

A plausible explanation for the slab thickness effect observed in the AASHO Road Test backcalculation results is that the subgrade is not quite a true dense liquid, but possesses some low level of shear strength, albeit far less than is assumed if the soil is considered an elastic solid. The thicker the tested slab is, the larger the mass of soil within the radius of influence is, and the more net shear resistance to deformation is mobilized. For the range of slab thicknesses at the AASHO Road Test, which encompasses about the full range of typical concrete highway pavement thicknesses in the United States, and for the relatively low shear strength subgrade soil at the site, the slab thickness effect on k value does not appear to be very significant. For soils of higher shear strength and for thicker (e.g., airport) pavements, the slab thickness effect may be more significant.

Resilient Modulus versus k: AASHO Road Test Loop 1

The flexible pavement sections in Loop 1 were also tested on the same day that the rigid pavement sections were tested. The data and backcalculation results are shown in Table A-7. The flexible sections were tested primarily to measure the subgrade strength, rather than to backcalculate the pavement layer moduli, so the AC mix temperature was not monitored. A load sequence of 12, 12, 5, 8, and 12 kips [53, 53, 22, 36, and 53 kN] was applied; measurements from the last three drops were used for backcalculation. The results shown in Table A-7 were obtained from analysis of the deflections measured at 36 inches [914 mm] from the center of the load, using the procedure in the 1993 AASHTO Guide.

The overall mean backcalculated resilient modulus of about 11,600 psi [80 MPa] exceeds by a factor of 3.85 the M_R value of 3,000 psi [20.7 MPa] which was assigned to the AASHO Road Test soil in the derivation of the flexible pavement design equation. The 3,000 psi value [20.7 MPa] is consistent with laboratory resilient modulus tests (wet of optimum, 6 psi [41 kPa] deviator stress) on soil samples from the site. The backcalculated moduli show a decreasing trend with increasing load level, which suggests possible stress-dependent behavior. The backcalculated moduli do not show any increasing trend with increasing pavement thickness, which suggests that for all of the sections tested the 36-inch [914 mm] deflection measurement distance was adequate for measuring the subgrade response independent of any significant influence of the upper layers.

The mean backcalculated modulus of 11,600 psi [80 MPa], while high with respect to the laboratory value of 3,000 psi [20.7 MPa], is still indicative of a weak subgrade, which is consistent with the plate load k value and backcalculated k value results.

Table A-7. AASHO Road Test Loop 1 flexible pavement backcalculation results.

Sta	AC (in)	Base (in)	Sub (in)	Load (lbs)	Δ_{36} (mils)	M_R (psi)	Mean M_R (psi)
288.68	3	6	16	4,904 7,216 10,328	3.26 5.31 8.04	10,029 9,060 8,564	9,217
285.08	5	0	0	5,016 7,464 10,288	2.09 3.46 4.98	16,000 14,382 13,772	14,718
sect 829	3	0	8	5,064 7,704 10,352	2.53 4.38 5.31	13,344 11,726 12,997	11,859
280.30	3	6	8	4,656 7,160 10,352	2.29 3.62 5.31	13,555 13,186 12,997	13,246
278.90	1	6	8	4,320	1.77	16,271	16,271
278.13	3	6	0	4,728 7,224 10,072	3.42 5.87 9.00	9,216 8,204 7,461	8,294
sect 869	3	0	8	4,072 6,408 9,288	2.53 4.26 5.83	10,730 10,028 10,620	10,460

Notes: 1 in = 25.4 mm, 1 pound = 4.45 kN, 1 mil = 25.4 μ m, 1 psi = 6.89 kPa

M_R calculated from 1993 AASHTO Guide equation $M_R = (0.24 P) / (d_r r)$,
where P = load (lbs), d_r = deflection (in), r = radial distance (in)

Overall mean backcalculated $M_R = 11,561$ psi [79.65 MPa]

Backcalculated versus Static k: Willard Airport

The University of Illinois' Willard Airport in Savoy, Illinois has several concrete pavements which have been monitored for many years by destructive and nondestructive testing and condition surveys. The results of plate bearing tests conducted on the silty clay subgrade yielded a mean k value of 73 psi/in [20 kPa/mm]. The subgrade soil has a density of about 93 lbs/ft³ [1490 kg/m³] and a CBR value of about 5.3. [78]

FWD testing was conducted on several pavements at Willard Airport in 1992. The pavements included new and old concrete slabs on stabilized or granular bases, two bonded concrete overlays, and an unbonded concrete overlay. The backcalculation results for these pavements are summarized in Table A-8.

The mean backcalculated k value for the Willard Airport pavements was 234 psi/in [63 kPa/mm]. This value is about three times higher than the k value obtained from the static plate load tests. The backcalculated k values are higher for the pavements with greater total PCC thickness (original slab plus overlay). This is probably due to the finite slab size effect, for which these backcalculation results were not adjusted. A total PCC thickness of 15 inches [381 mm] or more for a relatively small joint spacing L produces an L/ℓ ratio far less than the L/ℓ of about 8 needed to approximate infinite slab behavior.

For the thinner pavements, the mean backcalculated k value is 148 psi/in [40 kPa/mm], which when divided by 2 yields an estimated static k value of 74 psi/in [20 kPa/mm], practically the same as the plate load k value.

Table A-8. Backcalculation results for concrete pavements and concrete overlays at Willard Airport.

Pavement	Description	Backcalc k (psi/in)	Backcalc k / 2 (psi/in)	Backcalc Concrete E (million psi)
New Apron	15-in PCC 4-in OGATB	332	166	5.10
New Taxiway	18-in PCC no base	194	97	3.95
Southwest Taxiway	7-in BOL 8-in PCC 8-in gran	252	126	4.90
Runway 18-36	8-in PCC (very old) 8-in gran	142	71	6.90
Northwest Taxiway	11-in BOL 8-in PCC 8-in gran	242	121	3.70
Gen Aviation Ramp	6-in UBOL separation layer 9-in PCC (old, D-cracked) 8-in gran	320	160	(see note)
Old Ramp	9-in PCC (old, D-cracked) 8-in gran	154	77	< 1.00

1 in = 25.4 mm, 1 psi/in = 0.27 kPa/mm, 1 million psi = 6890 MPa

OGATB = open-graded asphalt-treated base, BOL = bonded concrete overlay, UBOL = unbonded concrete overlay, gran = granular base

Concrete E values for overlaid sections were backcalculated two ways, with overlay thickness only and with total thickness, to assess bond. Values shown for Southwest Taxiway and Northwest Taxiway are effective E of total thickness.

Northwest Taxiway was constructed as "partially bonded" (no surface preparation, no separation layer). Backcalculation results indicates the layers are bonded.

General Aviation Ramp backcalculation using only 6-in [152 mm] overlay thickness yields unreasonably high value (about 13 million psi [89570 MPa]). Backcalculation using the total 15-in [381 mm] thickness of overlay and original slab yields unreasonably low value (about 1 million psi [6890 MPa]). These results suggest a significant degree of friction between the two slabs, and possibly that the old pavement's sound concrete thickness is less than 9 inches.

Subgrade and Base Type versus k: RPPR Field Studies

Field evaluations of 95 in-service JPCP and JRCP highway pavements located throughout the United States were conducted for the FHWA's "Rigid Pavement Performance and Rehabilitation" (RPPR) study. [79] Deflection testing was conducted on these pavements using an FWD. The backcalculated k values are summarized by subgrade soil classification in Table A-9. The values shown are estimated static values obtained by dividing the backcalculated values by 2.

Table A-9. Backcalculated k values by soil class, from RPPR data. [79]

Subgrade Class	Number of Projects	Minimum Static k value (psi/in)	Maximum Static k value (psi/in)
A-1-a	10	116	310
A-1-b	0	---	---
A-2-4	22	64	374
A-2-5	0	---	---
A-2-6	8	64	336
A-2-7	1	128	128
A-3	2	189	265
A-4	17	95	314
A-5	0	---	---
A-6	22	78	311
A-7	1	170	170

1 psi/in = 0.27 kPa/mm

The ranges of estimated static k values for the various soil classes appear to be very reasonable in most cases. A great many unknown factors can produce scatter in these results, including such things as the season in which the pavement was tested, the uniformity of the subgrade with depth, whether or not the pavement was in a cut or fill section, and whether a rigid layer is present at a shallow depth. These backcalculation results have also not been adjusted for slab size effects. Presumably deflection testing was conducted at times of the day when the slabs were not curled. Nonetheless, the results shown in Table A-9 demonstrate that backcalculated k values can be used to estimate static k values which are of reasonable magnitude for the subgrade type, even when the slab is constructed on a stiff base. About half of these pavements were built on stabilized bases (asphalt-treated, cement-treated, and lean concrete) and the other half were built on aggregate bases or no base at all.

In general, the sections with treated bases had a somewhat higher average k value than the sections with aggregate base or no base (estimated mean static of 255 psi/in for treated bases, versus 186 psi/in for untreated bases and no base). However, the results are mixed when examined for specific experimental projects which have different base types on the same subgrade, as shown in Table A-10.

This magnitude of increase for the treated base sections is much less than would be predicted by the conventional top-of-base k value charts, and much less than the composite k values that would be predicted for treated bases by the 1986 Guide procedure. One possible explanation for the difference is slab size effect: the L/ℓ ratio for a slab with a bonded, stabilized base is lower than the L/ℓ ratio for a slab of the same dimensions on a granular base or no base at all. The lower the L/ℓ ratio is below 8, the less applicable are the infinite slab theory backcalculation methods, without adjustment.

Table A-10. Effect of treated and untreated bases on k, for projects with different bases at the same location, from RPPR data. [79].

Location (State) of Project	Backcalculated k (psi/in)		
	Aggregate Base	Treated Base	Ratio
North Carolina	554	535	< 1.0
Ohio	395	482	1.2
New York	577	560	< 1.0
Michigan	304	468	1.5
Minnesota	200	270	1.3
Arizona	425	602	1.4

1 psi/in = 0.27 kPa/mm

These comparisons, and others in this appendix, are based on the rule of thumb division of dynamic k values by a factor of two to estimate static k values. It is extremely difficult to provide a more sophisticated method for converting dynamic k values to static k values, due to the complexities of modelling dynamic soil behavior and the sparsity of available data on side-by-side comparisons of dynamic and static soil response. The division-by-two rule has been shown to produce reasonable values in many cases. Nonetheless, it may be true, and future research may discover, whether the relationship between backcalculated and static k values varies in a predictable way as a function of soil properties, loading characteristics, or other factors.

Subgrade Type versus k: LTPP Study

Some preliminary analyses of the deflection data collected from the GPS 3 and GPS 4 sections in the LTPP study have been conducted to date. Subgrade k values and concrete E values were backcalculated using the SHRP LTPP method described in Appendix B. The subgrade k value results are presented by subgrade class in Table A-11.

Table A-11. Backcalculated k values by soil class, from LTPP GPS 3 and 4.

Subgrade Class	Number of Projects	Minimum Static k (psi/in)	Maximum Static k (psi/in)	Average Static k (psi/in)
A-1-a	5	108	181	142
A-1-b	5	92	334	208
A-2-4	16	48	535	188
A-2-5	0	---	---	---
A-2-6	2	101	370	235
A-2-7	4	68	239	133
A-3	13	60	271	135
A-4	24	54	395	154
A-5	2	66	102	84
A-6	26	61	512	146
A-7-5	5	79	181	117
A-7-6	18	48	248	126

1 psi/in = 0.27 kPa/mm

The k value results for the LTPP sections are similar in many respects to the results for the RPPR sections shown in Table A-9. In both data sets, the range of k values obtained for subgrades identified as A-1 material (about 100 to 300 psi/in [27 to 81 kPa/mm]) is considerably lower than the A-1 k value range suggested by the Corps of Engineers and PCA charts (300 psi/in [81 kPa/mm] or more). Since it is very rare for a natural subgrade to be an A-1 material, these low values may indicate that the pavement and base are built on a layer of A-1 material above the natural subgrade.

The LTPP results are also similar to the RPPR results in that the k values are generally within the ranges suggested by the Corps of Engineers and PCA charts for the respective subgrade classes, even though the data set includes pavements with a variety of untreated and treated bases, from granular materials to lean concrete. Although the base type does seem to have a significant effect on the backcalculated concrete E value, the LTPP data do not indicate that base type significantly affects backcalculated k values.

Plate Load k on High-Strength Base: Japan

A Japanese study of deflection and strain measurements on concrete airfield pavements provides an interesting comparison of top-of-base plate load k values and k values backcalculated from slab deflections. [80] Each section of concrete pavement was constructed on a crushed stone layer either 4 or 8 inches [102 or 203 mm] thick, which was in turn placed on a 12-in [305 mm] layer of pit gravel. Plate load tests were conducted on top of the base to determine k values.

After the concrete slabs were constructed, static load tests were conducted on the slabs with a 12-in [305 mm] diameter plate. A 45-ton [400 kN] truck provided the

reaction force for the load tests at the slab interiors, edges, and corners.

Westergaard's equations were used to backcalculate k values using the maximum deflections and the concrete E determined from laboratory tests.

The k values measured on top of the base were consistently two to four or more times the k values backcalculated from slab deflections, and this discrepancy increased with increasing load level. These results confirm again that plate tests on base layers yield misleadingly high k values, as slab deflection test results show.

Effect of Rigid Layer Beneath Subgrade: Dulles Airport

Dulles International Airport near Washington, D. C. provides an interesting example of the effect of a shallow rigid layer on deflections and backcalculated k values. [81] The site upon which the airport was built has shallow bedrock (stratified red shale), varying in depth from 0 to 6 ft [1.8 m] throughout most of the airport property. The overlying soils are red clayey silt and silty clay (FAA class E-7, liquid limit 34, plasticity index 17, dry density 104 lb/ft³ [1666 kg/m³]). If the bedrock layer were not present and this soil were present to a substantial depth, it might be expected to have a static k value in the range of about 100 to 250 psi/in [27 to 67 kPa/mm].

The concrete slabs are all 15 inches [381 mm] thick. The elastic modulus of the concrete was estimated at 5.4 million psi [37200 MPa] from sonic modulus tests on cores and from backcalculation of WES Vibrator and FWD deflection data. The backcalculated k values for the 35 pavement sections tested ranged from 260 to 1000 psi/in [70 to 270 kPa/mm], and averaged 480 psi/in [130 kPa/mm]. These correspond to an estimated static k value range of 130 to 500 psi/in [35 to 135 kPa/mm], and an estimated average static k value of 240 psi/in [65 kPa/mm]. There

is, however, considerable variation in fill heights and depths to bedrock within a section, and a corresponding variation in k values, as shown in Figure A-33.

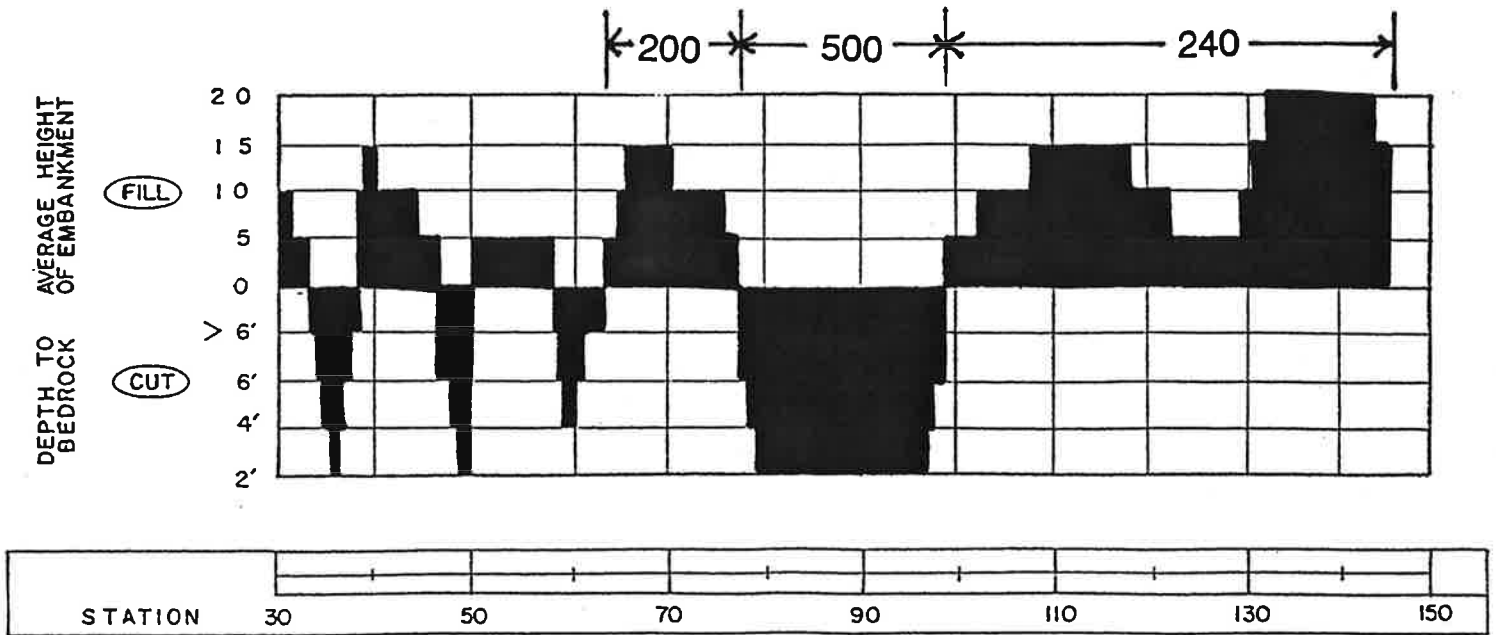
The average static k value is within but near the high end of the range of values predicted for the subgrade soil type, which means that about half of the values are above the range expected for the subgrade type. The highest values (500 psi/in [135 kPa/mm]) are twice the expected upper limit (about 250 psi/in [67 kPa/mm]) for the subgrade type. The highest values were reported for areas with bedrock at a very shallow depth (0 to 2 ft [0.6 m]).

These results suggest that bedrock or a similar stiff layer at a shallow depth (i.e., within 10 ft [3 m] of the subgrade surface) may increase k values to as much as twice the level which would otherwise be assigned to the subgrade soil based on its classification, density, and other properties. This type of field information is valuable because a shallow rigid layer is considered to be significant in producing an effectively stiffer foundation, but the magnitude of the increase which should be expected due to a rigid layer is extremely difficult to quantify. Simulating the effect of a rigid layer in an elastic layer computer analysis can yield much greater changes in k value (e.g., by a factor of five or more), which may be very erroneous. Additional collection and analysis of field data on rigid layer depth and its effect on subgrade k values is needed to more accurately quantify this effect.

Soft Subgrade K Value with Stabilized Base: Utah I-15 in Salt Lake City [84]

This highway pavement consists of a 9-in [229 mm] undowelled JPCP over a 4-in [102 mm] cement-treated base, over a 12-in [305 mm] granular borrow layer consisting of AASHTO A-1 and A-2 materials. Beneath the borrow layer is some embankment material of varying thickness. Below the embankment are very soft lake

Backcalculated k value:



1 ft = 0.3 m, 1 psi/in = 0.27 kPa/mm

Backcalculated k value:

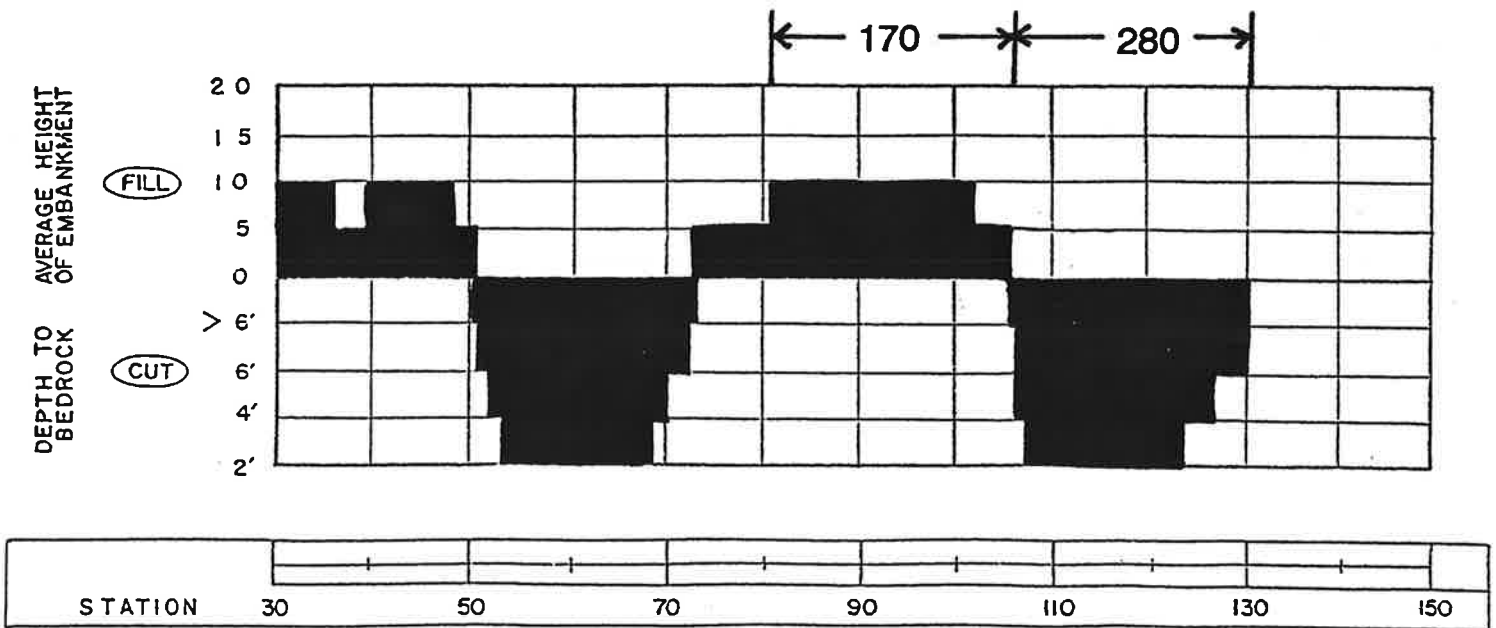


Figure A-33. Effect of fill and bedrock on backcalculated k values at Dulles International Airport. [81]

bed clays with CBR values of 0 to 3 percent. During the construction of I-15, vertical sand drains were installed in these soft soils to drain water as the soils consolidated under the weight of the embankment. The embankment had to be constructed in 1-ft [0.3 m] increments because of the large volume of water that was drained from the underlying soils during consolidation.

This pavement is over 25 years old and has shown excellent performance with virtually no cracking and little faulting. The pavement was tested with an FWD, and the k value was backcalculated using the 1993 AASHTO Guide procedure described in Appendix B. The backcalculated k values ranged from 49 to 234 psi/in [13 to 63 kPa/mm], corresponding to a range of estimated static k values of 25 to 115 psi/in [7 to 31 kPa/mm]. These are among the lowest k values observed anywhere, despite the presence of the embankment, borrow layer, and cement-treated base. The k values were higher in one end of the project where the embankments were over 10 ft [3 m] high, and lower in the other end where the embankments were shallower.

It is also interesting to note that this pavement has shown no fatigue-related cracking in over 25 years of heavy traffic for a relatively thin slab. A structural analysis conducted assuming that the slab and base were not bonded indicated that the pavement should have failed long ago from fatigue damage. A second analysis conducted assuming that the cement-treated base was bonded to the slab indicated that there should be very little structural fatigue damage, which is consistent with the performance observed. [84]

Effect of K Value on Slab Cracking: Chile

A major research study has been underway in Chile for several years to monitor the deterioration of undowelled JPCP. [85] Twenty of these pavements were

instrumented and tested in a variety of ways. Results from this monitoring show a "permanent upward curling of slabs in all pavement sections ... The curling is demonstrated in the field by the perceptible rocking of the slabs under the early morning traffic and by the systematic transverse cracking and corner breaks of some rather new pavements with no signs of pumping. Cracking seems to start from the surface downward and from the edges inward." [85] The researchers have also concluded that moisture gradients in the concrete slabs have produced slab stresses, deformations, and increased deflections under load as significant as those caused by temperature gradients. [86]

Deflection data from the slab centers and an estimate of the concrete modulus of elasticity were obtained and the k value backcalculated using Westergaard's center deflection equation. The backcalculated k values ranged from 87 to 675 psi/in [23.5 to 182 kPa/mm] and seemed to vary considerably depending on the subgrade and to a lesser extent on the base type. The base types include untreated aggregate base and cement-treated base. Some of the bases were constructed on new alignments where the subgrade was uniform, and some were constructed over old AC or PCC pavement. Differences in slab thickness, joint spacing and traffic loadings between the sections make it difficult to make direct comparisons. However, the results shown in Table A-12 do indicate some interesting trends.

Pavements constructed over old deteriorated pavements had backcalculated k values about two times the k value of pavements constructed on a new alignment with a typical subgrade. This may be due to the low L/ℓ of these pavements (small slab size with respect to their total thickness and stiffness). Pavements constructed over old pavements had about four times the percent slabs cracked that pavements constructed on new alignments had. The old pavements may have provided a stiffer

Table A-12. Mean backcalculated k values from 20 Chilean JPCP test sections.

Base Type	New Alignment	Constructed Over Old AC or PCC Pavement
Untreated Aggregate*	k = 137 psi/in n = 4 (no. sections) C = 11 % slabs cracked	k = 287 n = 6 C = 15
Cement-Treated Aggregate	k = 232 n = 1 C = 0	k = 448 n = 9 C = 31
Mean k value Total no. sections Mean cracking	k = 185 n = 5 C = 6 %	k = 368 n = 15 C = 23

* Three sections included cement-stabilized material.
1 psi/in = 0.27 kPa/mm

foundation and contributed to increased stresses in the slabs when deformed by temperature and moisture gradients, producing increased cracking. These results are consistent with the 3D finite element analyses done in this study and proposed revised AASHTO design procedure.

REFERENCES FOR APPENDIX A

1. Winkler, E., "Die Lehre von der Elastizität und Festigkeit," (The Theory of Elasticity and Stiffness), H. Dominicus, Prague, 1867.
2. McCullough, B. F. and Boedecker, K. J., "Use of Linear-Elastic Layered Theory for the Design of CRCP Overlays," Highway Research Record No. 291, 1968.
3. Hertz, H., "Über das Gleichgewicht schwimmender elastischer Platten," (On the Equilibrium of Floating Elastic Plates), Wiedemann's Annalen der Physik und Chemie, volume 22, 1884, pp. 449-455.
4. Föppl, A., Technische Mechanik, volume 5, 1907, pp. 288-294.
5. Koch, J. J., "Berekening van vlakke platen, ondersteund in de hoekpunten van een willekeurig rooster," De Ingenieur, No. 6, 1925.
6. Schleicher, F., "Über Kreisplatten auf elastischer Unterlage," Festschrift sur Hundertjahrfeier der Technischen Hochschule Karlsruhe, 1925.
7. Selvadurai, A. P. S., Elastic Analysis of Soil-Foundation Interaction, Developments in Geotechnical Engineering, Volume 17, Elsevier Scientific Publishing Company, the Netherlands, 1979.
8. Peck, R. B., W. E. Hanson, and T. H. Thornburn, Foundation Engineering, second edition, John Wiley and Sons, New York, 1974.

9. Westergaard, H. M., "Computation of Stresses in Concrete Roads, Proceedings, Highway Research Board, 1925. Also published as "Stresses in Concrete Pavements Computed by Theoretical Analysis," Public Roads, Volume 7, Number 2, 1926.
10. Westergaard, H. M., "Theory of Stresses in Road Slabs," Proceedings, Fourth Annual Meeting of the Highway Research Board, 1925.
11. Bijls, A., Essais de Résistance et D'Élasticité du Terrain de Fondation de la Nouvelle Écluse Maritime D'Ymuiden (Hollande), Le Génie Civil, Vol. 82, 1923.
12. Goldbeck, A. T., "Researches on the Structural Design of Highways by the United States Bureau of Public Roads," Transactions, American Society of Civil Engineers, Volume 88, 1925.
13. Goldbeck, A. T. and M. J. Bussard, "The Supporting Value of Soil as Influenced by the Bearing Area, Public Roads, Vol. 5, No. 11, 1925.
14. Teller, L. W. and E. C. Sutherland, "The Structural Design of Concrete Pavements, Part 1, A Description of the Investigation," Public Roads, Vol. 16, No. 8, 1935.
15. Teller, L. W. and E. C. Sutherland, "The Structural Design of Concrete Pavements, Part 2, Observed Effects of Variations in Temperature and Moisture on the Size, Shape and Stress Resistance of Concrete Pavement Slabs," Public Roads, Vol. 16, No. 9, 1935.
16. Teller, L. W. and E. C. Sutherland, "The Structural Design of Concrete Pavements, Part 3, A Study of Concrete Pavement Cross Sections," Public Roads, Vol. 16, No. 10, 1935.

17. Teller, L. W. and E. C. Sutherland, "The Structural Design of Concrete Pavements, Part 4, A Study of the Structural Action of Several Types of Transverse and Longitudinal Joint Designs," Public Roads, Vol. 17, Nos. 7 and 8, 1936.
18. Teller, L. W. and E. C. Sutherland, "The Structural Design of Concrete Pavements, Part 5, An Experimental Study of the Westergaard Analysis of Stress Conditions in Concrete Pavements of Uniform Thickness," Public Roads, Vol. 23, No. 8, 1943.
19. Kelley, E. F., "Application of the Results of Research to the Structural Design of Concrete Pavements," Public Roads, Vol. 20, No. 5, 1939.
20. U.S. Army Corps of Engineers, "Wright Field Slab Tests," Ohio River Division, Cincinnati Testing Laboratories, Cincinnati, Ohio, 1942.
21. U. S. Army Corps of Engineers, "Report on Special Field Bearing Tests on Natural Subgrade and Prepared Subbase Using Different Size Bearing Plates," Ohio River Division, Cincinnati Testing Laboratories, 1943.
22. Sale, J. P. and Hutchinson, R. L., "Development of Rigid Pavement Design Criteria for Military Airfields," Journal of the Air Transport Division, Proceedings of the American Society of Civil Engineers, Vol. 85, No. AT3, July 1959.
23. Sale, J. P., "Rigid Pavement Design for Airfields," Proceedings, First International Conference on Concrete Pavement Design, Purdue University, West Lafayette, Indiana, 1977.

24. Phillippe, R. R., "Field Bearing Tests Applied to Pavement Design," Symposium on Load Tests of Bearing Capacity of Soils, American Society for Testing and Materials, Special Technical Publication No. 79, 1947.
25. U. S. Department of Defense, "Test Method for Pavement Subgrade, Subbase, and Base-Course Materials," Military Standard MIL-STD-621A.
26. U. S. Army Corps of Engineers, "Rigid Plate-Bearing Test Investigation," Waterways Experiment Station, Vicksburg, Mississippi, 1945.
27. U. S. Army Corps of Engineers, "Determination of High Values of the Subgrade Modulus, k , from the Plate Bearing Test," Rigid Pavement Laboratory, Ohio River Division, Mariemont, Ohio, 1953.
28. Middlebrooks, T. A. and G. E. Bertram, "Soil Tests for Design of Runway Pavements," Proceedings, Highway Research Board, 1942.
29. U. S. Department of the Army, Technical Manual TM 5-824-3.
30. U.S. Department of the Army, "Rigid Airfield Pavements," Engineering and Design Manual EM 1110-45-303, Office of the Chief of Engineers, 1958.
31. Portland Cement Association, "Thickness Design for Concrete Pavement," 1966.
32. Packard, R. G., "Design of Concrete Airport Pavement," Portland Cement Association Engineering Bulletin, 1973.
33. Campen, W. H. and J. R. Smith, "Use of Load Tests in the Design of Flexible Pavements," Symposium on Load Tests of Bearing Capacity of Soils, American Society for Testing and Materials, Special Publication No. 79, 1947.

34. Hittle, J. E. and W. H. Goetz, "Factors Influencing the Load-Carrying Capacity of Base-Subgrade Combinations," Proceedings, Highway Research Board, 1946.
35. McLeod, N. W., "A Canadian Investigation of Load Testing Applied to Pavement Design," Symposium on Load Tests of Bearing Capacity of Soils, American Society for Testing and Materials, Special Technical Publication No. 79, 1947.
36. Ahlvin, R. G., "Origin of Developments for Structural Design of Pavements," Technical Report GL-91-26, U.S. Army Corps of Engineers, Waterways Experiment Station, Vicksburg, Mississippi, 1991.
37. Highway Research Board, "The AASHO Road Test, Report 1, History and Description of Project," Special Report 61A, 1961.
38. Highway Research Board, "The AASHO Road Test, Report 2, Materials and Construction," Special Report 61B, 1962.
39. Highway Research Board, "The AASHO Road Test, Report 3, Traffic Operations and Pavement Maintenance," Special Report 61C, 1962.
40. Highway Research Board, "The AASHO Road Test, Report 4, Bridge Research," Special Report 61D, 1962.
41. Highway Research Board, "The AASHO Road Test, Report 5, Pavement Research," Special Report 61E, 1962.
42. Highway Research Board, "The AASHO Road Test, Report 6, Special Studies," Special Report 61F, 1962.

43. Highway Research Board, "The AASHO Road Test, Report 7, Final Summary," Special Report 61G, 1962.
44. Highway Research Board, "The AASHO Road Test, Proceedings of a Conference Held May 16-18, 1962, St. Louis, Mo.," Special Report 73, 1962.
45. Langsner, G., T. S. Huff, and W. J. Liddle, "Use of Road Test Findings by AASHO Design Committee," from "The AASHO Road Test, Proceedings of a Conference Held May 16-18, 1962, St. Louis, Mo.," Highway Research Board Special Report No. 73, 1962.
46. U.S. Army Corps of Engineers, "Results of Modulus of Subgrade Reaction Determination at the AASHO Road Test Site by Means of Pavement Volumetric Displacement Test," Ohio River Division Laboratories, April 1962.
47. Hudson, W. R., "Comparison of Concrete Pavement Load-Stresses at AASHO Road Test with Previous Work," Highway Research Record No. 42, 1963.
48. Vesic, A. S. and S. K. Saxena, "Analysis of Structural Behavior of AASHO Road Test Rigid Pavements," NCHRP Report No. 97, 1970.
49. Childs, L. D. and Kapernick, J. W., "Tests of Concrete Pavements on Crushed Stoned Subbases," Proceedings of the American Society of Civil Engineers, Vol. 89, No. HW-1, 1963.
50. Childs, L. D., "Cement-Treated Subbases for Concrete Pavements," Highway Research Record No. 189, 1967.

51. Nussbaum, P. J. and Larsen, T. J., "Load-Deflection Characteristics of Soil-Cement Pavements," Highway Research Record No. 86, 1965.
52. Packard, R. G., "Design of Concrete Airport Pavement," Portland Cement Association, Engineering Bulletin, 1973.
53. Crovetti, J. A., "Evaluation of Jointed Concrete Pavement Systems Incorporating Open-Graded Permeable Bases," Ph.D. thesis, University of Illinois at Urbana-Champaign, 1994.
54. American Association of State Highway and Transportation Officials, "Interim Guide for Design of Pavement Structures," Washington, D. C., 1972.
55. Darter, M. I., "Design of Zero-Maintenance Plain Jointed Concrete Pavement, Volume 1 -- Development of Design Procedures," University of Illinois at Urbana-Champaign, Report No. FHWA-RD-77-111, 1977.
56. Darter, M. I. and E. J. Barenberg, "Design of Zero-Maintenance Plain Jointed Concrete Pavement, Volume 2 -- Design Manual," University of Illinois at Urbana-Champaign, Report No. FHWA-RD-77-112, 1977.
57. Thompson, M. R. and Q. L. Robnett, "Resilient Properties of Subgrade Soils," Illinois Cooperative Highway Research Program, Report No. UILU-ENG-76-2009, University of Illinois and Illinois Department of Transportation, 1976.
58. American Association of State Highway and Transportation Officials, Guide for Design of Pavement Structures, Washington, D.C., 1986.

59. American Association of State Highway and Transportation Officials, Guide for Design of Pavement Structures, Volume 2 -- Appendices, Washington, D. C., 1986.
60. L. A. Palmer, "Field Loading Tests for the Evaluation of the Wheel-Load Capacities of Airport Pavements," American Society for Testing and Materials, Special Technical Publication No. 79, Symposium on Load Tests of Bearing Capacity in Soils, Atlantic City, N.J., June 16-20, 1947.
61. Sprague, J. C., F. M. Bell, and K. W. Schwartz, Discussion of "Field Loading Tests for the Evaluation of the Wheel-Load Capacities of Airport Pavements," American Society for Testing and Materials, Special Technical Publication No. 79, Symposium on Load Tests of Bearing Capacity in Soils, Atlantic City, N.J., June 16-20, 1947.
62. Rutledge, P. C., "Relation of Undisturbed Sampling to Laboratory Testing," Transactions, American Society of Civil Engineers, No. 109, 1944.
63. Peck, R. B., "Sampling Methods and Laboratory Tests for Chicago Subway Soils," Proceedings, Purdue Conference on Soil Mechanics and its Applications, Purdue University, West Lafayette, Indiana, July 1940.
64. American Association of State Highway and Transportation Officials, Guide for the Design of Pavement Structures, Washington, D.C., 1993.
65. McCullough, B. F. and G. E. Elkins, "CRC Pavement Design Manual," Austin Research Engineers, Inc., 1979.

66. Scrivner, F. H., C. H. Michalak, and W. M. Moore, "Calculation of the Elastic Moduli of a Two-Layer Pavement System from Measured Surface Deflection," Highway Research Record No. 431, 1973.
67. Hoffman, M. S. and M. R. Thompson, "Mechanistic Interpretation of Nondestructive Pavement Testing Deflections," Transportation Engineering Series No. 32, Illinois Cooperative Highway and Transportation Research Series No. 190, University of Illinois at Urbana-Champaign, 1981.
68. ERES Consultants, Inc., "Nondestructive Structural Evaluation of Airfield Pavements," prepared for U.S. Army Corps of Engineers Waterways Experiment Station, Vicksburg, Mississippi, 1982.
69. Foxworthy, P. T., "Concepts for the Development of a Nondestructive Testing and Evaluation System for Rigid Airfield Pavements," Ph.D. thesis, University of Illinois at Urbana-Champaign, 1985.
70. Barenberg, E. J. and K. A. Petros, "Evaluation of Concrete Pavements Using NDT Results," Project IHR-512, University of Illinois and Illinois Department of Transportation, Report No. UILU-ENG-91-2006, 1991.
71. Ioannides, A. M., "Dimensional Analysis in NDT Rigid Pavement Evaluation," Transportation Engineering Journal, American Society of Civil Engineers, Volume 116, No. TE1, 1990.
72. Westergaard, H. M., "Stresses in Concrete Runways of Airports," Proceedings, Highway Research Board, Volume 19, 1939.

73. Losberg, A., Structurally Reinforced Concrete Pavements, Doktorsavhandlingar Vid Chalmers Tekniska Högskola, Göteborg, Sweden, 1960.
74. Ioannides, A. M., E. J. Barenberg, and J. A. Lary, "Interpretation of Falling Weight Deflectometer Results Using Principles of Dimensional Analysis," Proceedings, Fourth International Conference on Concrete Pavement Design and Rehabilitation, Purdue University, West Lafayette, Indiana, 1989.
75. Hall, K. T., "Performance, Evaluation, and Rehabilitation of Asphalt-Overlaid Concrete Pavements," Ph.D. thesis, University of Illinois at Urbana-Champaign, 1991.
76. Potter, C. J. and K. L. Dirks, "Pavement Evaluation Using the Road RaterTM Deflection Dish," Final Report, Project MLR-89-2, Iowa Department of Transportation, 1989.
77. Hall, K. T., "Backcalculation Solutions for Concrete Pavements," technical memo prepared for SHRP Contract P-020, "Long-Term Pavement Performance Data Analysis," 1992.
78. Barenberg, E. J. and B. L. Ratterree, "Fully Bonded Concrete Overlay for an Airport Runway," Proceedings, ASCE International Air Transportation Conference, New Orleans, Louisiana, 1979.
79. Smith, K. D., D. G. Peshkin, M. I. Darter, A. L. Mueller, and S. H. Carpenter, "Performance of Jointed Concrete Pavements, Phase I, Volume IV -- Appendix A, Project Summary Reports and Summary Tables," Report No. FHWA-RD-89-139, 1990.

80. Kogure, K. and Sakai, T., "Measurements of Deflection and Strain of Airfield Rigid Pavement for Deterioration and Evaluation," Proceedings, International Conference on Bearing Capacity of Roads and Airfields, Minneapolis, Minnesota, July 1994.
81. Crawford, Murphy, and Tilly, Inc.; ERES Consultants, Inc.; E. J. Barenberg; and M. Y. Shahin; "Evaluation of Airfield Pavements at Dulles International Airport," report for U.S. Department of Transportation, Federal Aviation Administration, 1984.
82. Sparkes, F. N. and A. F. Smith, Concrete Roads, copyright Edward Arnold and Company, London, 1952.
83. Ioannides, A. M. and Khazanovich, L., "Backcalculation Procedures for Three-Layered Concrete Pavements," Proceedings, Fourth International Conference on Bearing Capacity of Roads and Airfields, Minneapolis, Minnesota, 1994.
84. Beckemeyer, C. B. and M. I. Darter, "Utah I-15 Pavement Evaluation," Final Report for Utah DOT, ERES Consultants, Inc., 1993.
85. Poblete, M., R. Salsilli, R. Valenzuela, A. Bull, and P. Spratz, "Field Evaluation of Thermal Deformations in Undowelled PCC Pavement Slabs," Transportation Research Record No. 1207, 1989.
86. Poblete, M., A. Garcia, J. David, P. Ceza, and R. Espinosa, "Moisture Effects on the Behaviour of PCC Pavements," Proceedings, Second International Workshop on the Design and the Evaluation of Concrete Pavements, Sigüenza, Spain, October 1990.

APPENDIX B
METHODS FOR DETERMINING K VALUE

INTRODUCTION

Three categories of methods for determining a k value for use in concrete pavement design are presented in this appendix. The first category is the correlation methods category. Guidelines are presented for selecting an appropriate k value based on other information available, including soil classification, resilient modulus, moisture level, density, California Bearing Ratio (CBR), Hveem Stabilometer data (R-value), or Dynamic Cone Penetrometer (DCP) data. These correlation methods are anticipated to be used routinely for design.

The second category of methods for determining k value is the deflection testing and backcalculation methods category. These methods are suitable for determining k value for design of overlays of existing pavements, or for design of a reconstructed pavements on existing alignments, or for design of similar pavements in the same general location on the same type of subgrade. An agency may also use backcalculation methods to develop correlations between nondestructive deflection testing results and subgrade types and properties.

The third category of methods for determining k value is the plate testing methods category. The standard ASTM, AASHTO, and Corps of Engineers nonrepetitive and repetitive plate loading test methods are summarized, as well as the German plate load test. The American standard test methods are the most direct methods of determining the elastic k value of the soil under static loading, but because these tests are costly and time-consuming, it is not anticipated that they will be conducted routinely.

CORRELATION METHODS

K Values and Correlations for Cohesive Soils (A-4 through A-7)

The characteristics of the various classes of cohesive soils are summarized below:

A-4: Nonplastic or slightly plastic silts, may have some coarse material.

Comparable Unified classes: ML, OL

Typical dry density range: 90 to 125 lb/ft³ [14300 to 19900 N/m³]

Typical CBR range: 4 to 15 percent

A-5: Poorly graded silts, usually micaceous or diatomaceous, may be highly elastic.

Comparable Unified class: MH

Typical dry density range: 80 to 100 lb/ft³ [12700 to 15900 N/m³]

Typical CBR range: 4 to 8 percent

A-6: Plastic clays, sometimes with moderate coarse fraction, usually exhibit high volume change from wet to dry states.

Comparable Unified class: CL

Typical dry density range: 100 to 125 lb/ft³ [15900 to 19900 N/m³]

Typical CBR range: 5 to 15 percent

A-7-5: Elastic clays, moderate plasticity index. May be highly elastic, may undergo considerable volume changes.

Comparable Unified class: CL, OL

Typical dry density range: 90 to 125 lb/ft³ [14300 to 19900 N/m³]

Typical CBR range: 4 to 15

A-7-6: Elastic clays, high plasticity index. May be highly elastic, may undergo extremely high volume changes.

Comparable Unified class: CH, OH

Typical dry density range: 80 to 110 lb/ft³ [12700 to 17500 N/m³]

Typical CBR range: 3 to 5

The bearing capacity of these cohesive soils is strongly influenced by their degree of saturation (S_r , percent), which is a function of water content (w , percent), dry density (γ , lb/ft³), and specific gravity (G_s):

$$S_r = \frac{w}{\left(\frac{62.4}{\gamma}\right) - \left(\frac{1}{G_s}\right)} \quad (\text{B-1})$$

In an extensive field and laboratory study of Illinois soils, Thompson and Robnett developed regression equations for each of the soil classes listed above to predict the resilient modulus (at 6 psi deviator stress) of a soil as a linear function of degree of saturation. [1] Under a concrete pavement, deviator stresses in the subgrade due to traffic loads are likely to be much lower than 6 psi [41 kPa] (e.g., 0.5 to 2 psi [3.4 to 13.8 kPa]). Thompson's research indicates that for these cohesive

soil classes, the resilient modulus increases between about 1000 and 1500 psi [6890 and 10335 kPa] (average 1200 psi [8270 kPa]) for every 1 psi [6.9 kPa] of deviator stress less than 6 psi [41 kPa], up to a maximum resilient modulus which occurs at a stress level of about 2 psi [13.8 kPa]. To estimate the resilient moduli for these soils at a stress level likely to exist under a concrete pavement, resilient moduli at 6 psi [41 kPa] were predicted for a range of degrees of saturation, and the resulting values were increased by 4800 psi [33 MPa] (4 times 1200 psi [8270 kPa]) to estimate resilient moduli at 2 psi [13.8 kPa].

These modulus values, which ranged from about 5 to 27 ksi [34.5 to 186 MPa], were used to model subgrades for a range of slab thicknesses in the elastic layer program BISAR. The deflections predicted for a 9000-lbf [40 kN] load were used to backcalculate k values, using the procedure given in the 1993 AASHTO Guide. The relationship of backcalculated k value to input E was very strong; although theoretically the relationship of k to E for a given load size is dependent on slab thickness, for a 6- to 12-in [152 to 305 mm] range of highway slab thicknesses, the thickness effect is minor. Therefore, the predicted resilient moduli as a function of degree of saturation were used to predict k values versus degree of saturation. The results are shown in Figure B-1. Bear in mind when examining this figure that each line represents the middle of a band of reasonable values for k. The height of those bands is consistently about 40 psi/in [11 kPa/mm]. So, for example, an A-6 soil might be expected to exhibit k values between about 180 and 260 psi/in [49 and 70 kPa/mm] at 50 percent saturation, and k values between about 45 and 115 [12 and 31 kPa/mm] at 100 percent saturation.

The k values ranges indicated in Figure B-1 are in remarkably good agreement for nearly all of the cohesive soil types with the k value ranges recommended for the same soil classes by the Corps of Engineers and PCA (see Appendix A).

1 psi/in = 0.27 kPa/mm,
1 lb/ft³ = 159 N/m³

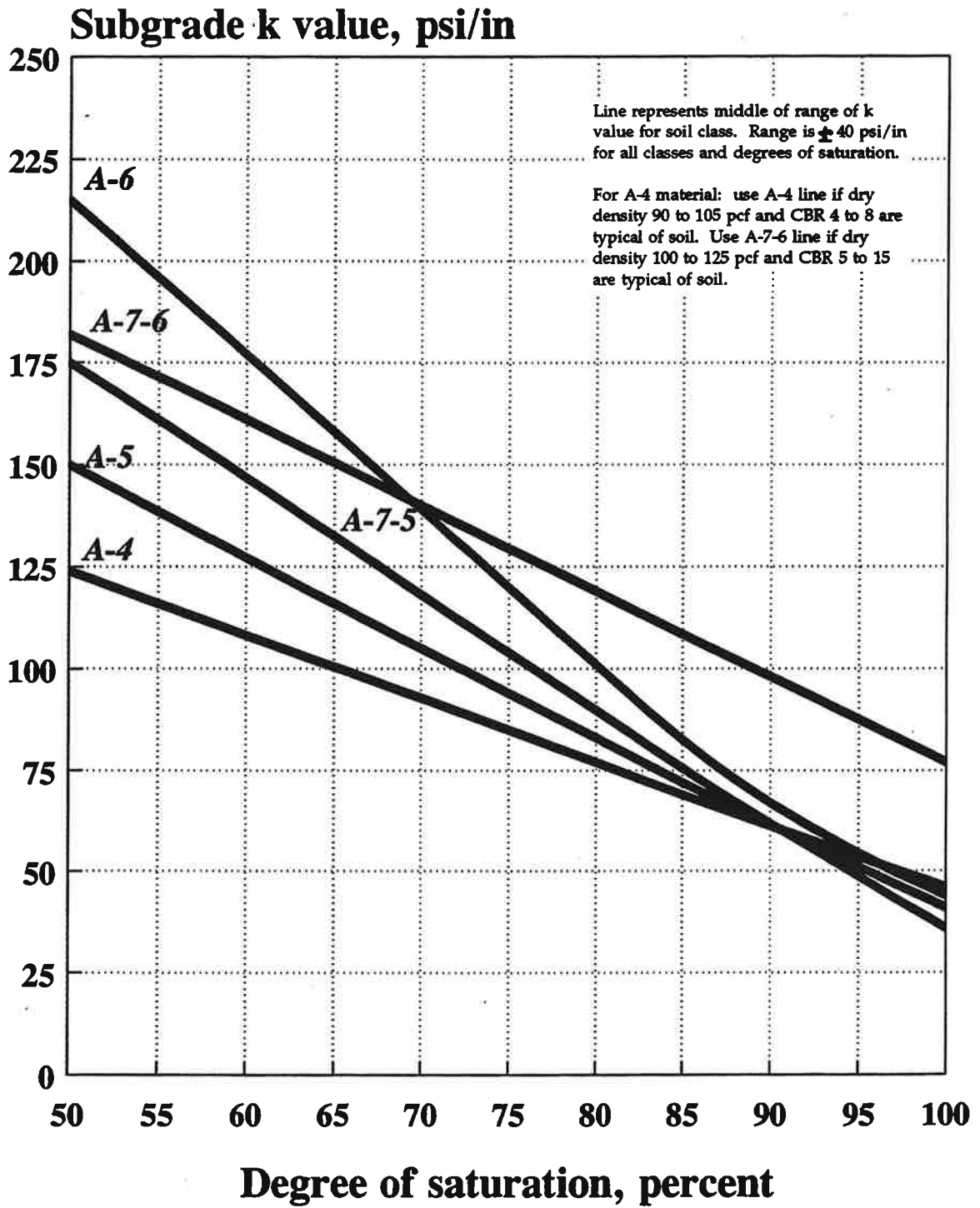


Figure B-1. k values versus degree of saturation for cohesive soils.

The one exception is A-4, for which Figure B-1 indicates a lower range of k values than the range indicated by the COE and PCA correlations. This may be due to the fact that two somewhat different types of materials can be classified as A-4: predominantly silty materials (at least 75 percent passing the #200 sieve, possibly organic), and also mixtures of silt, sand, and gravel (up to 64 percent retained on #200 sieve). The former type may have a density between 90 and 105 lb/ft³ [14300 and 16700 N/m³], a CBR between 4 and 8, and a k value between 100 and 175 psi/in [27 and 47 kPa/mm], according to old Bureau of Public Roads correlations (see Appendix A, Figure A-7). The latter may have a density between 100 and 125 lb/ft³ [15900 and 19900 N/m³], a CBR between 5 and 15, and a k value between 150 and 300 psi/in [40.5 and 81 kPa/mm]. It is possible that the available resilient modulus regression equation for A-4 is more representative of the weaker subset of this class. Therefore, if the material in question is A-4, but possesses the properties of the stronger subset of materials in the A-4 class, a higher k value at any given degree of saturation (for example, along the line labelled A-7-6 in Figure B-1) is appropriate.

K Values and Correlations for Cohesionless Soils (A-1 and A-3)

The characteristics of the various classes of cohesionless soils are summarized below:

A-1-a: Predominantly stone fragments and gravel, with or without binder.

Comparable Unified classes: GW, GP

Typical dry density range:

125 to 140 lb/ft³ [19900 to 22200 N/m³] if well graded,

120 to 130 lb/ft³ [19100 to 20700 N/m³] if poorly graded

Typical CBR range: 60 to 80 if well graded, 35 to 60 if poorly graded

A-1-b: Predominantly coarse sand with or without binder.

Comparable Unified class: SW

Typical dry density range: 110 to 130 lb/ft³ [17500 to 20700 N/m³]

Typical CBR range: 20 to 40

A-3: Fine beach or desert sand without fines. Also alluvial mix of poorly graded fine sand and small amounts of coarse sand and gravel.

Comparable Unified class: SP

Typical dry density range: 105 to 120 lb/ft³ [16700 to 19100 N/m³]

Typical CBR range: 15 to 25

Cohesionless materials can be characterized by their shear modulus G , which is fairly insensitive to moisture variation and is predominantly a function of their void ratio and overall stress state. The elastic modulus E can be related to the shear modulus G through the Poisson's ratio μ (about 0.35 for clean sands and gravels):

$$E = 2 G (1 + \mu) \quad (\text{B-2})$$

where

$$G = \frac{1230 (2.97 - e)^2}{1 + e} (\sigma_0^{0.5}) \quad (\text{B-3})$$

Equation B-3 is one of many available empirical equations which yield reasonable values for the shear modulus (G , psi) of cohesionless sands and gravels as a function of the void ratio (e) and all-around confining pressure (σ_0). The void ratio can be calculated from the dry density, as shown below:

$$e = \frac{\text{void volume}}{\text{solid volume}} = \frac{V_v}{V_s} = \frac{1 - V_s}{V_s} \quad (\text{B-4})$$

$$V_s = \frac{\gamma_d}{\gamma_w G} = \frac{\gamma_d}{62.4 G} \quad (\text{B-5})$$

At any given depth below the surface, the overburden pressure on an element of soil is the sum of the pressure due to the pavement structure's weight and the pressure due to the weight of the soil above the soil element. Assuming about 1 psi [7 kPa] of pressure on the subgrade due to the weight of a typical concrete highway slab and base, and assuming a value of 0.6 for the coefficient of earth pressure at rest, the all-around confining pressure (σ_0) can be calculated from the horizontal pressure σ_3 and the overburden pressure σ_1 , for a given density (γ , lb/ft³) and depth (z , ft):

$$\sigma_1 \text{ psi} = 1 \text{ psi} + \frac{\gamma \text{pcf } z \text{ft}}{144} \quad (\text{B-6})$$

$$\sigma_3 = 0.6 \sigma_1 \quad (\text{B-7})$$

$$\sigma_0 = \frac{\sigma_1 + 2 \sigma_3}{3} = \frac{2.2 \sigma_1}{3} = 0.733 \sigma_1 \quad (\text{B-8})$$

These equations were used to compute E values for soils with densities from 90 to 150 lb/ft³ [14300 to 23800 N/m³] for two-foot [0.6 m] depth increments in the subgrade. Research on cohesionless soils has also shown that these materials approach a maximum shear modulus when the strain amplitude falls below about 0.001 percent shear strain. To determine at what depth in a subgrade a maximum E might be reached for a cohesionless soils, a series of BISAR runs was conducted for a series of E values corresponding to densities from 90 to 150 lb/ft³ [14300 to

23800 N/m³], with E increasing as a function of depth. The BISAR output was examined to determine the depth at which the shear strain fell below 0.001 percent, when a 9000-lbf [40 kN] load was applied to a 9-in [229 mm] concrete slab on top of the subgrade. This occurred at about 10.75 ft [3.3 m] for the 90 lb/ft³ [14300 N/m³] material, and at lesser depths for higher-density materials. It was therefore concluded that for any of the densities modelled, the E could be presumed constant beyond a depth of about 10 to 12 ft [3 to 3.7 m].

Having established the E values to represent various cohesionless soil densities, a series of BISAR runs were conducted to calculate slab deflections, and k values were backcalculated for the soils from these deflections. On the basis of the results, the following k value ranges are suggested:

<u>Soil Class</u>	<u>K Range (psi/in)</u>	<u>Dry Density Range (lb/ft³)</u>
A-1-a, well graded	300 - 450	125 - 140
A-1-a, poorly graded	300 - 400	120 - 130
A-1-b	200 - 400	110 - 130
A-3	150 - 300	105 - 120

[1 psi/in = 0.27 kPa/mm 1 lb/ft³ = 159 N/m³]

These ranges agree well with the Corps of Engineers and PCA correlation charts, although both the Corps and PCA allow a very high upper limit on A-1. The Corps chart suggests a range of 225 to 700 psi/in [60 to 190 kPa/mm] for all A-1 materials, while the PCA chart suggests a range of 250 to 700 psi/in [67 to 190 kPa/mm]. For A-3 sands, the Corps chart suggests a range of 200 to 330 psi/in [54 to 89 kPa/mm] while PCA suggests a range of 200 to 700 [54 to 190 kPa/mm].

K Values and Correlations for A-2 Soils

Soils in the A-2 class are all granular materials falling between A-1 and A-3. Although they are difficult to characterize, some properties are described below:

A-2-4 and A-2-5: Gravel and coarse sand with fines content in excess of A-1 limits, and fine sand with fines content in excess of A-3 limits. The fraction passing the #40 sieve behaves like nonplastic (A-4 and A-5) clays and silts.

Gravelly A-2-4 and A-2-5 (silty gravel or silty sandy gravel):

Comparable Unified class: GM

Typical dry density range: 130 to 145 lb/ft³

Typical CBR range: 40 to 80

Sandy A-2-4 and A-2-5 (silty sand or silty gravelly sand):

Comparable Unified class: SM

Typical dry density range: 120 to 135 lb/ft³

Typical CBR range: 20 to 40

A-2-6 and A-2-7: Gravel and coarse sand with fines content in excess of A-1 limits, and fine sand with fines content in excess of A-3 limits. The fraction passing the #40 sieve behaves like plastic (A-6 and A-7) clays and silts.

Gravelly A-2-6 and A-2-7 (clayey gravel or clayey sandy gravel):

Comparable Unified class: GC

Typical dry density range: 120 to 140 lb/ft³

Typical CBR range: 20 to 40

Sandy A-2-6 and A-2-7 (clayey sand or clayey gravelly sand):

Comparable Unified class: SC

Typical dry density range: 105 to 130 lb/ft³

Typical CBR range: 10 to 20

It is evident from the above list that a wide variety of materials fall into the A-2 class, and that the division into subcategories by the relative elasticity of the fines (A-2-4 versus A-2-5 and A-2-6 versus A-2-7) is not as useful to selecting an appropriate k value as division into gravelly and sandy subcategories would be.

Specific aspects of A-2 behavior can be difficult to predict. Some A-2 soils exhibit stress-hardening behavior while others are stress-softening. How much influence moisture variation has on the bearing capacities of various A-2 soils is unknown. One might think intuitively that, because A-2 soils are in the middle between coarse-grained (A-1 and A-3) and fine-grained (A-4 through A-7), their typical k values might lie somewhere between the k ranges for coarse- and fine-grained soils.

On the contrary, the k value range recommended by the PCA and Corps for A-2-4 and A-2-5 soils is just as high as those for A-1 soils (300 to 700 psi/in). The lower limit of the recommended k range for A-2-6 and A-2-7 is somewhat lower (about 180 psi/in) than for the A-2-4 and A-2-5, but still much higher than the

appropriate ranges for fine-grained soils. Comparison of the dry density and CBR ranges for the A-2 soils and the other soil categories also indicates that the A-2 materials are, in terms of bearing capacity and shear modulus, much more likely to behave like A-1 and A-3 soils than like A-4 through A-7 soils. Therefore, k ranges were selected for the various A-2 soils by comparison with the k ranges, density ranges and CBR ranges of other soil types. Wider k ranges in the A-2-6 and A-2-7 groups than in the A-2-4 and A-2-5 groups appear to be appropriate because the former have wider ranges of density and CBR. The following k value ranges are suggested for A-2 soils:

<u>Soil Class</u>	<u>K Range (psi/in)</u>	<u>Dry Density Range (lb/ft³)</u>
A-2-4 gravelly	300 - 500	130 - 145
A-2-5 gravelly	300 - 500	130 - 145
A-2-4 sandy	300 - 400	120 - 135
A-2-5 sandy	300 - 400	120 - 135
A-2-6 gravelly	200 - 450	120 - 140
A-2-7 gravelly	200 - 450	120 - 140
A-2-6 sandy	150 - 350	105 - 130
A-2-7 sandy	150 - 350	105 - 130

[1 psi/in = 0.27 kPa/mm 1 lb/ft³ = 159 N/m³]

Correlation of K Value to Other Tests

The following correlations are also available for estimating k value from other types of soil test data:

California Bearing Ratio: Figure B-2 illustrates the range of k values which might be expected for a soil with a given California Bearing Ratio. This figure was developed by comparing the typical CBR ranges to the typical k ranges for different soil classes. It is intended as an approximate illustration of the trend of k with CBR.

R-Value: Figure B-3 illustrates the general relationship between k value and R-value.

Dynamic Cone Penetrometer. Figure B-4 illustrates the range of k values which might be expected for a soil with a given penetration rate (inches per blow) measured with a Dynamic Cone Penetrometer. This is a rapid hand-held testing device which can be used to quickly test dozens of locations along an alignment. The DCP can also penetrate AC surfaces and surface treatments to test the foundation below. Figure B-4 was developed using Figure B-3 and an available correlation between CBR and DCP penetration rate.

Determination of Seasonally Adjusted K Value for Design

A k value should be selected for the subgrade soil for each of the four seasons of the year. The guidelines provided in the previous section may be used to select a k for each season, or the backcalculation methods or plate testing methods described later in this appendix may be used.

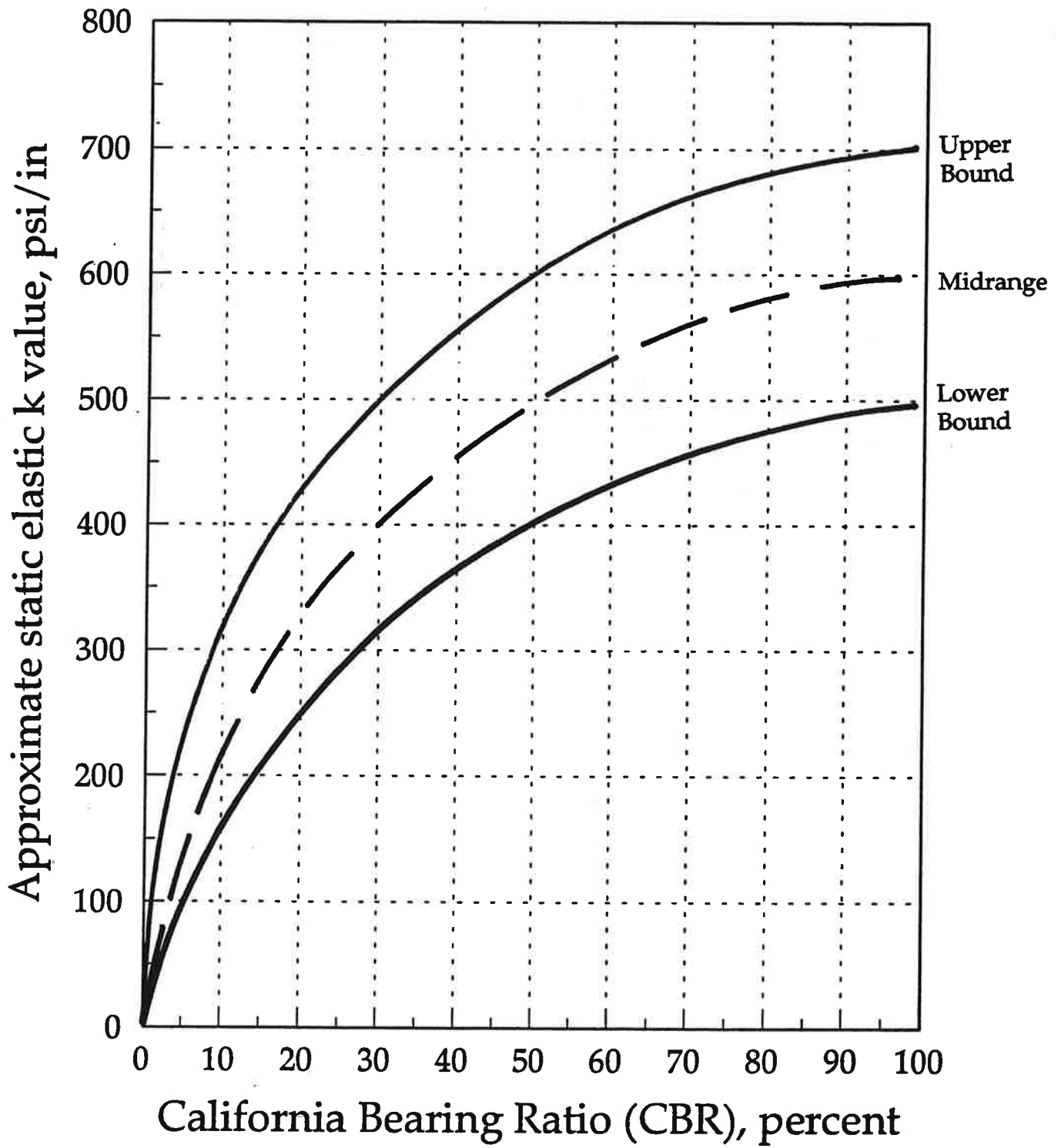


Figure B-2. Approximate relationship of k value range to CBR.

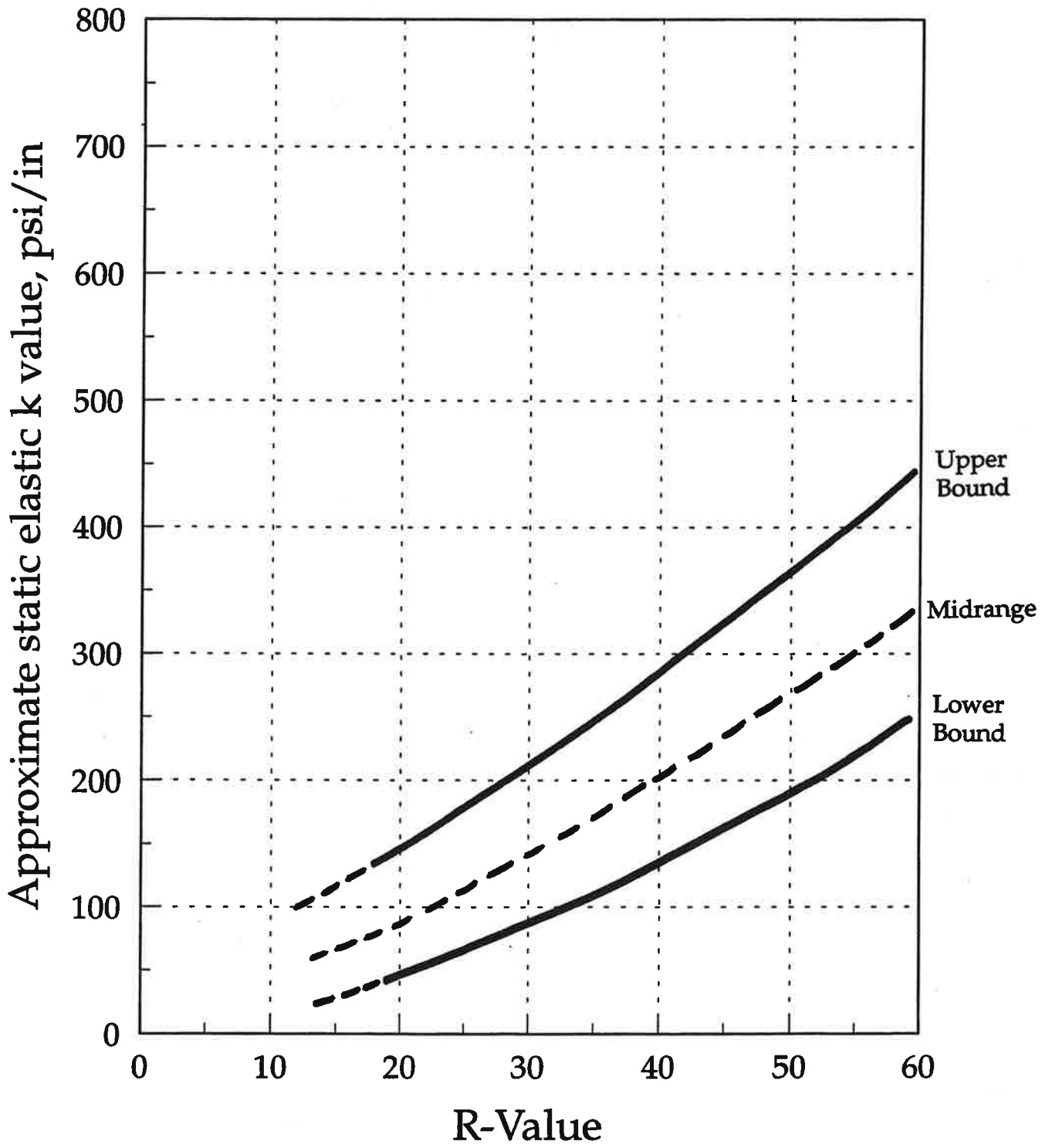


Figure B-3 Approximate relationship of k value to R-value.

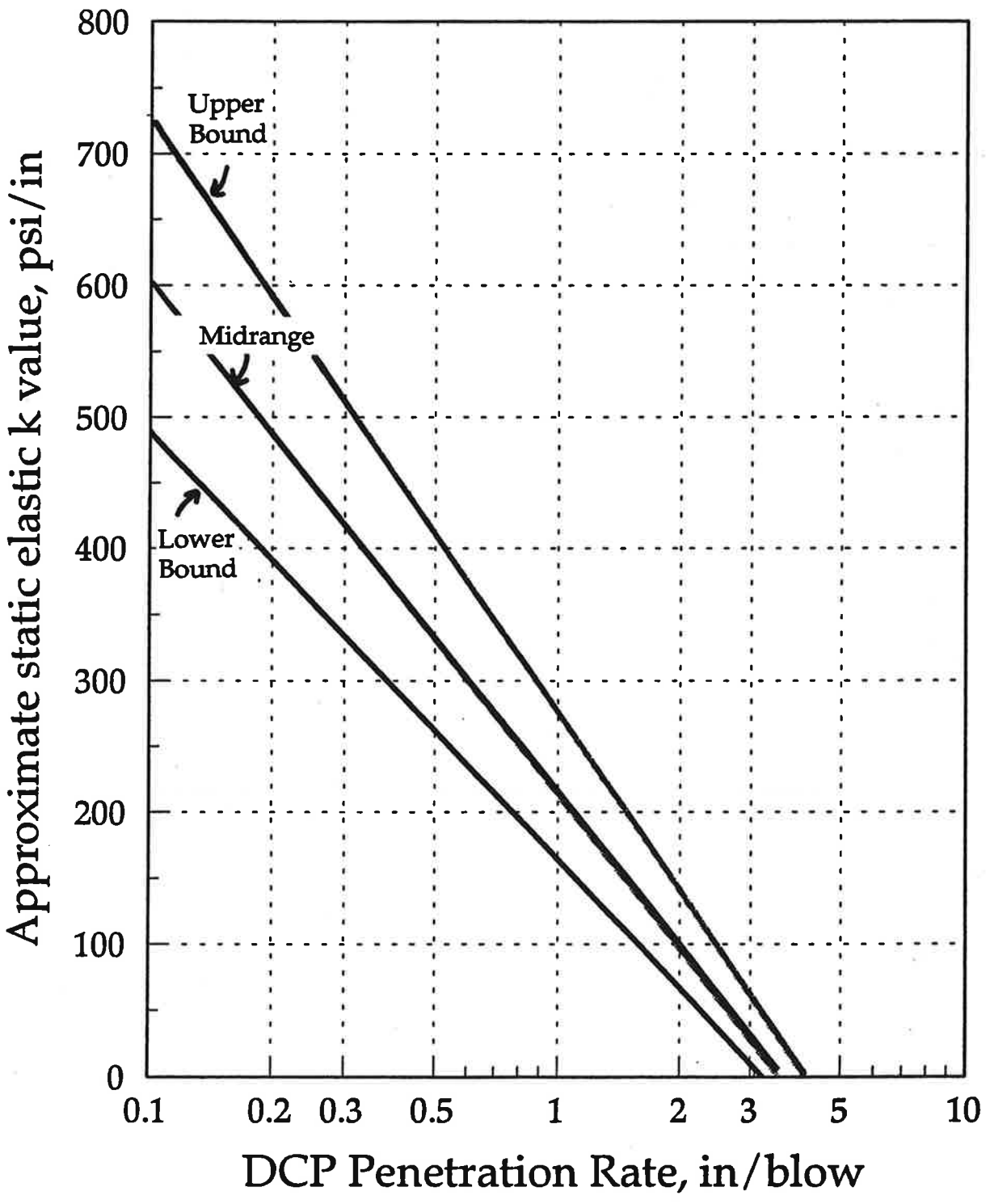


Figure B-4. Approximate relationship of k value range to DCP penetration rate.

Among the factors which should be considered in selecting seasonal k values are the seasonal movement of the water table, seasonal precipitation levels, winter frost depths, number of freeze-thaw cycles, and the extent to which the subgrade will be protected from frost by embankment material. A "frozen" k may not be appropriate for the winter season, even in a cold climate, if the frost will not reach and remain in a substantial thickness of the subgrade throughout the winter. If it is anticipated that a substantial depth (e.g., a few feet) of the subgrade will be frozen, a k value of 500 psi/in would be an appropriate "frozen" k.

The seasonal variation in degree of saturation is difficult to predict, but in wetter climates, in locations where a water table is constantly present at a depth of less than about 10 ft, it is reasonable to expect that fine-grained subgrades will remain at least 70 and 90 percent saturated, and may be completely saturated for substantial periods in the spring. County soil reports can provide data on the position of the high water table (i.e., the typical depth to the water table at the time of the year that it is at its highest). Unfortunately, county soil reports do not provide data on the variation in depth to the water table throughout the year.

Once a k value for each season has been selected, a seasonally adjusted effective k value is determined using the method given in Appendix E.

Adjustment to K Value for Embankment

A nomograph is provided in Figure B-5 for adjustment of the seasonally adjusted effective subgrade k value if (a) a substantial thickness of fill material will be placed above the natural subgrade, and/or (b) a rigid layer (e.g., bedrock or hardpan clay) is present at a depth of 10 ft or less beneath the existing subgrade surface. Note that the rigid layer adjustment should only be applied if the subgrade

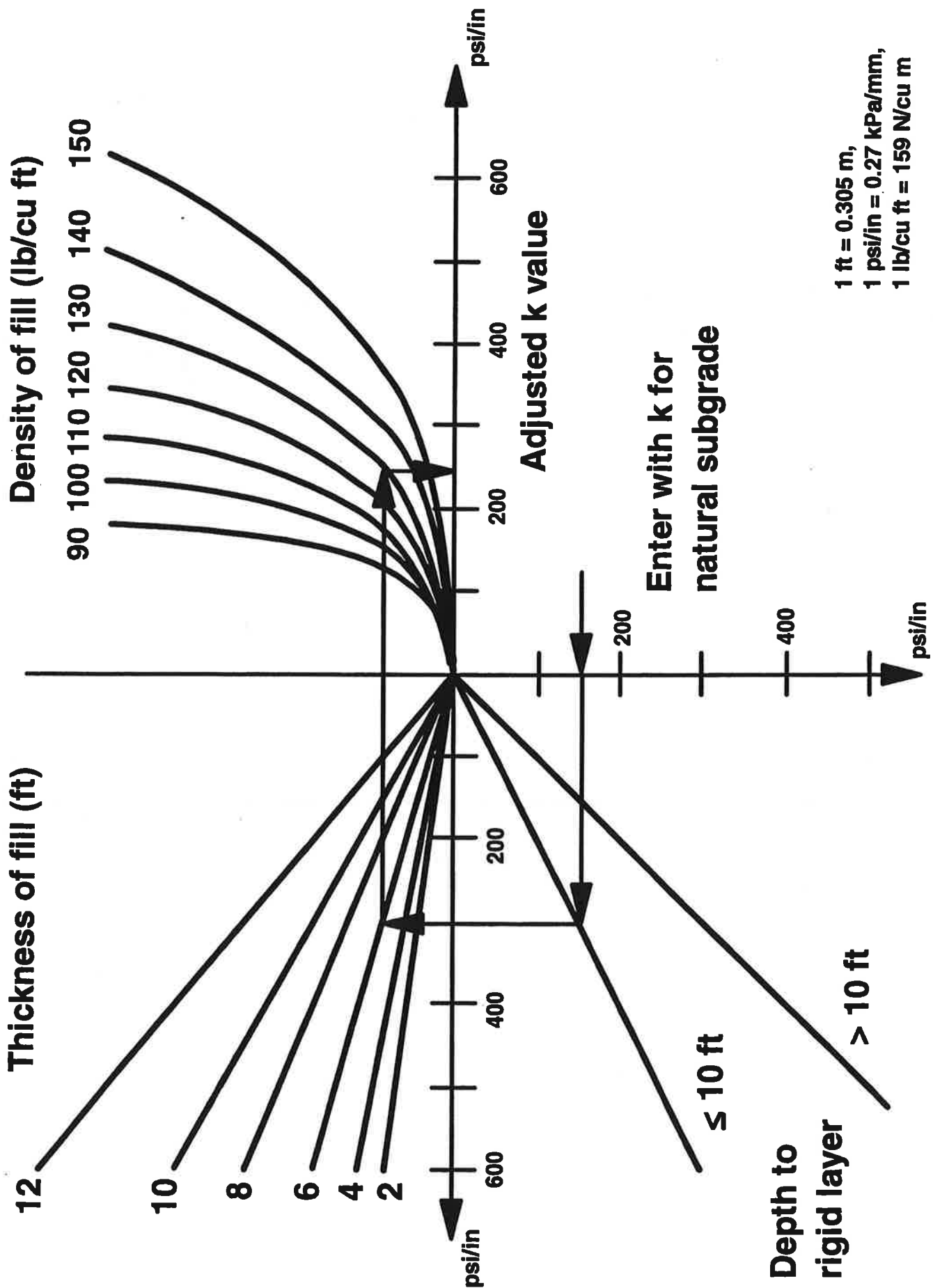


Figure B-5. Adjustment to k for fill and/or rigid layer.

k was determined on the basis of soil type or similar correlations. If the k value was determined from nondestructive deflection testing or from plate bearing tests, the effect of a rigid layer, if present at a depth of less than 10 ft, is already represented in the k value obtained.

DEFLECTION TESTING AND BACKCALCULATION METHODS

1993 AASHTO Guide

Equations for backcalculation of concrete elastic moduli and subgrade k values for concrete and composite pavements were developed by Hall [2] and incorporated in the overlay design procedures in the 1993 AASHTO Guide. [64] This solution method is also based on deflection of an infinite slab. The relationship between AREA and ℓ is shown in Figure B-6 and given by the following equation:

$$\ell = \left[\frac{\ln \left(\frac{36 - \text{AREA}}{1812.279} \right)}{-2.559} \right]^{4.387} \quad (\text{B-9})$$

The k value and concrete E value may be obtained from Figures B-7 and B-8 respectively, or from the following equations:

$$k = \left(\frac{P}{8 d_0 \ell^2} \right) \left\{ 1 + \left(\frac{1}{2\pi} \right) \left[\ln \left(\frac{a}{2\ell} \right) + \gamma - 1.25 \right] \left(\frac{a}{\ell} \right)^2 \right\} \quad (\text{B-10})$$

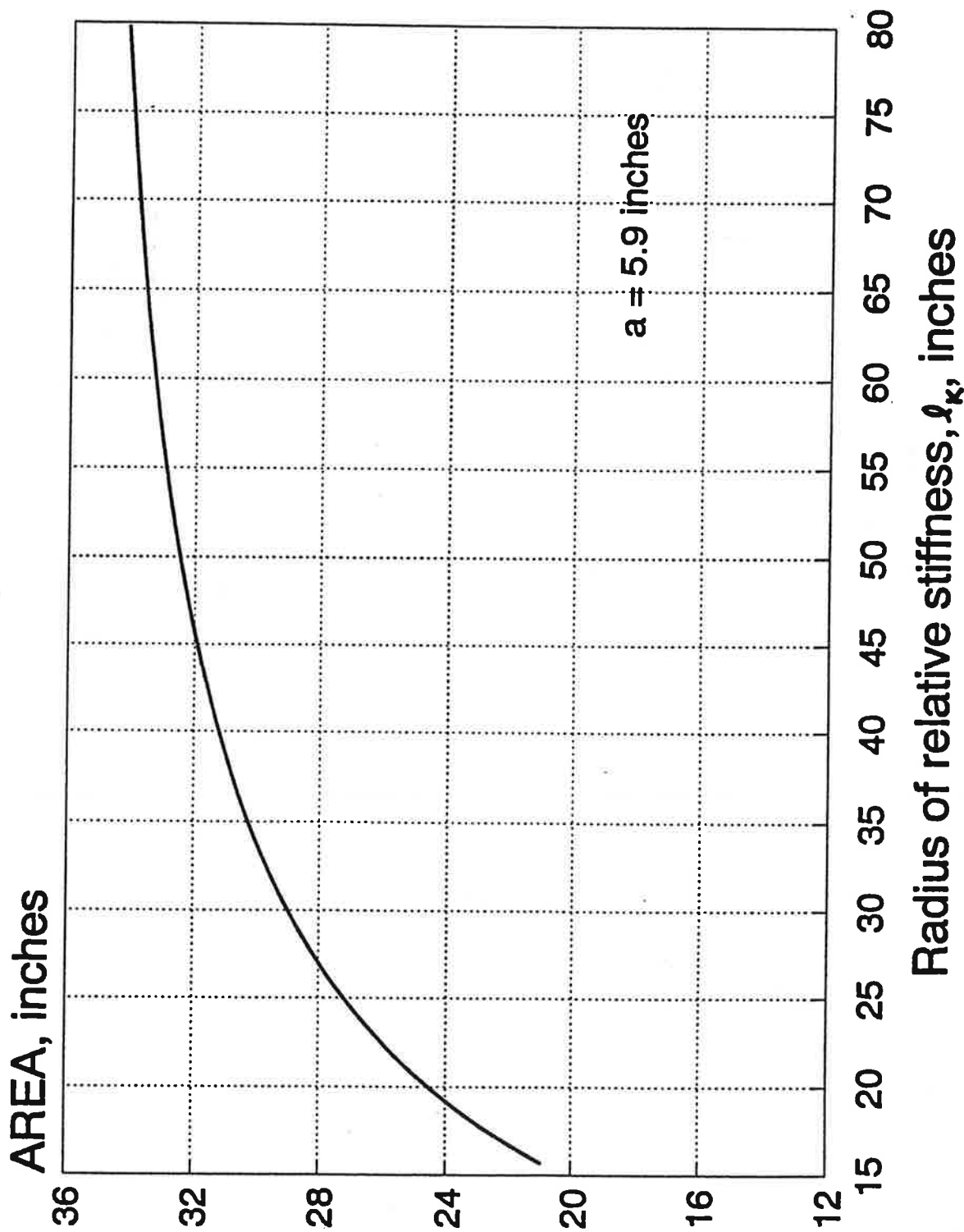


Figure B-6. Relationship of AREA to l_k . [2]

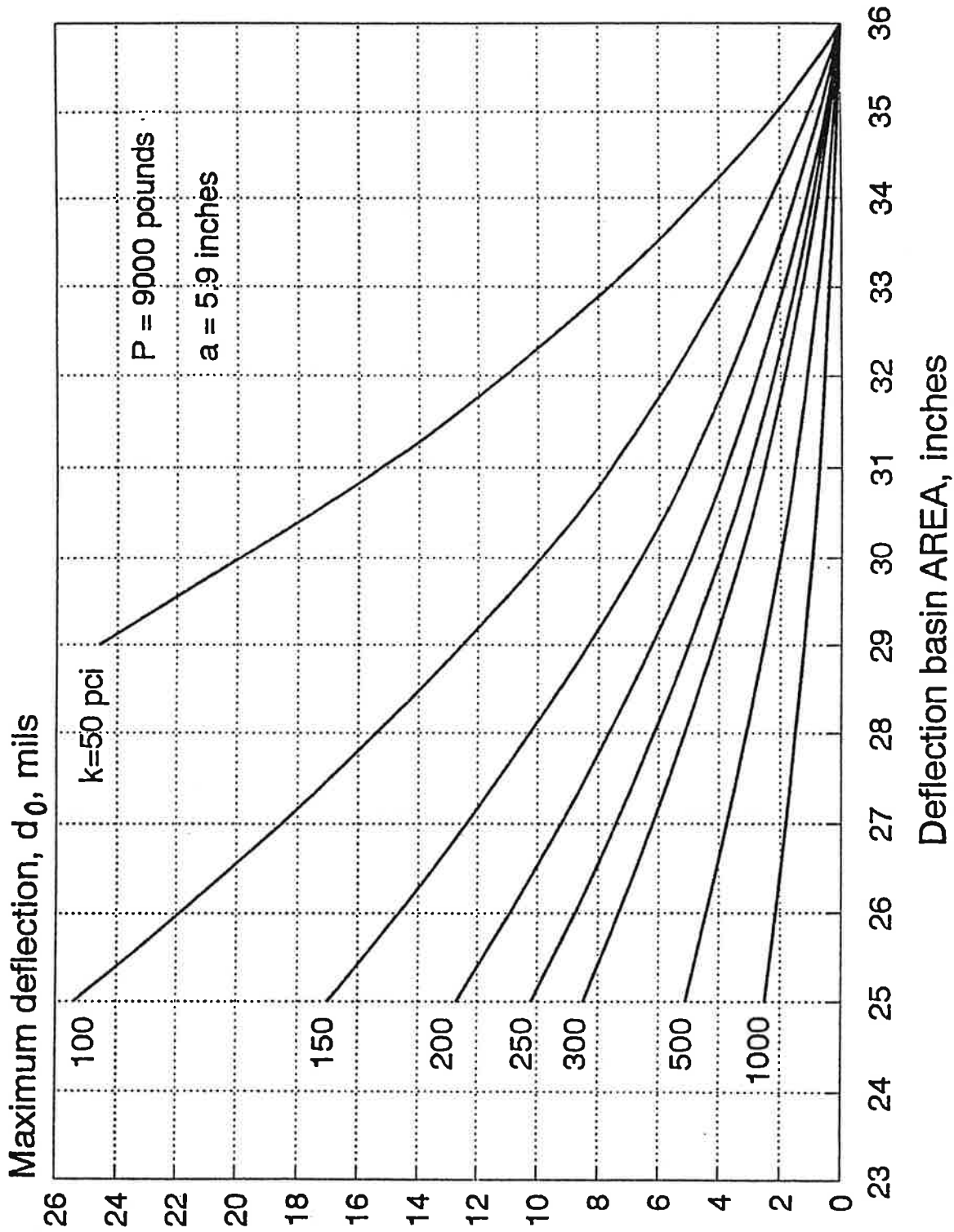


Figure B-7. Dynamic k value determination from d_0 and AREA. [2]

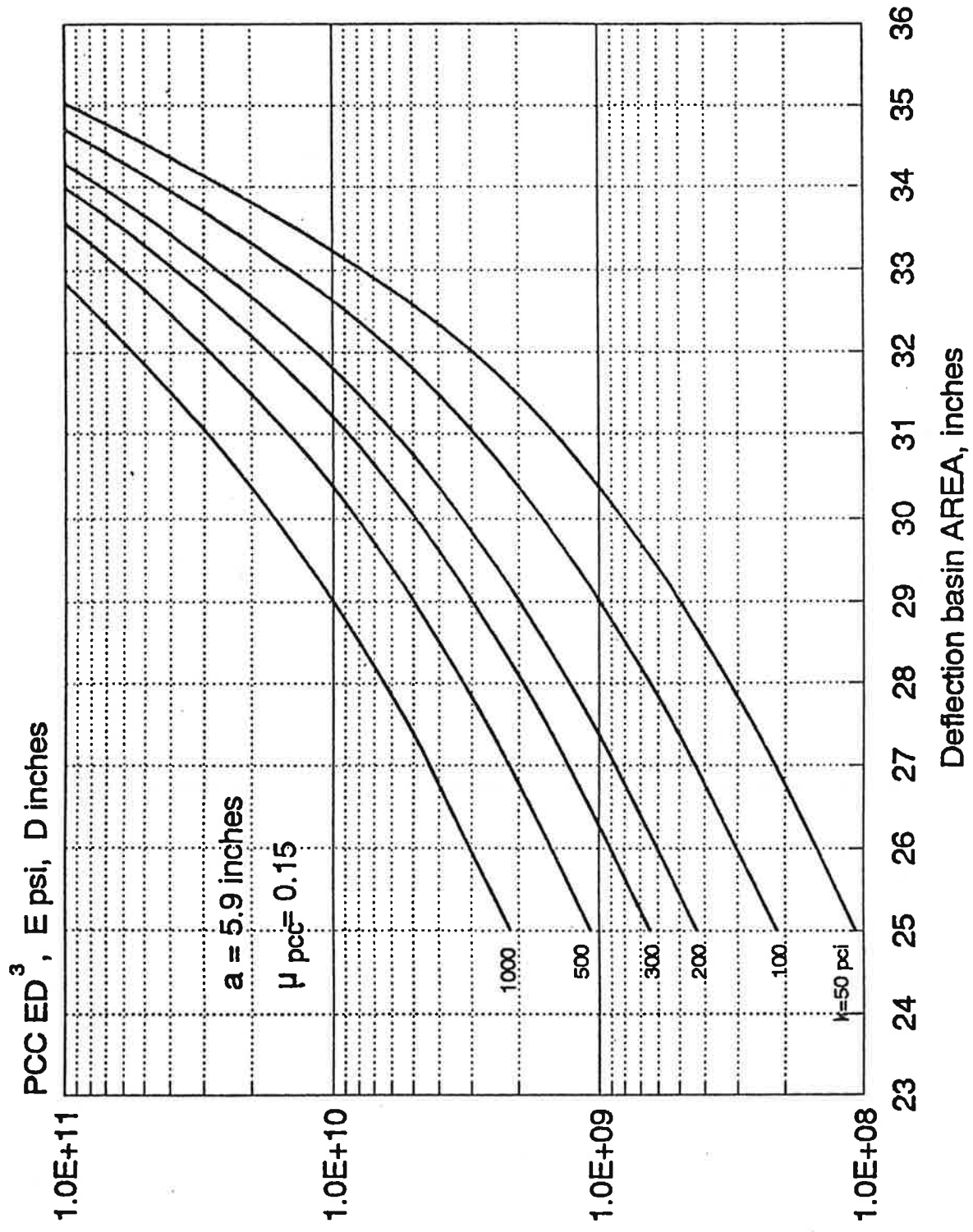


Figure B-8. Concrete E determination from k value, AREA, and slab thickness. [2]

where d_0 = maximum deflection, inches

P = load, pounds

γ = 0.57721566490 (natural logarithm of Euler's constant γ)

$$E = \frac{12 (1 - \mu^2) k \ell^4}{h^3} \quad (\text{B-11})$$

where E = concrete elastic modulus, psi

μ = Poisson's ratio for concrete (typically 0.15)

h = slab thickness, inches

These equations may be applied to AC-overlaid PCC pavements if the AREA and the k value are calculated with a maximum deflection d_0 which has been corrected for compression in the AC surface. The following equations were provided for the correction factor $d_{0 \text{ compress}}$ which is subtracted from the measured d_0 :

AC/PCC BONDED:

$$d_{0 \text{ compress}} = -0.0000328 + 121.5006 \left(\frac{D_{ac}}{E_{ac}} \right)^{1.0798} \quad (\text{B-12})$$

AC/PCC UNBONDED:

$$d_{0 \text{ compress}} = -0.00002132 + 38.6872 \left(\frac{D_{ac}}{E_{ac}} \right)^{0.94551}$$

where $d_{0 \text{ compress}}$ = AC compression at center of load, inches

D_{ac} = AC thickness, inches

E_{ac} = AC elastic modulus, psi

Which of the two equations should be used depends on whether or not the AC overlay and PCC slab are considered to be bonded. The AC elastic modulus may be determined from the Asphalt Institute equation [3] or from diametral resilient modulus tests on cores, in accordance with ASTM D 4123.

The k value backcalculated with the 1993 Guide equations from deflections measured by an FWD or similar dynamic loading device are expected to be higher than the k values which would be obtained from a static load test on the subgrade or on the slab. The 1993 Guide recommended that these backcalculated dynamic k values be divided by two to approximate static k values for use in design.

SHRP LTPP Solutions

The AREA concept was further developed for use with the six-sensor arrangement used to test SHRP LTPP experiment sections. [4] For the SHRP sensor positions of 0, 8, 12, 18, 24, 36, and 60 inches, AREA is calculated from the following equation:

$$AREA_{SHRP} = 4 + 6 \left(\frac{d_8}{d_0} \right) + 5 \left(\frac{d_{12}}{d_0} \right) + 6 \left(\frac{d_{18}}{d_0} \right) + 9 \left(\frac{d_{24}}{d_0} \right) + 18 \left(\frac{d_{36}}{d_0} \right) + 12 \left(\frac{d_{60}}{d_0} \right) \quad (B-13)$$

The radius of relative stiffness is calculated from the following equation:

$$\ell = \left[\frac{\ln \left(\frac{60 - AREA_{SHRP}}{289.708} \right)}{-0.698} \right]^{2.566} \quad (B-14)$$

AREA_{SHRP} values between 35 and 50 correspond to typical ℓ values of 25 to 55 for concrete highway pavements. (The corresponding range of AREA values according to the four-sensor definition would be 27 to 33). It is important to note

that although theoretically the two AREA definitions should yield the same ℓ , in analysis of actual measured deflection basins from in-service pavements, the two may give slightly different ℓ values. This is not surprising considering that one equation includes a deflection at a considerably farther distance from the load than the other equation. Which equation gives higher ℓ values for a given pavement may vary from location to location and may depend on slab dimensions and subgrade properties.

The subgrade k value and concrete E value may be calculated from the maximum deflection d_0 using Equations B-9 and B-10, or may be calculated from each of the sensor deflections. The actual deflection at the surface of a slab on a dense liquid foundation, at any radial distance from the load, is a function of a nondimensional deflection coefficient (d_r^*), the load magnitude, and the pavement system parameters, as shown by the following equations:

$$d_r^* = \frac{d_r k \ell^2}{P} = \frac{d_r D}{P \ell^2} \quad (\text{B-15})$$

where

$$D = \frac{E h^3}{12 (1 - \mu^2)} \quad (\text{B-16})$$

The nondimensional deflection coefficient is in turn a function of the load radius a , the radial distance r , and ℓ . For a load radius $a = 5.9055$ inches (for the 300-mm-diameter FWD load plate), d_r^* at any given radial distance r is thus a function solely of ℓ , as illustrated in Figure B-9. These relationships can be expressed by a model of the following general form:

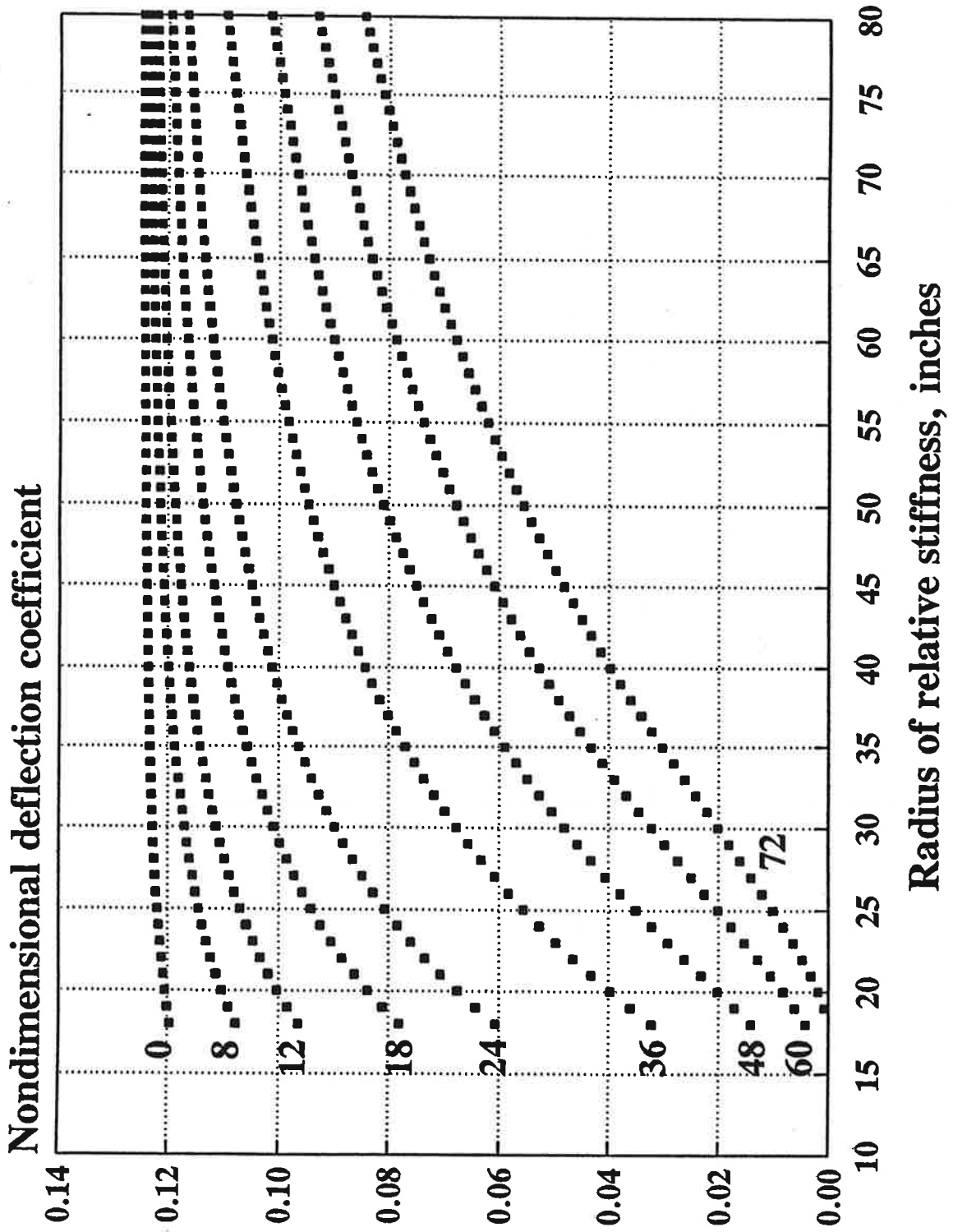


Figure B-9. Nondimensional deflection coefficients versus k_r . [4]

$$d_r^* = a e^{-b e^{(-c \ell)}} \quad (B-17)$$

The values for the a, b, and c constants obtained for each of the SHRP sensor positions are given in Table B-1.

With ℓ determined from AREA, and the nondimensional deflection at any sensor location determined from d_r , an estimate of the k value may be obtained from any measured deflection by rearranging Equation B-14:

$$k = \frac{P d_r^*}{d_r \ell^2} \quad (B-18)$$

An estimate of the slab's elastic modulus may also be obtained from each of the measured sensor deflections by rearranging Equations B-14 and B-15:

$$D = \frac{P \ell^2 d_r^*}{d_r} \quad (B-19)$$

$$E = \frac{12 D (1 - \mu^2)}{h^3} \quad (B-20)$$

$$E = \frac{12 (1 - \mu^2) P \ell^2 d_r^*}{d_r h^3} \quad (B-21)$$

Backcalculating a k value and slab E at each sensor may be useful for such things as identifying an individual bad sensor reading. However, these individual k and E values should not be considered independent estimates, because they are all derived from a common ℓ value which was determined from the AREA computed from all of the deflections.

Table A-1 Regression coefficients for d^* versus l relationships.

Radial distance	a	b	c
0 in	0.1245	0.14707	0.07565
8	0.12323	0.46911	0.07209
12	0.12188	0.79432	0.07074
18	0.11933	1.38363	0.06909
24	0.11634	2.06115	0.06775
36	0.10960	3.62187	0.06568
60	0.09521	7.41241	0.06255

Notes: $R^2 \geq 99.7$ percent (predicted versus actual values) for all models.
 $\sigma_Y \leq 0.001$ for all models.

General Solution for Any Arbitrary Sensor Arrangement

The backcalculation methods based on the traditional four-sensor definition of AREA or any other sensor arrangement such as that used for SHRP sections are limited in their use to data collected with the same sensor arrangement. It is also possible to solve for ℓ from any two deflections at any two radial distances greater than 0. The curves shown in Figure B-9 for radial distances greater than 0 may be transformed into a single curve, as shown in Figure B-10. The following equation was developed for this curve:

$$d^* = 0.12497 e^{-0.46308 \left(\frac{r}{\ell}\right)^{1.55212}} \quad (\text{B-22})$$

Given any two deflections d_x and d_y at radial distances x and y :

$$\frac{w_x}{d_x} = \frac{w_y}{d_y} = \frac{k \ell^2}{P} \quad (\text{B-23})$$

$$\frac{d_x}{d_y} = \frac{w_x}{w_y} = \frac{0.12497 e^{-0.46308 \left(\frac{x}{\ell}\right)^{1.55212}}}{0.12497 e^{-0.46308 \left(\frac{y}{\ell}\right)^{1.55212}}} \quad (\text{B-24})$$

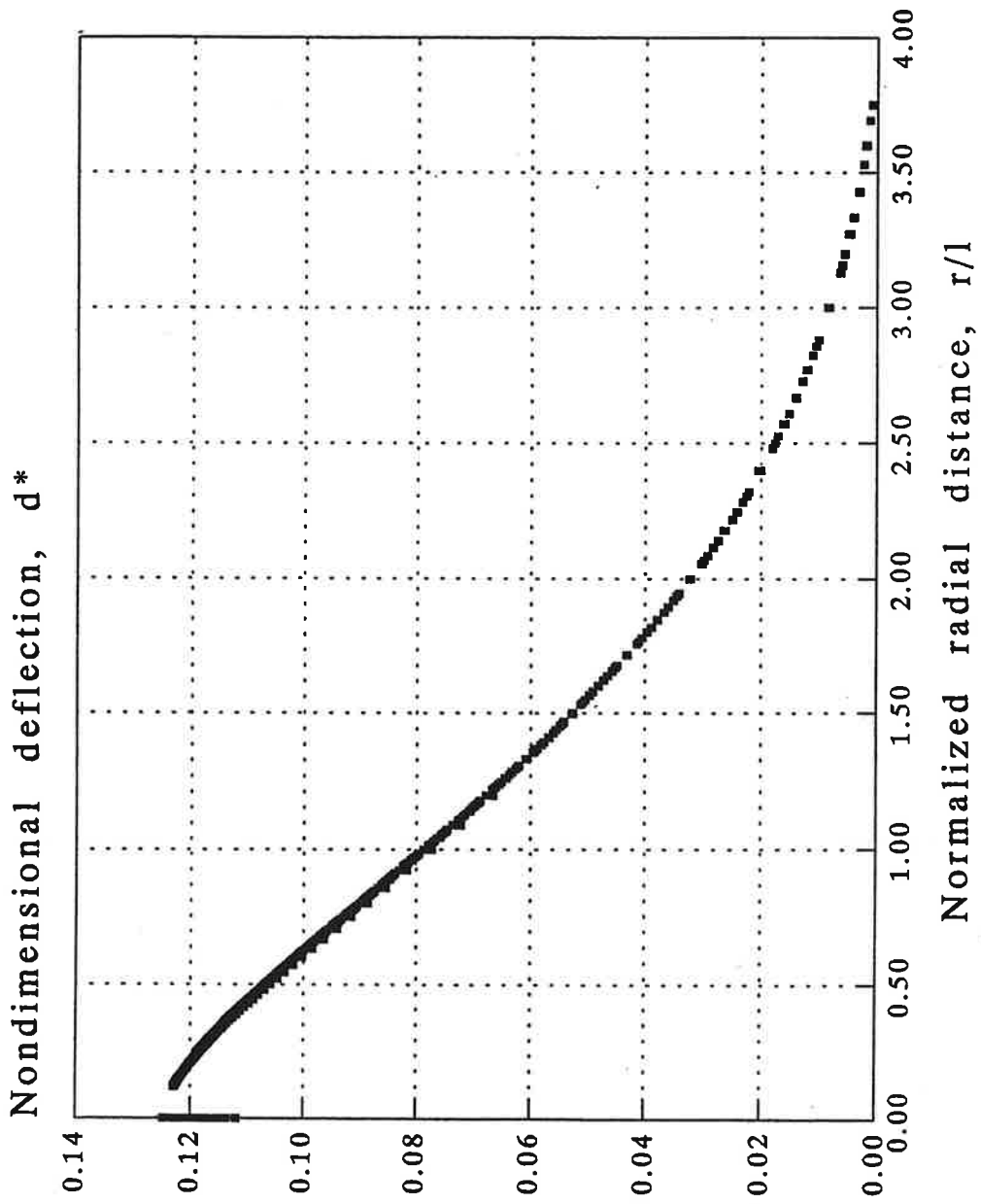


Figure B-10. Nondimensional deflection versus normalized radial distance.

Taking the natural logarithm of both sides of this equation, and rearranging to solve for ℓ :

$$\ell = \sqrt[1.55212]{\frac{-0.46308 (x^{1.55212} - y^{1.55212})}{\ln\left(\frac{d_x}{d_y}\right)}} \quad (\text{B-25})$$

For example:

$$P = 9000 \text{ pounds}$$

$$E = 3 \text{ million psi}$$

$$h = 10 \text{ inches}$$

$$d_{12} = 0.006537 \text{ inch}$$

$$d_{24} = 0.005695 \text{ inch}$$

$$\ell = \sqrt[1.55212]{\frac{-0.46308 (24^{1.55212} - 12^{1.55212})}{\ln\left(\frac{0.005695}{0.006537}\right)}} \quad (\text{B-26})$$

$$\ell = 40.039 \text{ inches}$$

The two deflections d_{12} and d_{24} in this example were actually computed from the above values for P , E , and h , using Equation 21 and $\ell = 40$ inches.

Effect of Load Radius

The above equations and all of the AREA-based backcalculation equations presented in this section were developed for a load radius of 5.9 inches [30 cm], which corresponds to the Falling Weight Deflectometer testing device. The equations are not very sensitive to the load radius, so they may be used with reasonable accuracy for other deflection testing devices with circular load plates of similar radius

or multiple loading pads for which an equivalent circular radius would be similar. In fact, comparable equations which have been developed for the large FWD plate which has a radius of 9 inches [45 cm] are only slightly different.

Edge and Corner Solutions and Slab Size Effects

In 1993, Croveti developed equations for backcalculation of foundation k values from interior, edge, and corner deflection measurements, and correction of infinite slab solutions for finite slab size effects. [53] As Croveti has shown, Westergaard's edge, interior, and corner deflection equations can all be represented by quadratic equations of the following form:

$$\frac{\Delta_0 D}{P \ell^2} = a + b \left(\frac{a_r}{\ell} \right) + c \left(\frac{a_r}{\ell} \right)^2 \quad (\text{B-27})$$

where Δ_0 = maximum deflection

D = bending stiffness of slab (from Equation B-15)

P = applied load

ℓ = radius of relative stiffness

a_r = radius of applied load

a, b, c = constants of the quadratic equation

The equations for interior, edge, and corner loading become: [53]

$$\text{Interior: } \frac{\Delta_0 D}{P \ell^2} = 0.1253 - 0.008 \left(\frac{a_r}{\ell} \right) - 0.028 \left(\frac{a_r}{\ell} \right)^2 \quad (\text{B-28})$$

$$\text{Edge: } \frac{\Delta_0 D}{P \ell^2} = 0.4311 - 0.707 \left(\frac{a_r}{\ell} \right) - 0.2899 \left(\frac{a_r}{\ell} \right)^2 \quad (\text{B-29})$$

Each of these equations can be rearranged to isolate ℓ on the right side and solve for ℓ as a root of the quadratic equation:

$$\text{Corner: } \frac{\Delta_0 D}{P \ell^2} = 1.148 - 1.50 \left(\frac{a_r}{\ell} \right) + 0.6565 \left(\frac{a_r}{\ell} \right)^2 \quad (\text{B-30})$$

$$\ell = \frac{-b - \sqrt{b^2 - 4 a c}}{2 a} \quad (\text{B-31})$$

where, for example, for the interior deflection equation:

$$a = 0.1253$$

$$b = -0.008 a_r$$

$$c = -0.028 a_r^2 - (\Delta_0 D / P)$$

This approach to determining ℓ can be used with the maximum deflection d_0 alone, if the concrete modulus is known or assumed. Alternatively, the AREA method or the SHRP LTPP method can be used to determine the ℓ and thus the concrete modulus from interior deflection basins, and this concrete modulus can then be used to backcalculate edge and corner k values from maximum deflections measured at those positions.

Crovetti also developed equations for adjustments to the measured d_0 and calculated ℓ to account for finite slab sizes. If L/ℓ , the ratio of least slab dimension (length or width in inches) to radius of relative stiffness, is less than about 8, incorrect k and E values may be backcalculated unless a slab size correction is applied. For interior deflection measurements, this correction involves the following steps:

1. Estimate ℓ from any of methods presented above.
2. Calculate L/ℓ_{est} where L = least slab dimension
3. Calculate adjustment factors for maximum deflection (d_0) and ℓ from the following equations:

$$AF_{d_0 i} = 1 - 1.15085 e^{-0.71878 \left(\frac{L}{\ell_{est}} \right)^{0.80151}} \quad (B-32)$$

$$AF_{\ell_{est}} = 1 - 0.89434 e^{-0.61662 \left(\frac{L}{\ell_{est}} \right)^{1.04831}} \quad (B-33)$$

4. Calculate adjusted $d_0 = \text{measured } d_0 * AF_{d_0}$
5. Calculate adjusted $\ell = \ell_{est} * AF_{\ell}$
6. Backcalculate k value and concrete E using adjusted d_0 and ℓ .

These correction equations were developed for slab with equal length and width and no load transfer. Croveti has also studied rectangular slabs and corrections for partial load transfer at transverse and longitudinal edges. Both of these effects are complex, and require additional research to develop efficient and reliable methods for a range of slab sizes and load transfer conditions.

Limitation of Plate Theory Backcalculation Methods

All of the k value backcalculation methods developed to date are based on plate theory, assuming pure bending of the concrete slab. A base layer, if it is considered, is generally also considered to exhibit plate behavior. In future work on k value backcalculation methods for concrete pavements, three-dimensional finite element analysis is recommended to model the behavior of the slab and base as elastic layers on a k foundation. The effects on backcalculated k value of slab size, joint load transfer, slab/base interface friction, and slab deformation due to temperature or moisture gradients could also be examined more realistically using 3D finite element analysis.

Iowa Road Rater Method

The Iowa Department of Transportation has developed a method for determining springtime static k values from Road Rater deflection measurements. The method was developed over several years by comparing Road Rater deflection data from concrete pavements of various thicknesses and types of subgrades with static plate load k value data for subgrades of the same type.

The Model 400 Road Rater used by Iowa is a steady-state deflection device which applies a peak-to-peak force of about 2000 pounds to rigid and composite pavements. The load is applied through two rectangular plates, each 7 in by 4 in, spaced about 9.5 inches center to center. Deflections are measured between the two load plates, and at 12, 24, and 36 inches from the load center, with strain-gauge-type force transducers. [5]

The Iowa DOT conducts deflection testing for the purpose of determining subgrade k values only in April and May, after the spring thaw, as explained below:

"Subgrades are generally saturated in April and May and can be identified by soil type or density through Road Rater deflection testing in this condition. All other times of the year, all subgrades are firm and deflect in a similar manner when tested with the Road Rater. It is extremely difficult or impossible to seasonally adjust Road Rater deflection data taken at other times of the year to a springtime condition unless detailed soils information is available. The only exception is a wet fall following an unusually cool and wet summer when Road Rater testing conditions may be similar to springtime conditions." [6]

Iowa characterizes subgrades by k values which were developed by correlating plate load test data to standard Proctor density and AASHTO group index values. In order to include a wider range of soil types, these correlations were supplemented with the correlations developed by Darter for k value versus soil type and degree of saturation. [7] For concrete pavements with subgrades of known soil type, density, and group index, Road Rater deflection testing was done to correlate deflection basin parameters to the k values assigned to the subgrades. The results are shown in Figure B-11.

The X axis on the chart, average sensor 1 deflection in mils, is the average deflection measured between the two load plates. The Y axis, SCI/SENS1 ratio, is the ratio of Surface Curvature Index (sensor 1 deflection, at the load center, minus sensor 2 deflection, at 12 inches from the load center) to sensor 1 deflection. From these two basin parameters, the k value may be determined from Figure B-11 for a given slab thickness. The maximum k value which can be determined from the chart is 225 psi/in [61 kPa/mm]. Note from the chart that for a given slab thickness, a granular base produces a higher k value.

The k value obtained in this manner is considered a static k value, i.e., what would be obtained in a static plate load test on the subgrade, and is also considered representative of springtime conditions only. The Iowa DOT's concrete pavement design procedure uses this static springtime k value as the subgrade input. The comments quoted above suggest that the peak force of 2000 lbf [8900 N] applied by the Road Rater may not be adequate to reliably determine k values in other seasons with this device. Nonetheless, the Iowa Road Rater procedure is attractive in that it is to date the only procedure in which static k values have been directly correlated to pavement deflections measured by a dynamic loading device.

Soil Support K Values For Rigid & Composite Pavements From Road Rater Deflection Dishes

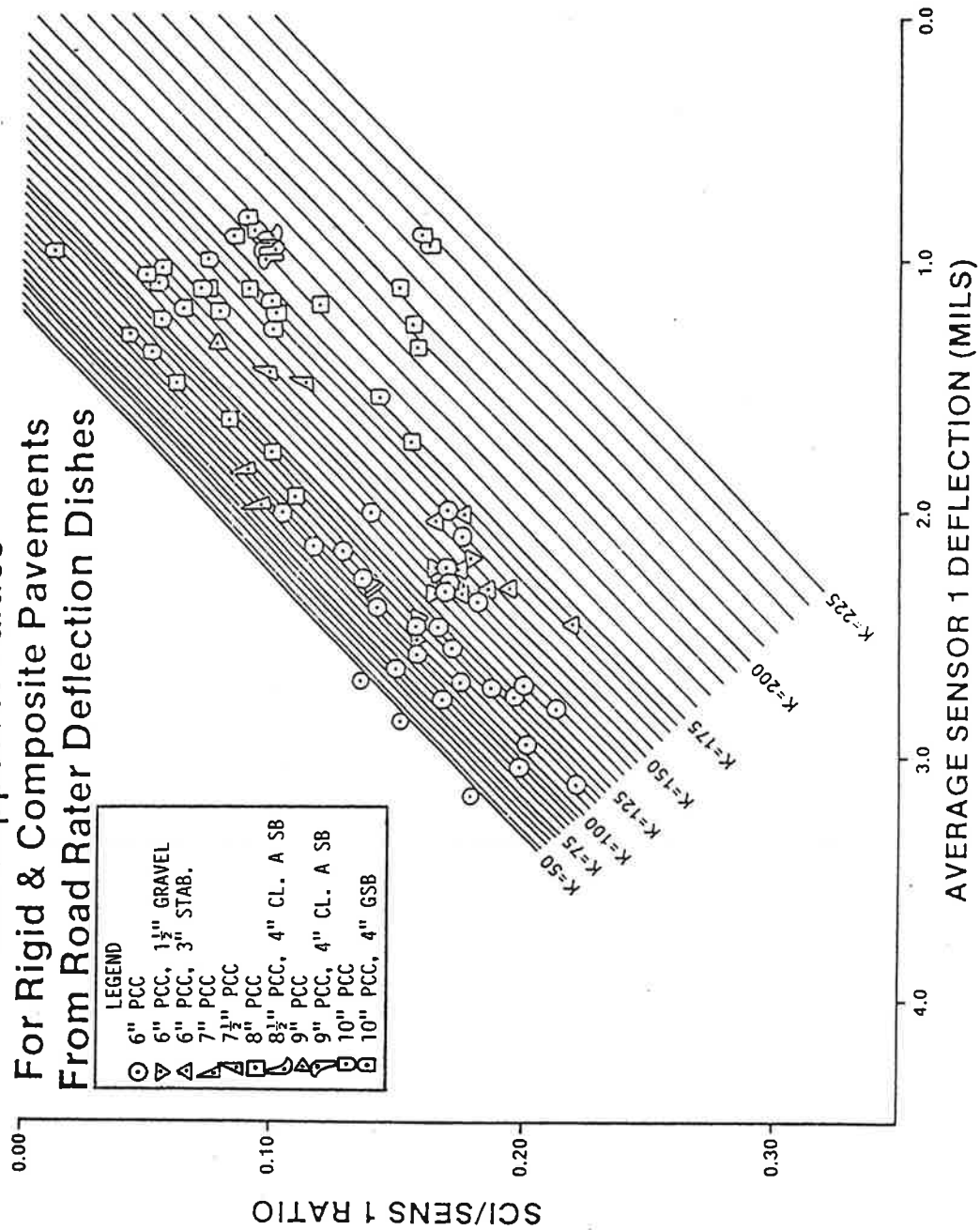


Figure B-11. Iowa Road Rater method for determining springtime static k value. [6]

PLATE TESTING METHODS

The available standardized plate bearing test methods for determining k value are reviewed and compared in this section. Four standard-setting bodies are referred to: the American Society for Testing and Materials (ASTM), the American Association of State Highway and Transportation Officials (AASHTO), the Corps of Engineers (COE), and the Deutsches Institut fuer Normung (DIN, German Institute for Standardization). Note that these tests are used for a variety of purposes other than concrete pavement design; thus the guidance provided is not specifically targeted to determination of k values for concrete pavement design. Comments on the test methods pertaining specifically to the purpose of this study, determination of static elastic k values for concrete pavement design, have been added.

The two types of plate bearing tests are repetitive static and nonrepetitive static plate loading. ASTM D 1195 and AASHTO T 221 are repetitive tests; ASTM D 1196 and AASHTO T 222 are nonrepetitive tests. The original COE test was nonrepetitive; the Corps later developed a repetitive test as well. The German DIN 18134 is a nonrepetitive test. The differences between the repetitive and nonrepetitive tests lie in the seating, loading, and k value calculation procedures.

For the purpose of concrete pavement design, the recommended subgrade input parameter is the static elastic k value. This may be determined from either a repetitive or nonrepetitive test. In a repetitive test, the elastic k value is determined from the ratio of load to elastic deformation (the recoverable portion of the total deformation measured). In a nonrepetitive test, the load-deformation ratio at a deformation of 0.05 in [1.25 mm] is considered to represent the elastic k value, according to extensive research by the Corps of Engineers.

Equipment

The equipment necessary to carry out a plate bearing test includes the following: a load application device, load plates, a pressure application device, settlement measurement devices, and auxiliary equipment.

Load Application Device

This may be a truck, trailer, tractor-trailer, or tram which can be properly anchored. ASTM, AASHTO, and COE recommend that the loading device supports be at least 8 ft [2.4 m] from the circumference of the largest loading plate. DIN specifies that the clearance between the load plate and the supports be at least 2.5 ft [0.75 m] for a 12-in [300 mm] diameter plate, at least 3.6 ft [1.1 m] for a 24-in [600 mm] plate, and at least 4.3 ft [1.3 m] for a 30-in [762 mm] plate. AASHTO specifies a dead load of at least 25,000 pounds [112 kN]. DIN recommends a loading capability of at least 2240 pounds [10 kN] greater than the maximum test load.

Load Plates

ASTM and AASHTO recommend circular bearing plates at least 1 in [25 mm] thick, ranging in diameter from 6 in [152 mm] to 30 in [762 mm]. The number of plates and plate sizes used may vary depending on the purpose of the test. If several plates are used, they should be stacked in pyramidal fashion to ensure rigidity and provide a uniform vertical strain to the subgrade. The diameters of sequential stacked plates must not differ by more than 6 in [152 mm]. None of the test methods specifically require a certain plate size for a certain purpose, but based on the findings of this study, testing with a 30-in [762 mm] plate is recommended for concrete pavement design purposes because this plate size has been found to produce

k values which match k agree with k values calculated from slab deflections. Tests made with smaller plate sizes will yield higher k values.

Pressure Application Device

The American standards recommend applying the load with a hydraulic jack assembly. ASTM and AASHTO specify that the assembly have a spherical bearing attachment for incremental application of loads and a gauge to measure the magnitudes of applied loads. DIN recommends an oil pressure pump connected to a hydraulic press by a high-pressure hose. The setup must also have a mechanical or electrical force transducer to indicate the magnitudes of applied loads to a maximum of 1 percent of the greatest test load.

Settlement Measurement Device

AASHTO and COE require at least three dial gauges to measure movements; ASTM requires two. The gauges must be properly supported to insure that they will not be affected by loading conditions. The mounting beam for the dial gauges should be at least 18 ft [5.5 m] long resting on supports at least 8 ft [2.44 m] (4 ft [1.22 m] in the AASHTO nonrepetitive test) from the circumference of the bearing plate or nearest wheel or supporting leg. The COE specifies that the gauges be able to read to units of 0.001 in [0.03 mm] and able to read a maximum deflection of 1 in [25 mm]. The gauges should be positioned to measure the average vertical movement of the plate (e.g., at third points around the plate, 1 in [25 mm] from the edge of the bearing plate).

The German standard recommends at least three dial gauges able to read to units of 0.0004 in [0.01 mm] and able to read a maximum deflection of 0.4 in

[10 mm], or electronic displacement transducers. The deflection is measured at the center of the plate by a long beam with a supporting frame, similar in appearance to a Benkelman Beam. The beam length can be varied from about 3 to 6 ft [1 to 2 m].

Auxiliary Equipment

This includes such things as levels, spades, rulers, a plumb bob, brushes or brooms to level the site, and plaster of Paris or sand on which to seat the plate if necessary. The AASHTO nonrepetitive test also uses a consolidometer apparatus for cutting undisturbed specimens of the soil into a consolidometer test ring. This is done to determine the moisture content of the soil.

Test Site

ASTM and AASHTO specify that if an unconfined test is to be conducted on material at some depth below the existing grade, surrounding material must be removed to provide clearance of one and a half to two times the diameter of the bearing plate, to eliminate surcharge or confining effects. If the test is intended to be confined, the excavated area may be the minimum required to accommodate the bearing plate.

AASHTO and COE further specify that if the subgrade is to be composed of fill material, a test embankment of at least 30 in [762 mm] in height should be made from the proposed fill material and compacted to the required moisture and density which will be required in actual construction, and the plate load test conducted on top of this test embankment. COE also specifies that if the subgrade is exposed by cut, the test area must be uncovered to eliminate any surcharge effect.

Plate Load Assembly

The stacked load plates shall be set level on a thin bed of pure sand, pure plaster, or a combination of the two. This shall serve as a cushion layer for uniform contact of the plate to the subgrade. A minimum amount of cushion material should be used, and COE specifies a maximum grain size of 0.25 in [6 mm]. If plaster is used, DIN recommends that the bottom surface of the plate be oiled and that testing commences only when the plaster has set. ASTM, AASHTO, and DIN take loss of moisture from the subgrade into account and cover an area within a radius of 6 ft [1.8 m] from the load with a tarpaulin or waterproof paper to protect the test area from drying.

Seating Procedure

The bearing plates and assembly are seated by quick application and release of load until the dial gauges measure at least 0.01 in [0.25 mm] displacement or at most 0.02 in [0.51 mm] by the ASTM and AASHTO repetitive standards. Before the load is reapplied the dial gauges are zeroed. The plate is reseated with an application of half the load which produced the displacement between 0.01 and 0.02 in [0.25 and 0.51 mm].

The nonrepetitive AASHTO procedure suggests another seating procedure in addition to the one described above. For a pavement design thickness of less than 15 in [381 mm], a load of 707 lbs [3.15 kN] is applied to produce 1 psi [6.89 kN/m²] pressure, or if the pavement design thickness is 15 in [381 mm] or more, 1414 lbs [6.30 kN] is applied to produce 2 psi [13.7 kN/m²] pressure. The seating load, or "zero load" is maintained until complete deformation has taken place, a reading is

then taken, and this is used as the "zero" reading. To ensure good seating of the apparatus and bearing plate, cyclic loading under the seating load may be used.

COE seats the equipment by application of at most 5 psi [34.6 kN/m²] depending on the type of soil being tested. The revised COE procedure seats the load system and bearing plate with 1000 pounds (4.46 kN) applied in 30 seconds, immediate load release, and zeroing of the dial gauge.

DIN recommends seating the load plate prior to testing with 1.45 psi [10 kN/m²] for about 30 seconds. The dial gauges are then set to zero.

Loading Procedure

The ASTM and AASHTO procedure for repetitive loading is as follows:

- Apply load until a deflection of 0.04 in [1 mm] is reached. Start stopwatch.
- Maintain load until the rate of deflection is at most 0.001 in per minute [0.03 mm per minute] for three successive minutes.
- Apply and release the load in the above manner six times.
- Record the dial gauge readings.
- Increase the load until a deflection of 0.20 in [5.1 mm] is reached; proceed with the second through fourth steps.
- Increase the load until a deflection of 0.40 in [10.2 mm] is reached; proceed with the second through fourth steps.

For all the loads, the load is maintained until the rate of displacement slows to less than 0.001 in per minute [0.03 mm per minute]. Readings from the dial gauges resting on the plate shall be recorded every minute. For dial gauges set beyond the

perimeter of the load plate, readings shall be recorded just before load application and just before release for each repetition. At half hour intervals, air temperature readings should also be taken near the load plate.

The ASTM procedure for nonrepetitive loading is as follows:

- Apply unspecified loads at a moderately rapid rate and in uniform increments. The magnitude of the loads must be small enough to just permit recording of a sufficient number of load-deflection points (6 or more) to produce an accurate load-deflection curve.
- Maintain load until the rate of deflection is at most 0.001 in per minute [0.03 mm per minute] for three successive minutes.
- Record deflections corresponding to the load increment.
- Continue until the total deflection (initially chosen) is reached or until the load capacity of the apparatus is reached.
- Maintain each load level until the rate of deflection is at most 0.001 in per minute [0.03 mm per minute] for three successive minutes.
- Record total deflection.
- Release load until "zero" load is returned (the load at which the dial gauges were set to zero).
- Maintain this zero load until the rate of recovery is at most 0.001 in per minute [0.03 mm per minute] for three successive minutes.
- Record the deflection at the zero-setting load.

An average settlement for each load application is then obtained by taking the average of each of the individual gauge readings for each load level.

AASHTO provides two nonrepetitive loading procedures, one being the same as ASTM's above, and the other one being intended to determine the k value as the ratio of load to 10 psi pressure. This method is not presented in detail here since the first method, in which k can be determined at a selected deflection level, is considered the appropriate procedure for concrete pavement design.

The COE nonrepetitive procedure recommends incremental application of 3 to 5 psi [20.7 to 34.6 kN/m²] depending on existing soil conditions. Complete settlement must be allowed to take place before application of a new load. Full release of the load should be done in one increment. To ensure that consolidation is sufficiently complete in cohesive soils, a time-deformation curve should be plotted. The test may be done beyond the yield point of the material.

The revised COE procedure specifies the following steps:

- Within 10 seconds of seating, a 7070-pound [31.5 kN] load for 10 psi [69 kN/m²] is applied and held for 40 seconds.
- Dial gauge readings are recorded. The load is released 5 seconds thereafter. Readings are taken again after 5 more seconds.
- The cycle is repeated at the same load level 10 times.
- After the release of the tenth load, pause for 10 minutes before reading the gauges.

- Apply a load of 7070 pounds [31.5 kN] in 10 seconds, and record the dial gauge readings at periods equal to the square of the unit numbers (i.e., 1, 4, 9, 16, etc.).
- Plot movements with respect to the square root of time.
- Continue the test as long as the relationship is linear; otherwise, the load is released and the test is stopped.

Evaluation of Results

Selection of a static, elastic k value for use in concrete pavement design may be obtained from the results of static load testing in either of two ways:

- **From a repetitive test:** Plot the deformations during loading and unloading, and calculate the average elastic deformation from the total deformation for a given loading minus the nonrecoverable deformation measured at the end of unloading. The ratio of load to elastic deformation is the elastic k value.
- **From a nonrepetitive test:** Plot the load-deformation curve, and determine the load level that corresponds to a deformation of 0.05 in [1.25 mm]. The load divided by the deformation at this point is a good estimate of the elastic k.

Finally, it should be noted that a 30-in-diameter [762 mm] plate should be used to determine the k value for concrete pavement design.

REFERENCES FOR APPENDIX B

1. Thompson, M. R. and Q. L. Robnett, "Resilient Properties of Subgrade Soils," Illinois Cooperative Highway Research Program, Report No. UILU-ENG-76-2009, University of Illinois and Illinois Department of Transportation, 1976.
2. Hall, K. T., "Performance, Evaluation, and Rehabilitation of Asphalt-Overlaid Concrete Pavements," Ph.D. thesis, University of Illinois at Urbana-Champaign, 1991.
3. Asphalt Institute, "Research and Development of the Asphalt Institute's Thickness Design Manual (MS-1) Ninth Edition," Research Report 82-2, 1982.
4. Hall, K. T., "Backcalculation Solutions for Concrete Pavements," technical memo prepared for SHRP Contract O-020, "Long-Term Pavement Performance Data Analysis," 1992.
5. Smith, R. E. and R. L. Lytton, "Synthesis of Nondestructive Testing Devices for Use in Overlay Thickness Design of Flexible Pavements," FHWA Report No. RD/83/097, 1984.
6. Potter, C. J. and K. L. Dirks, "Pavement Evaluation Using the Road Rater TM Deflection Dish," Final Report, Project MLR-89-2, Iowa Department of Transportation, 1989.
7. Darter, M. I., "Design of Zero-Maintenance Plain Jointed Concrete Pavement," Volume 1 -- Development of the Design Procedures," University of Illinois at Urbana-Champaign, Report No. FHWA-RD-77-111, 1977.

APPENDIX C

LOSS OF SUPPORT CONCEPTS AND METHODS

LOSS OF SUPPORT OVER THE DESIGN LIFE

Loss of support refers to any gap or void that may occur between the base and slab or between a stabilized base and the subgrade, causing increased deflection of the slab surface. There are three basic types of "loss of support" that a concrete slab exhibits over time.

- Erosion of the base and/or subgrade from beneath the slab, resulting in increased deflections (faulting) and stresses (cracking) in the slab.
- Settlement or consolidation of the base and/or subgrade, usually resulting in slab cracking in the vicinity of the settlement.
- Temperature curling and moisture warping of the slab, resulting in increased deflections and stresses in the slab. Permanent construction curling presents a potential for very serious loss of support and early failure of jointed concrete pavements.

Loss of support can have a major impact on slab deflections and stresses, and thus pavement life. Erosion also has a major effect on joint faulting, which is a critical distress related to life.

LOSS OF SUPPORT FROM EROSION

Pumping results in loss of support over time beneath either the slab itself or beneath a treated base. Either of these situations can lead to increased deflections and stresses in the concrete slab and are of concern to the design engineer.

AASHO Road Test Erosion

The extensive amount of loss of support that occurred at the AASHO Road Test site is well documented. [2]

- Extensive pumping and erosion of the sand-gravel base occurred causing loss of support beneath the corners and edges of the slab. The amount of material pumped onto the shoulder was measured in a cubic foot container over the two-year period. A "pumping index" (PI) was computed as cubic inches of pumped material per inch along the pavement. The PI ranged from 0 to over 200 depending on slab thickness and axle loading. Photos exist of persons shoving a yard stick under the concrete slab corner. [2]
- "By removing the concrete from a few failed sections and sampling the underlying material, it was observed that subbase material had apparently been removed by erosive action of water moving across the top of the subbase, and that the remaining subbase material was relatively undisturbed ... Inasmuch as the great majority of the sections which failed pumped severely prior to failure, many of these sections would have survived the two years of traffic had the subbase material been stabilized effectively to resist erosion by water." [2]

Note that this erosion occurred even though the transverse joints were adequately dowelled to prevent faulting. If the joints had not been dowelled, erosion would have occurred sooner leading to much earlier failure. The AASHTO design model for concrete pavements thus inherently includes the effect of this extent of loss

of support. If erosion could be controlled, a pavement should perform better than predicted by the AASHTO design model, all other things being equal.

Predicting Loss of Support from Erosion

No methodology currently exists to predict the amount of loss of support that may occur from erosion. To directly consider this in design, the designer would need to be able to approximately predict the amount of loss of support that may develop beneath a slab over the design life so that the increased stresses can be predicted and their effect on fatigue cracking considered. This is a problem of great complexity because of many other factors that play a role. One key factor is the presence of dowel bars at the joint which decreases the amount of differential deflection across the joint and thus the amount of erosion potential. Other factors include the drainability of the pavement structure (the time that free water is available), the climate (freeze-thaw, precipitation, saturation levels), traffic loadings, slab thickness, subgrade and base stiffness, and joint sealing.

A second main effect of erosion is joint and crack faulting. An erodible base layer would normally result in increased faulting and thus, decreased service life. Joint faulting can be predicted from several available prediction models. A design check can be made to determine if joint faulting is excessive, and if so, a modified joint design could be proposed and evaluated.

As far as the AASHTO design method is concerned, the extensive loss of support that occurred during the test period had a very significant effect on pavement load-carrying capacity. It is hard to imagine a greater amount of loss of support than that which occurred at the AASHO Road Test site. Therefore, loss of support is already fully considered in the AASHO rigid pavement design equation. Increasing slab thickness for loss of support is overdesign and is not recommended.

For other design procedures, however, the impact of erosion and loss of support on the load carrying capacity could be more fully considered. This would involve a complex analysis of the erodibility of underlying base and subgrade materials, erosion of the concrete slab itself, the friction between the base and concrete slab, the magnitude of deflections and load transfer at the joints, the number of axles, and a subdrainage analysis of the pavement section. The development of a predictive model for this complex phenomenon would be extremely difficult.

The next section discusses the amount of loss of support that occurs for temperature curling and moisture warping. This is quite significant and results in increased slab stresses that might otherwise be caused by erosion and loss of support. Of course, in the field both of these mechanisms go on at the same time (erosion and curling/warping). In fact, significant upward curling or warping may be a catalyst for increased erosion if water gets between the curled slab and the base course.

PIARC Recommendations on Erosion

The most comprehensive recommendations available on ways to minimize erosion and loss of support are provided by the PIARC Technical Committee on Concrete Roads from eight European countries and the USA. A document entitled "Combatting Concrete Pavement Slab Pumping" is available that provides excellent guidelines for design and construction. [20] The general principles are [21]:

- The erodibility of subbase and shoulder materials is an essential property that must be taken into account in the design of new pavements and in the diagnosis of existing pavements, because the erosion of materials at interfaces causes pumping and destabilizes the slabs of the concrete pavement.

- Simple tests have been developed for characterizing the erodibility of materials. They offer the data required for comparing results using a common language understood in all countries.

Tests are conducted in the laboratory to classify a material in terms of its type and binder content in five erodibility classes based upon a decreasing order of erodibility resistance. The erodibility resistance ratio is in the order of about 5 between each class. These materials classes and criteria are as follows:

Class A - Extremely erosion resistant. Examples: lean concrete with 7-8 percent cement; bituminous concrete with at least 6 percent bitumen.

Class B - Erosion resistant. Example: cement treated granular material with 5 percent cement manufactured in a plant (five more times erodible than Class A when tested in the laboratory).

Class C - Erosion resistant under certain conditions. Examples: cement treated granular material with 3.5 percent cement manufactured in the plant; bitumen-treated granular materials with 3 percent bitumen (five more times erodible than Class B).

Class D - Fairly erodible. Examples: granular material treated in place with 2.5 percent cement, fine soils treated in place, untreated granular materials (five times more erodible than Class C).

Class E - Very erodible. Example: contaminated untreated granular material; untreated fine soils (five times more erodible than Class D).

Base erodibility is of course closely related to traffic loadings, subdrainage, dowelling of joints, and transverse and longitudinal joint sealing. Table C-1 shows

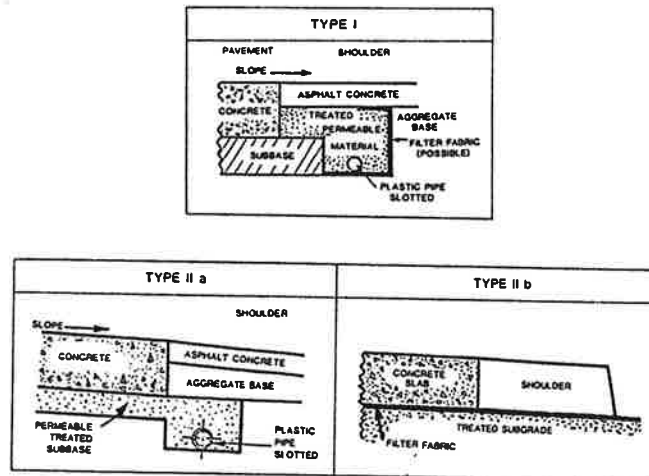
Table C-1. Design provisions proposed for combatting pumping in concrete pavements by PIARC.

TRUCK TRAFFIC	HIGH			MEDIUM			LOW		
SURFACE WATER EXPOSURE TIME	High	Medium	Low	High	Medium	Low	High	Medium	Low
CONSTRUCTIONAL ARRANGEMENTS									
INTERFACE DRAINAGE (TYPE)	I or I Ia	I or I Ia	I or* I Ib	I or I Ia or I Ib	I or* I Ib	OPTIONAL			
SUBBASE AND SHOULDER EDGE MATERIAL (ERODABILITY CLASS)	A	A or B	B	B	B or C	C	C or D	C or D	D or E
JOINT SEALING	yes	yes	yes	yes	Optional with B yes with C	OPTIONAL			

* Subject to checking of stresses in concrete with filter layer actually used.

- Legend :

1 - Drainage



2 - Significant materials of erodability classes (examples)

- A : lean concrete with 8 % cement ; bituminous concrete with 6 % bitumen
- B : cement-treated material with 5 % cement produced in the plant
- C : cement-treated material with 3.5 % produced in the plant ; bitument-treated material with 3 % bitume
- D : material treated in place with 2.5 % cement, treated soils
- E : untreated, unprocessed material

the recommendations for combating pumping in concrete pavements. The traffic loading (High = > 2000 trucks/day/lane, Medium = 400-2000, Low = < 400), subdrainage (Type I, II, III shown) and joint sealing (Yes or No) where each of these classes of materials are recommended are given in Table C-1. Subdrainage Type IIa includes a permeable subbase that would apparently be a Type A material.

Laboratory Erosion Testing

Several tests have been developed to measure the degree of erodibility of different materials. These tests include the Surface Abrasion Test developed by California [27], a brush test, a jetting test, and a vibrating table test used in France [28, 29], and a rotational shear apparatus [26].

Three of these tests (brush, jetting, and rotational shear) were evaluated in 1989 by Van Wijk and Lovell. [26] Each of the tests was found to have some advantages. For example, the jetting test was only used on nonstabilized materials; the brush test on cement-treated, lean concrete and asphalt-treated materials; and the rotational shear device on cement stabilized materials.

"The brush test was appropriate for comparing the erosion of different lean concrete samples, but was inappropriate for comparing the effect of the different compaction efforts used in preparing lean concrete and cement-stabilized samples on erosion. Use of the jetting test to characterize the erosion of nonstabilized materials was the least successful. Use of the rotational shear device was successful for determining the critical shear stresses and erosion rates of portland cement-stabilized materials." [26]

Van Wijk and Lovell concluded:

"... any impervious unstabilized material used in rigid pavements will erode ... portland cement content is the most important factor in the erodibility of cement-stabilized materials. The compaction effort and gradation are also important, but to a lesser extent ... The erosion of asphalt-stabilized materials is affected by the asphalt content, the compaction effort, and environmental factors. Wetting and drying have greater influence on the erosion of asphalt-stabilized materials than freezing and thawing." [26]

The water-cement ratio also affected the erodibility of lean concrete in addition to cement content.

Birmann of the Technical University of Munich, Germany conducted laboratory erosion tests on six different types of asphalt-stabilized bases using a pavement model with concrete slabs. He found that erosion occurs on asphalt-treated bases when the asphalt content is less than 4 percent and the void content is greater than 5 percent. The materials which performed poorly in the pavement model also showed considerable loss of mass when submitted to the French brush test. Also, the materials which performed well in the pavement model showed small quantities of loss of mass in the French brush test. [30]

LOSS OF SUPPORT FROM TEMPERATURE CURLING AND MOISTURE WARPING

At least three different temperature and moisture mechanisms are occurring that contribute to a deformed slab surface causing gaps or voids beneath the slab and

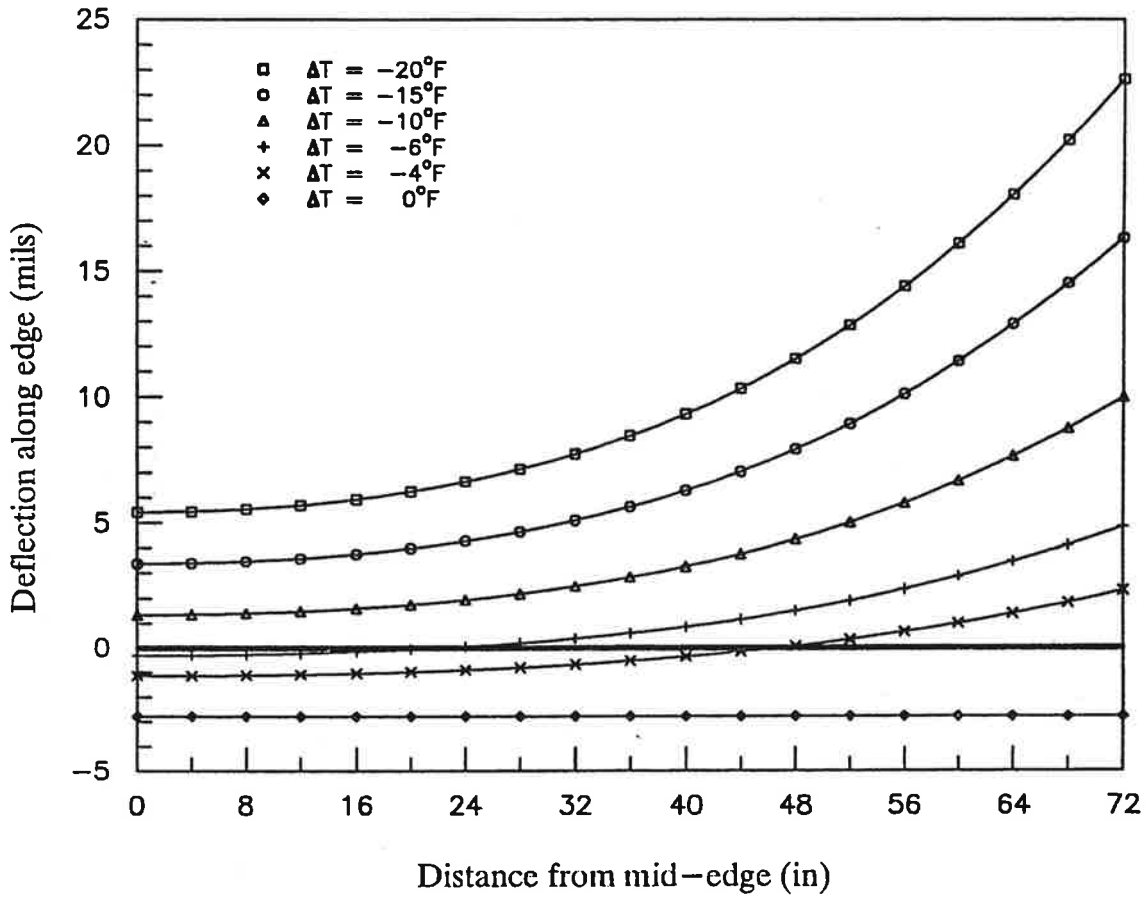
increased deflections and stresses: (1) negative (nighttime) temperature differential from the top to bottom of the slab which occur daily, (2) permanent curling resulting when the slab hardens with a high positive (daytime) temperature gradient after placement, and (3) moisture differentials from top to bottom of the slab, which may be permanent to some degree and also seasonally cyclic.

Negative Temperature Differential Through Slab

Normal curling of a slab is caused by temperature differential through the slab which occurs on a daily basis. A negative (top cooler than bottom) temperature differential results in the corners and edges displacing upward, creating the potential for a gap or void between the slab and the base or subgrade. Figure C-1 illustrates the magnitude of slab corner uplift from curling for a range of nighttime temperature differentials. When this happens, any load near the corner or joint will cause an increased stress on the surface of the slab that could lead to corner breaks, diagonal cracks, or even transverse cracks several feet from the joint. Figure C-2 shows this increase in stress for a given negative temperature differential.

Construction Permanent Curl

A permanent form of curling from a temperature differential at construction has been identified in England, Germany and Chile. [7, 8, 22, 36, 37] If a high positive temperature differential through the slab exists in the slab when it hardens (at which time the slab is flat), upward corner and edge curling may occur shortly thereafter when the temperature gradient dissipates. A high positive temperature differential occurs particularly on days with high solar radiation and when conventional curing procedures are used. This temperature differential has not been measured extensively and its magnitude is not well known. [7, 8, 22, 36, 37]



Notes: Midslab is at 0 inches and the corner is at 72 inches [1829 mm]
 Joint spacing L = 12 ft [3.7 m]
 k = 250 psi/in [68 kPa/mm]
 Slab thickness D = 8 in [203 mm]
 Concrete elastic modulus E_c 4 million psi [27560 MPa]
 ΔT = top temperature - bottom temperature, °F
 $1^\circ\text{F} = 0.55^\circ\text{C}$, 1 in = 25.4 mm, 1 mil = 25.4 μm

Figure C-1. Illustration of corner deflection due to a negative temperature differential through the slab, computed using 3DPAVE.

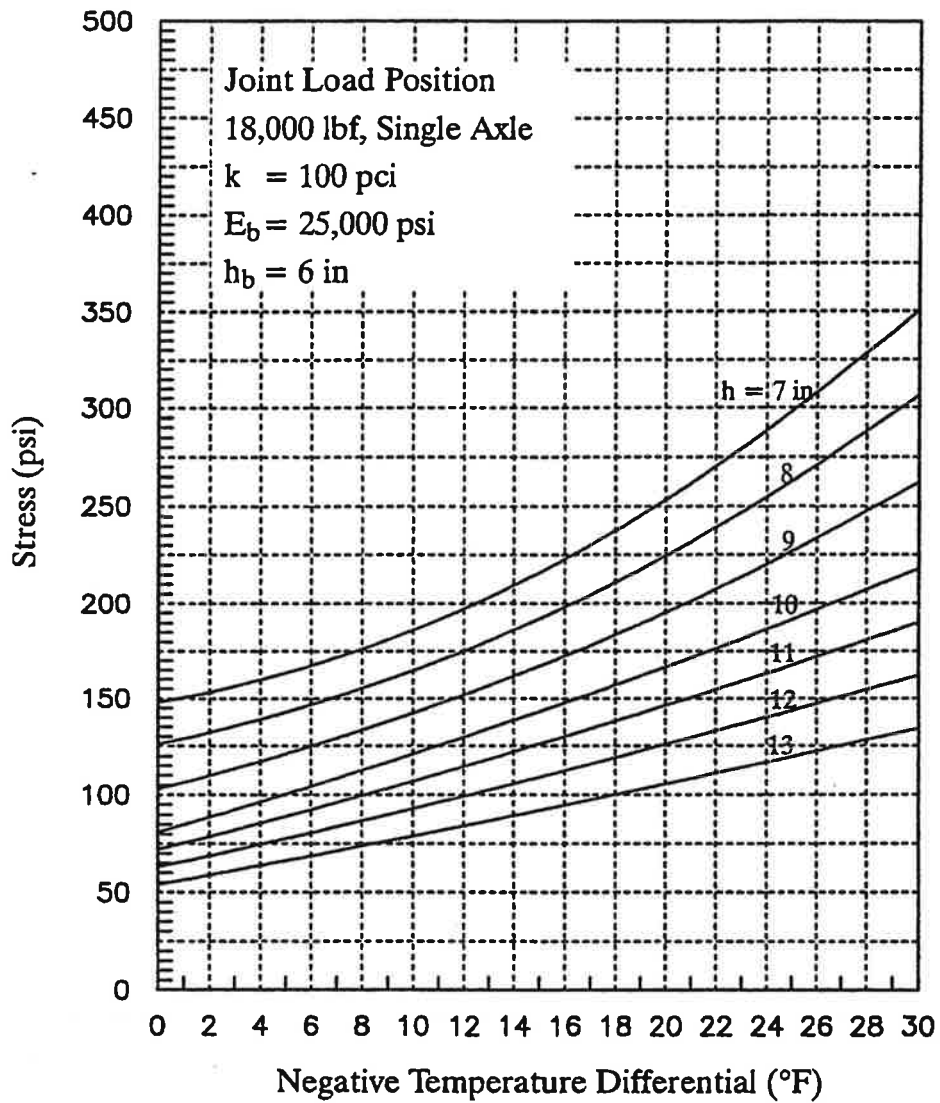
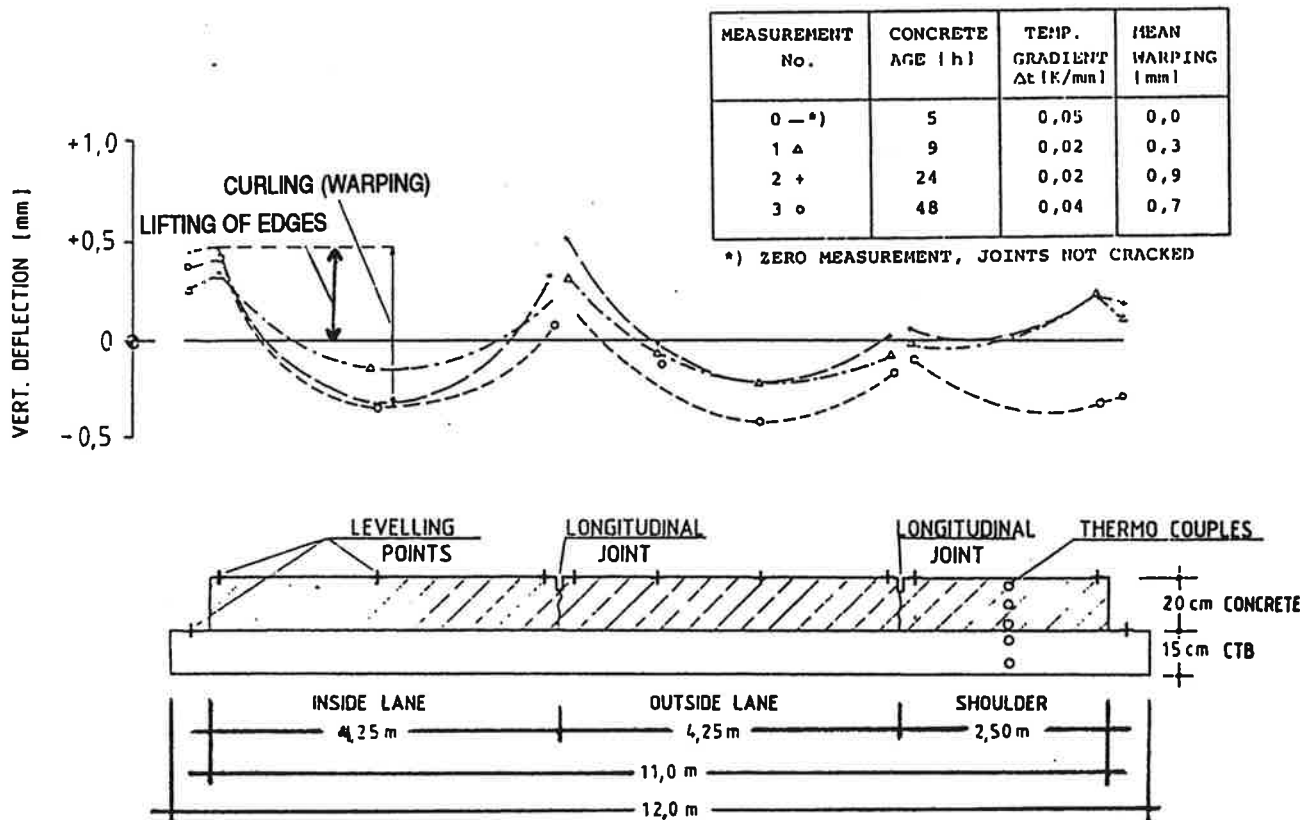


Figure C-2. Increase in tensile stress at top of slab from increased negative temperature differential from top to bottom of slab.

One set of data from Germany showed that 5 hours after placement in sunshine, the top of an 8-in [203 mm] slab had a temperature of 116°F [47°C] and the bottom 80°F [27°C] using a conventional curing compound. If the slab solidifies in a flat position with this large positive thermal gradient, the corners and edges will be permanently curled upward for any lower temperature gradient. Figure C-3 shows the permanent construction curling which developed within 48 hours after placement for a concrete pavement in Germany. An upward curling of the slab edges of about 0.012 in [0.3 mm] was observed 9 hours after paving in spite of the positive temperature differential of 7.2°F [4°C]. At 24 hours the mean upward curling had increased to 0.035 in [0.9 mm]. The researchers concluded that this upward curling within one day could not have been caused by shrinkage. The "construction curling" then is defined as the positive temperature differential that would be required to produce a flat slab (note that this is before any moisture shrinkage occurred at the top of the slab).

"Field tests at Munich Technical University ... indicated that the temperature development immediately after paving is of great importance [in] pavement curling ... Therefore the conclusion may be drawn that under normal paving conditions [in] warm weather always an upward curling will be created already a few hours after paving ... the advantages of wet curing clearly are evident: it reduces not only permanent shrinkage deformations in the plastic state of the "young" concrete but lowers as well the zero stress temperature at surface, thus preventing upward curling probably totally." [7]



1°F = 0.55°C, 1 psi = 6.89 kPa, 1 in = 25.4 mm, 1 lbf = 4.45 N, 1 psi/in = 0.27 kPa/mm

Figure C-3. Development of upward curling within 48 hours after paving in Munich, Germany. [37]

A 1969 study in the UK concluded the following:

"... it has been shown that weather conditions at the time of placing the concrete can have a considerable influence on the transverse cracking found in concrete roads. The most adverse conditions are a combination of high temperature and low humidity and, in general, cracking is more severe for concrete laid in the morning than it is for concrete laid in the afternoon ... When high air temperatures prevail during construction, precautions should be taken to ensure that changes of temperature gradient within the concrete are kept below 0.07 degrees C/mm for the first two or three days by suitable curing techniques." [22]

A study by Armaghani, Larson, and Smith in Florida found that a 9°F temperature difference through a test slab was required to bring it to a flat position. [5] Obviously, any such permanent upward curling would create a serious loss of support beneath the corners and edges of the slab. The deflection profile along a joint due to a change in the temperature differential for the Florida test is shown in Figure C-4. An uplift of 0.012 in [0.3 mm] was observed for only a 3°F [1.7°C] temperature difference between the top and the bottom of the slab. [5]

This phenomenon was also identified in Chile, where several undowelled pavements exhibited excessive corner cracking within a few years after placement:

"The results show a 'permanent' upward curling of slabs in all pavement sections included in the study, as modified by daily temperature variations. The curling is demonstrated in the field by the perceptible rocking of the slabs under the early morning traffic and by the systematic

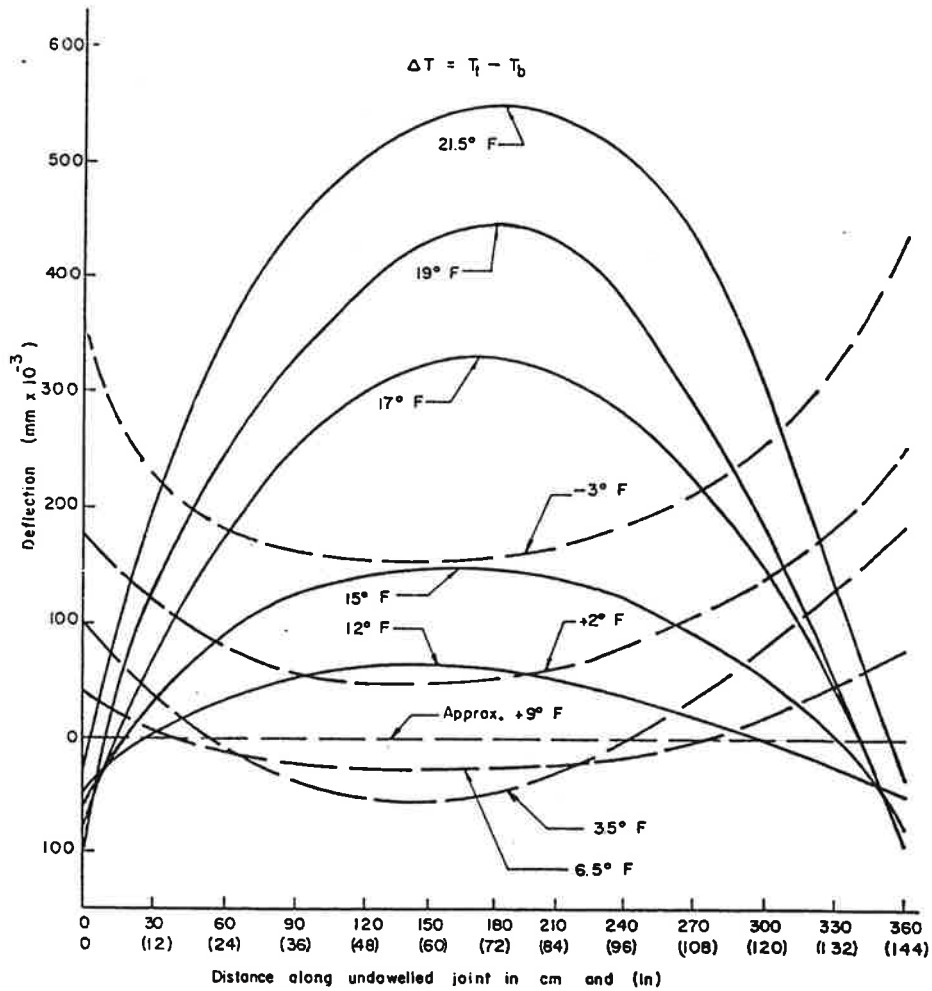


Figure C-4. Deflection profiles along a joint due to change in the temperature differential. [5]

transverse cracking and corner breaks of some rather new pavements with no signs of pumping. Cracking seems to start from the surface downward and from the edges inward." [14]

Moisture Shrinkage Warping

Moisture shrinkage warping of the top of the slab occurs over time has been observed frequently. [5, 7, 8, 9] Hatt reported in 1925 that slab warping occurred when moisture differences existed between the top and bottom surfaces of a slab in the laboratory. An uplift of 0.12 in [3 mm] at the corners and 0.05 in [1.3 mm] at the edge occurred during a period of 40 days. After water was introduced over the surface of the slab the corners and edges dropped 0.06 in [1.5 mm]. [23]

Researchers at the Arlington Tests in the 1930s observed:

"The curvature caused by moisture is principally an upward warping of the edges caused by a moisture loss from the upper surface of the pavement ... The edges of the slab reach their maximum position of upward warping from this cause during the summer and the maximum position of downward warping during the winter, the extent of the upward movement apparently exceeding that of the downward movement considerably." [24]

Janssen measured the moisture content variation through the thickness of concrete specimens at the University of Illinois:

"Pavement moisture contents ... indicated that substantial drying occurred only at the top surface, to a depth of less than 2 in. The rest of the pavement remained at 80 percent saturation or higher. A typical moisture distribution was determined ... a stress distribution was calculated. The tensile strength of the concrete at the surface was exceeded, and cracks could be expected to form to a depth of 0.75 in." [9]

Eisenmann and Leykauf presented a procedure to compute the amount of slab uplift from a moisture gradient. [31] Their model for uplift is as follows:

$$f = \frac{0.75 t e (D - t) L^2}{D^3} - \frac{2.24 \times 10^{-6} L^4}{E D^3} \quad (1)$$

where f = upward deflection of edge, mm

t = depth of shrinkage area, mm (typically < 50 mm)

e = shrinkage of concrete (dimensionless)

D = slab thickness, mm

L = joint spacing, mm

E = modulus of elasticity of concrete, N/mm²

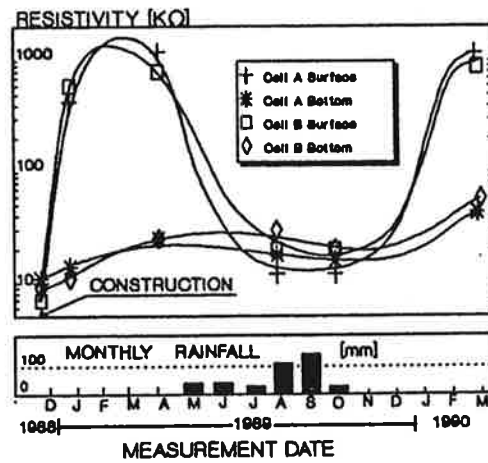
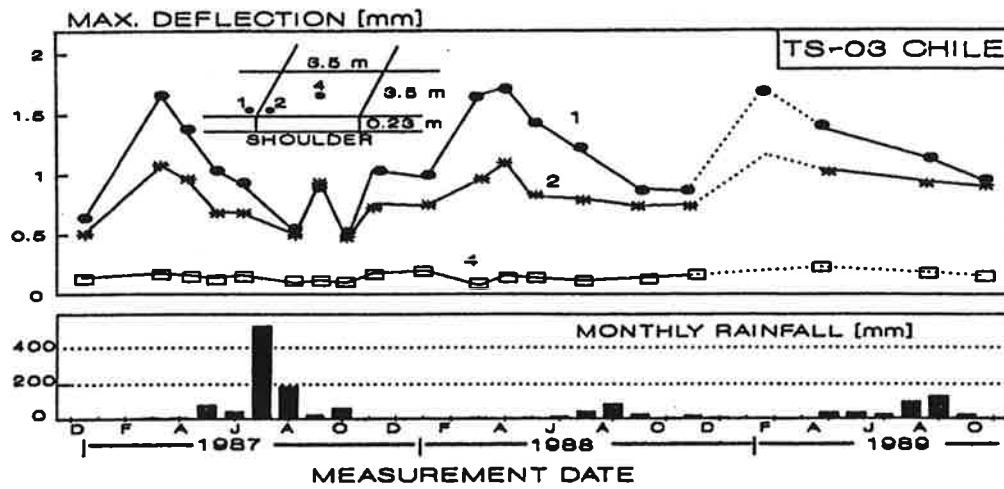
They present an example of a 203 mm [8-in] slab that was constructed under cloudy weather and relatively constant temperatures where 0.6 mm [0.024 in] of uplift was measured after two weeks. They calculated an upward deflection of 0.69 mm [0.027] assuming $t = 40$ mm, $L = 4250$ mm, $E = 30,000$ N/mm², and $e = 12 \times 10^{-5}$ using Eq C-1. Using 3DPAVE to model this pavement, this amount of edge uplift is equivalent to a negative thermal gradient of about 4 to 5°F (2.2 to 2.7°C), or about 0.5°F/inch (0.011°C/mm).

In other climates, greater drying and upward warping of the slab may develop. In Chile, for example, the dry climate is similar to that of portions of California. Figure C-5 illustrates data from Chile of seasonal warping of JPCP pavement in the absence of a temperature differential. During the rainy seasons, the slab uplift decreases. The corners are warped upward about 0.05 in [1.2 mm] during the dry season for a 9-in [229 mm] slab. [8] Using 3DPAVE, this magnitude of shrinkage warping uplift would require an equivalent negative temperature differential of -6°F (3.3°C), or about $-0.7^{\circ}\text{F}/\text{inch}$ ($0.015^{\circ}\text{C}/\text{mm}$).

"Deflections have been found to be maximum in the Autumn, after a long dry season, and minimum during the rainy Winter ... Results of immersion-drying laboratory tests on pavement concrete pieces show that the deformations produced by internal moisture variations are as important as those produced by temperature changes. On the other hand, indirect measurements of moisture through the slab thickness demonstrate the predominant existence of an hydraulic gradient, produced between the slab surface, which is directly exposed to solar radiation and wind, and the protected bottom, which is kept in a more humid environment." [8]

Combination of Temperature, Construction and Moisture

These three climatic conditions can all add together to cause a large tensile stress at the top of the slab near the joint which could eventually lead to serious slab cracking. Combined stresses from negative temperature differentials and from load can be estimated using 3DPAVE for use in pavement design.



Annual cyclic variation of electric resistivity at the slab surface and bottom cells in the experimental pavement and its relation to rainfall.

Figure C-5. Annual cyclic variations of slab deflections and its relation to rainfall in Chile (note: these data taken when no temperature differential existed through the slab). [8]

METHODS OF ASSESSING LOSS OF SUPPORT IN THE FIELD

Various test methods have been developed over the years to identify loss of support in concrete pavements. These methods have only been partially successful, but have been used to identify areas needing slab support improvement. They are important to this study in that future research into the prediction of loss of support is needed to develop prediction methods for use in design. The following methods were evaluated by Chapin. [25] He had difficulty locating "voids" with all of the procedures.

- FWD deflection load sweep.
- FWD deflection detailed analysis.
- Dynaflect deflection.
- 18-kip [80 kN] single-axle load and Benkelman Beam.
- Ground penetrating radar (GPR).
- Road Rater deflection.
- Infrared thermography.
- Spectral Analysis of surface waves.
- Impact echo response.
- Visual distress survey.
- Transient dynamic response.
- Epoxy/core test.

The most used procedures are probably the FWD load sweep and GPR testing. The authors have used the FWD load sweep method [33] successfully on many projects and also have found the epoxy/core test useful. Iowa has had success using a Road Rater for void detection. [36]

A recent study by Croveti [32] involved the development of a procedure to backcalculate a corner k value. By comparing the corner k value to the center-of-slab k value an indication of the amount of loss of support could be obtained. The method adjusts for temperature differential.

CONSIDERATION OF LOSS OF SUPPORT IN DESIGN

The following recommendations were developed for considering loss of support in the design process.

AASHTO Design Guide

An extensive amount of loss of support is already built in to the rigid pavement design models, so further increase in slab thickness for loss of support is not appropriate. The effects of less erodible materials than the AASHTO Road Test dense-graded granular base on predicted slab stress and predicted faulting are considered in the proposed revision to the AASHTO design equation. In addition, a design check is made for joint/corner loading where the total negative temperature differential is used to estimate critical stress in the slab. If this stress is greater than the maximum stress for midslab loading then a design modification is required.

Mechanistic Design

Direct consideration of loss of support for increased slab stresses (and thus cracking) and also for joint faulting is desirable in mechanistic design. Prediction of loss of support caused by thermal curling or moisture warping is possible and could be considered in design.

Negative temperature gradients can be computed using available heat transfer models for any given location. [35] An equivalent negative temperature gradient of

about 0.5 to 0.7°F per inch of slab thickness to account for shrinkage appears reasonable. The negative temperature gradient from construction is impossible to predict, but could be eliminated by improved curing methods.

Prediction of an additional loss of support from erosion is extremely difficult and would require a major research effort. Currently, it is recommended to determine the material requirements that would minimize the occurrence of erosion under varying climatic, traffic, and design conditions using the PIARC recommendations. [19, 20, 21] Then ensure that these conditions be met in the design and construction of the pavement.

In summary for mechanistic design, consider the combined effects of load at the corner position, nighttime negative thermal gradients, "built-in" construction curling from temperature gradient, and moisture shrinkage warping in the design process to control tensile stresses in the surface (slab cracking). Develop a design check for joint faulting that would provide for adequate load transfer, base type, and subdrainage to limit faulting to an acceptable level.

REFERENCES FOR APPENDIX C

1. Langsner, G., T. S. Huff, and W. J. Liddle, "Use of Road Test Findings by AASHO Design Committee," Special Report 73, Highway Research Board, 1962.
2. The AASHO Road Test Report 5, Pavement Research, Special Report 61E, Highway Research Board, 1962.
3. American Association of State Highway and Transportation Officials, Guide for Design of Pavement Structures, Washington, D.C., 1993.
4. Thompson, M. R. and E. J. Barenberg, "Calibrated Mechanistic Structural Analysis Procedures For Pavements Phase 2," Final Report, NCHRP Project 1,26, Transportation Research Board, 1992.
5. Armaghani, J. M, T. J. Larsen, and L. L. Smith, "Temperature Response of Concrete Pavements," Transportation Research Record 1121, Transportation Research Board, 1987.
6. Smith, K. D., et al., "Performance of Jointed Concrete Pavements, Volume IV - Appendix A," Report No. FHWA-RD-89-139, Federal Highway Administration, 1990.
7. Eisenmann, J. and G. Leykauf, "Effect of Paving Temperatures on Pavement Performance," Proceedings of the Second International Workshop on the Design and the Evaluation of Concrete Pavements, Siguenza, Spain, 1990.

8. Poblete, M., A. Garcia, J. David, P. Ceza, and R. Espinosa, "Moisture Effects on the Behaviour of PCC Pavements," Proceedings of the Second International Workshop on the Design and the Evaluation of Concrete Pavements, Siguenza, Spain, 1990.
9. Janssen, D. J., "Moisture in Portland Cement Concrete, Transportation Research Record 1121, Transportation Research Board, 1987.
10. Al-Omari, B. and M. I. Darter, "Effect of Pavement Deterioration Types on IRI and Rehabilitation," University of Illinois and Illinois Department of Transportation, 1993.
11. Hudson, W. R. and F. H. Scrivner, "AASHO Road Test Principal Relationships -- Performance with Stress, Rigid Pavements," Proceedings of the Saint Louis Conference, Special Report 73, Highway Research Board, 1962.
12. Darter, M. I., J. M. Becker, M. B. Snyder, and R. E. Smith, "Portland Cement Concrete Pavement Evaluation System – COPES," NCHRP Report No. 277, Transportation Research Board, 1985.
13. Miner, M. A., "Cumulative Damage in Fatigue," Transactions, American Society of Mechanical Engineers, Vol. 67, 1945.
14. Poblete, M., R. Salsilli, R. Valenzuela, A. Bull, and P. Spratz, "Field Evaluation of Thermal Deformations in Undoweled PCC Pavement Slabs," Transportation Research Record 1207, Transportation Research Board, 1989.
15. Sawan, J. S., M. I. Darter, and B. J. Dempsey, "Structural Analysis and Design of PCC Shoulders," Report No. FHWA/RD-81/122, Federal Highway Administration, 1982.

16. Thornthwaite, C. W., "An Approach Towards a Rational Classification of Climate," Geographical Review, Volume 38, 1948.
17. Darter, M. I., "Design of Zero-Maintenance Plain Jointed Concrete Pavement, Vol. I - Development of Design Procedures," Report FHWA-RD-77-111, Federal Highway Administration, 1977.
18. National Oceanic and Atmospheric Administration, "Climatic Atlas of the United States," U.S. Department of Commerce, Washington, D.C., 1983.
19. Christory, J. P., "Assessment of PIARC Recommendations on the Combatting of Pumping in Concrete Pavements," Proceedings of the Second International Workshop on the Design and the Evaluation of Concrete Pavements, Siguenza, Spain, 1990.
20. PIARC Technical Committee on Concrete Roads, "Combatting Concrete Pavement Slab Pumping," 1987.
21. Ray, M. and J. P. Christory, "Combatting Concrete Pavement Slab Pumping State of the Art and Recommendations," Proceedings of the Fourth International Conference on Concrete Pavement Design and Rehabilitation, Purdue University, West Lafayette, Indiana, USA, 1989.
22. Franklin, R. E., "The Effect Of Weather Conditions on Early Strains in Concrete Slabs," RRL Report No. LR 266, Road Research Laboratory, Crowthorne, Berkshire, UK, 1969.
23. Hatt, W. K., "Effect of Moisture on Concrete," Public Roads, Vol. 6, No. 1, March 1925; also Transactions of the American Society of Civil Engineers, Vol. 84, 1926.

24. Teller, L. W. and E. C. Southerland, "The Structural Design of Concrete Pavement," Part II - Observed Effects of Variations in Temperature and Moisture on the Size, Shape and Stress Resistance of Concrete Pavement Slabs, Public Roads, Vol. 16, No. 9, 1935.
25. Chapin, T. L., "Analysis of Loss of Support Detection Systems for Undersealing Concrete Pavements," Master's Thesis, Purdue University, 1989.
26. Van Wijk, A. J., C. W. Lovell, "Prediction of Subbase Erosion Caused by Pavement Pumping," Transportation Research Record 1099, Transportation Research Board, 1988.
27. Woodstrom, J. H., "Erodibility Testing And Development of Lean Concrete Base in California," International Seminar on Drainage and Erodibility at the Concrete Slab-Subbase-Shoulder Interface, Paris, France, 1983.
28. Pnu, N. C. and M. Ray, "The Erodibility of Concrete Pavement Subbase and Improved Subgrade Materials," Bulletin de Liaison des Laboratoires des Ponts et Chaussees, Special Issue 8, Paris, France, 1979.
29. Pnu, N. C. and M. Ray, "The Hydraulics of Pumping of Concrete Pavements," Bulletin de Liaison des Laboratoires des Ponts et Chaussees, Special Issue 8, Paris, France, 1979.
30. Birman, D. "Erosion von Asphalttragschichten unter Betondecken," (Erosion of Asphalt-Stabilized Bases Beneath Concrete Pavements), BITUMEN 55, 1993.
31. Eisenmann, J. and G. Leykauf, "Simplified Calculation Method of Slab Curling Caused by Surface Shrinkage," Proceedings of the Second International Workshop on the Design and the Evaluation of Concrete Pavements, Siguenza, Spain, 1990.

32. Croveti, J. A., "Design and Evaluation of Jointed Concrete Pavement Systems Incorporating Free-Draining Base Layers," Ph.D Thesis, University of Illinois at Urbana-Champaign, 1994.
33. Croveti, J. A. and M. I. Darter, "Appendix C - Void Detection Procedures," NCHRP Report 281, Transportation Research Board, 1985.
34. Potter, C. J. and K. L. Dirks, "Pavement Evaluation Using The Road Rater Deflection Dish," Final Report Project MLR-89-2, Iowa Department Of Transportation, Ames, Iowa, 1989.
35. Dempsey, B. J., W. A. Herlache, and A. J. Patel, "Climatic-Materials-Structural Pavement Analysis Program," Transportation Research Record No. 1095, Transportation Research Board, 1986.
36. Zachlehner, A., "Beanspruchung von Betonfahrbahnen durch Einflüsse durch Hydratation und Witterung, "(Concrete Pavement Stress due to the Influence of Hydration and Climatic Conditions), Ph.D. thesis, Technical University of Munich, Germany, 1989.
37. Zachlehner, A., "Restraint Stresses in Young Concrete Pavements," Proceedings, Sixth International Symposium on Concrete Roads, Madrid, Spain, October 1990.